Electrophysiological and pharmacological characterization of ion channels involved in moth olfactory transduction cascades

Elektrophysiologische und pharmakologische Charakterisierung von Ionenkanälen in den olfaktorischen Transduktionskaskaden von Nachtschmetterlingen

---

Dissertation zur Erlangung des Doktorgrades
der Naturwissenschaften (Dr. rer. nat.)

dem Fachbereich Biologie
der Philipps-Universität Marburg
vorgelegt von

Steffi Krannich
aus Zwickau

Marburg/Lahn
Juni 2008

Vom Fachbereich Biologie der Philipps-Universität Marburg
als Dissertation am 2008 angenommen.

Erstgutachter: Prof. Dr. Uwe Homberg
Zweitgutachterin: Prof. Dr. Monika Stengl (externe Gutachterin; Universität Kassel)

Tag der mündlichen Prüfung am 2008.

Der Flügelschlag eines Schmetterlings
kann einen Orkan auslösen.
(Edward N. Lorenz)

Contents

Erklärung: Eigene Beiträge und veröffentlichte Teile der Arbeit		1
Zusammenfassung		5
Introduction		11
Kapitel I.	Diacylglycerol activates cation channels in moth olfactory receptor neurons. Pézier A, Papaefthymiou C, Krannich S, Acquistapace A, Stengl M, Lucas P. J Neurophysiol, under review.	25
Kapitel II.	Diacylglycerol-dependent currents and TRP-like channels in the hawkmoth *Manduca sexta*. Krannich S, Ackermann F, Chubanov V, Gudermann T, Stengl M.	43
Kapitel III.	Pharmacological investigation of protein kinase C- and cGMP-dependent ion channels in cultured olfactory receptor neurons of the hawkmoth *Manduca sexta*. Dolzer J, Krannich S, Stengl M., Chem Senses, in press.	59
Kapitel IV.	Cyclic nucleotide-activated currents in cultured olfactory receptor neurons of the hawkmoth *Manduca sexta*. Krannich S, Stengl M., J Neurophysiol, under review.	79
Appendix A.	Hyperpolarization-activated cyclic nucleotide-modulated currents in cultured olfactory receptor neurons of *Manduca sexta*.	101
Appendix B.	Protein kinase C-dependent currents in cultured olfactory receptor neurons of *Manduca sexta*.	103
Appendix C.	Cross-talk of second messenger pathways in cultured olfactory receptor neurons of *Manduca sexta*.	107
Conclusions		111

Erklärung: Eigene Beiträge und veröffentlichte Teile der Arbeit

Der §8, Absatz 3 der Promotionsordnung der naturwissenschaftlichen Fachbereiche der Philipps-Universität Marburg in der Fassung vom 12. April 2000 schreibt vor, dass „die individuellen Leistungen des Doktoranden deutlich abgrenzbar und bewertbar sein müssen“, falls Teile der Dissertation aus gemeinsamer Forschungsarbeit entstanden. Dies betrifft die Kapitel 1, 2 und 3. Die individuellen Beiträge werden im Folgenden näher erläutert.

Kapitel I: **Diacylglycerol activates cation channels in moth olfactory receptor neurons.**
Pézier A, Papaefthymiou C, Krannich S, Acquistapace A, Stengl M, Lucas P.
J Neurophysiol, under review.

- Ausarbeitung, Durchführung und Auswertung von etwa einem Drittel der Experimente[1].

- Veröffentlichung: Die Arbeit wurde bei *Journal of Neurophysiology* eingereicht und wird zur Zeit überarbeitet. Das vorliegende Kapitel entspricht der eingereichten Version des Manuskripts.

Kapitel II: **Diacylglycerol-dependent currents and TRP-like channels in the hawkmoth *Manduca sexta*.**
Krannich S, Ackermann F, Chubanov V, Gudermann T, Stengl M.

- Aufbau des elektrophysiologischen Messstandes in Marburg.
- Ausarbeitung, Durchführung und Auswertung aller elektrophysiologischen Experimente.
- Auswertung der genetischen Untersuchungen[2].
- Verfassen des Manuskriptes in Zusammenarbeit mit Dipl.Biol. F. Ackermann und Prof. Dr. M. Stengl.

- Veröffentlichung: Die Arbeit liegt bisher nur als Manuskript vor. Zur Veröffentlichung der Daten fehlen noch Experimente.

[1] Die Ausarbeitung, Durchführung und Auswertung der Experimente wurde im Rahmen eines einjährigen Aufenthaltes am INRA Versailles/Frankreich in der Arbeitsgruppe von Dr. Philippe Lucas begonnen. Nach Abschluss meines Aufenthaltes wurden die Arbeiten von Dr. Chrisovalantis Papaefthimiou und Dr. Adeline Pézier vollendet. Die Ergebnisse dieser Arbeit sind ebenfalls Teil der Dissertation von Dr. Adeline Pézier (2007).

[2] Die genetischen Untersuchungen wurden in der Arbeitsgruppe von Prof. Dr. Thomas Gudermann (Philipps-Universität Marburg, Fachbereich Medizin - Pharmakologie & Toxikologie) im Rahmen der Diplomarbeit von Frauke Ackermann (2005) unter der Leitung von Prof. Dr. Monika Stengl durchgeführt. Die Abbildungen 6 und 7 im Manuskript wurden von Frauke Ackermann erstellt.

Kapitel III: **Pharmacological investigation of protein kinase C- and cGMP-dependent ion channels in cultured olfactory receptor neurons of the hawkmoth *Manduca sexta*.**
Dolzer J, Krannich S, Stengl M.
Chem Senses, in press.

- Statistische Auswertung eines Teils der Experimente[3].
- Verfassen der Veröffentlichung in Zusammenarbeit mit Prof. Dr. M. Stengl.

- Veröffentlichung: Die Arbeit wurde bei *Chemical Senses* zur Veröffentlichung angenommen.

Kapitel IV: **Cyclic nucleotide-activated currents in cultured olfactory receptor neurons of the hawkmoth *Manduca sexta*.**
Krannich S, Stengl M.
J Neurophysiol, under review.

- Ausarbeitung, Durchführung und Auswertung aller Experimente.
- Verfassen der Veröffentlichung in Zusammenarbeit mit Prof. Dr. M. Stengl.

- Veröffentlichung: Die Arbeit wurde bei *Journal of Neurophysiology* eingereicht. Das vorliegende Kapitel entspricht der überarbeiteten Version des eingereichten Manuskripts, nachdem die Änderungsvorschläge der Gutachter eingearbeitet wurden.

Appendix A: **Hyperpolarization-activated cyclic nucleotide-modulated currents in cultured olfactory receptor neurons of *Manduca sexta*.**

- Ausarbeitung, Durchführung und Auswertung aller Experimente.

Appendix B: **Protein kinase C-dependent currents in cultured olfactory receptor neurons of *Manduca sexta*.**

- Ausarbeitung, Durchführung und Auswertung aller Experimente.

Appendix C: **Cross-talk of second messenger pathways in cultured olfactory receptor neurons of *Manduca sexta*.**

- Ausarbeitung, Durchführung und Auswertung aller Experimente.

[3] Ausarbeitung, Durchführung und Auswertung aller Experimente durch Dr. Jan Dolzer im Rahmen seiner Dissertation (Dolzer 2002). Die von mir statistisch ausgewerteten Daten sind Grundlage der Abbildung 1 in der Veröffentlichung.

Über diese Arbeiten hinaus habe ich während meiner Doktorarbeit im Rahmen eines Aufenthaltes am Institut National de la Recherche Agronomique Versailles (Frankreich) unter der Leitung von Dr. Philippe Lucas an einem thematisch verwandten Projekt mitgearbeitet, das nicht Teil meiner Dissertation ist. Diese Arbeit befasste sich mit der elektrophysiologischen Charakterisierung von Ca^{2+}-aktivierten Cl^--Strömen in den olfaktorischen Rezeptorneuronen der Baumwolleule *Spodoptera littoralis*. Die Ergebnisse dieser Arbeit sind Teil der Dissertation von Dr. Adeline Pézier (2007). Die Arbeit liegt bisher nur als Manuskript vor und ist noch nicht zur Veröffentlichung vorgesehen.

Die Anfertigung der Dissertation in englischer Sprache wurde vom Dekan des Fachbereichs Biologie, Prof. Dr. A. Batschauer, am 29.04.2008 genehmigt.

Zusammenfassung

Für das Auffinden einer Nahrungsquelle, eines Sexualpartners oder einer geeigneten Stelle zur Eiablage orientieren sich Insekten wesentlich nach olfaktorischen Signalen aus ihrer Umwelt. So geben zum Beispiel die Weibchen nachtaktiver Schmetterlingsarten aus paarigen Drüsen am Hinterleibsende ein Gemisch von Pheromone ab. Pheromone sind Duftstoffe mit hormoneller Wirkung, die der innerartlichen Kommunikation dienen. Die Abgabe von Pheromonen durch Weibchen einer Art signalisiert Fortpflanzungsbereitschaft und wirkt auf Männchen der gleichen Art attraktiv. Männchen detektieren diese Lockstoffe mit Hilfe spezialisierter Riechsinneshaare auf ihren Antennen, den Sensilla trichoidea. Jedes Sensillum trichoideum enthält zwei olfaktorische Rezeptorneurone (ORNs), die von Hilfszellen mit Nährstoffen versorgt und vom umgebenden Gewebe elektrisch isoliert werden. Durch ihre Größe, ihre leichte Identifizierbarkeit und ihre Spezifität gegenüber bestimmten Pheromonen sind diese ORNs besonders geeignet für Untersuchungen der olfaktorischen Transduktionskaskaden und ihrer Modulation.
Die vorliegende Dissertation befasst sich mit der Transduktion von Duftstoffen in elektrische Signale und deren Modulation in den ORNs der Baumwolleule *Spodoptera littoralis* und des Tabakschwärmers *Manduca sexta*. Die olfaktorische Transduktion wird durch die Bindung eines Duftstoffes an seinen Rezeptor ausgelöst. Diese intrazelluläre Signalkaskade führt zur Modulation von Ionenkanälen. Ziel der Arbeit war es, mit elektrophysiologischen und pharmakologischen Methoden zu untersuchen, welche Transduktionskaskaden an der Modulation von olfaktorischen Signalen beteiligt sind. Deshalb wurden ORNs in primären Zellkulturen isoliert und kultiviert und anschließend mit Hilfe der *patch-clamp* Technik untersucht. Die *patch-clamp* Technik ermöglicht es, Ionenströme über die gesamte Zellmembran (*whole-cell*) oder durch einzelne Ionenkanäle zu messen (siehe Introduction, Fig. 6).
Die vorliegende Dissertation besteht aus vier Kapiteln, welche zwei Hauptthemen umfassen und je einen Signalweg in den ORNs von Insekten eingehend charakterisieren:

- Elektrophysiologische und pharmakologische Charakterisierung von Diacylglycerol-gesteuerten Ionenkanälen in ORNs von *S. littoralis* (Kapitel 1) und *M. sexta* (Kapitel 2, Appendix C). Außerdem Klonierung von Ionenkanälen, die in *M. sexta* an der olfaktorischen Transduktion beteiligt sein könnten (Kapitel 2).

- Elektrophysiologische und pharmakologische Charakterisierung von Proteinkinase C und zyklisch Nukleotid-gesteuerten Ionenkanälen, die eine Rolle bei der Adaptation der olfaktorischen Transduktion in den ORNs von *M. sexta* spielen. Die Ionenkanäle wurden sowohl auf Einzelkanalebene (Kapitel 3) als auch in *whole-cell* Konfiguration (Kapitel 4, Appendix A - C) untersucht.

Kapitel I: Diacylglycerol aktiviert Kationenkanäle in olfaktorischen Rezeptorneuronen von Nachtschmetterlingen.

Pézier A, Papaefthymiou C, Krannich S, Acquistapace A, Stengl M, Lucas P. Diacylglycerol activates cation channels in moth olfactory receptor neurons. *J Neurophysiol*, under review.

Es wird vermutet, dass Pheromone von G-Protein gekoppelten Rezeptoren in der dendritischen Membran der ORNs detektiert werden. Die Aktivierung des G_q-Proteins stimuliert die Phospholipase C (PLC), welche die sekundären Botenstoffe Inositoltriphosphat (IP_3) und Diacylglycerol (DAG) synthetisiert. In früheren Studien konnte gezeigt werden, dass IP_3 eine bedeutende Rolle bei der olfaktorischen Transduktion in den ORNs von Insekten spielt, während DAG bisher nur als Aktivator von Proteinkinase C (PKC) beschrieben wurde. Es ist deshalb bisher unbekannt, ob DAG ebenfalls bei der olfaktorischen Transduktion von Bedeutung ist. Mit *whole-cell* und *inside-out patch-clamp* Ableitungen konnten in dieser Arbeit erstmals DAG-gesteuerte Ionenkanäle in den ORNs von *S. littoralis* nachgewiesen werden.
In etwa 47 % der kultivierten ORNs führte die Applikation eines DAG-Analogons zur direkten Aktivierung eines bisher unbeschriebenen Kationenstroms. Bei dem charakterisierten Strom handelte es sich stets um einen linearen, unspezifischen Kationenstrom mit einem Umkehrpotential von ca. 0 mV. Der DAG-aktivierte Strom konnte unabhängig von PKC aktiviert und durch Lanthanum blockiert werden. Lanthanum ist ein unspezifischer Blocker von Ca^{2+}-permeablen Kationenkanälen. Dass der DAG-aktivierte Strom tatsächlich Ca^{2+} leitet, zeigte sich auch darin, dass die Reduktion der extrazellulären Ca^{2+}-Konzentration oder die Applikation eines Ca^{2+}/Calmodulin (CaM)-Antagonisten zu einem Anstieg der Stromamplitude führte. Wurde durch einen Inhibitor der DAG-Kinase der Abbau von endogenem DAG in den ORNs verhindert, trat ein konstanter Strom auf, der über die gleichen Eigenschaften wie der DAG-aktivierte Strom verfügte. In Abwesenheit von DAG zeigten die ORNs Spontanaktivität. Inhibition der PLC oder von Ca^{2+}-permeablen Kationenkanälen mittels Lanthanum führte zu verringerter Spontanaktivität. Die direkte Aktivierung von PKC durch Phorbolester führte in den ORNs von *S. littoralis* nicht zum Öffnen von Ionenkanälen.
Unsere Untersuchung zeigt, dass DAG entweder direkt oder über eines seiner Abbauprodukte (z.B. mehrfach ungesättigte Fettsäuren) an der Aktivierung von Ionenkanälen im olfaktorischen System von *S. littoralis* beteiligt ist und deshalb wahrscheinlich eine wichtige Rolle bei der Modulation der olfaktorischen Signaltransduktion spielt. Der beschriebene DAG-aktivierte Strom zeigte ähnliche Eigenschaften wie Ströme durch TRP-Kanäle (*transient receptor potential channels*), die in den sensorischen Systemen von Vertebraten und Invertebraten eine wichtige Rolle spielen.

Kapitel II: Diacylglycerol-abhängige Ströme und TRP-ähnliche Ionenkanäle im Tabakschwärmer *Manduca sexta*.

Krannich S, Ackermann F, Chubanov V, Gudermann T, Stengl M. Diacylglycerol-dependent currents and TRP-like channels in the hawkmoth *Manduca sexta*.

In der vorangegangenen Arbeit konnten von DAG aktivierte Kationenströme in den ORNs von *S. littoralis* nachgewiesen werden, die Ähnlichkeiten mit Strömen durch TRP-Kanäle zeigten. Um zu untersuchen, ob DAG ein genereller Botenstoff in der olfaktorischen Signaltransduktionskaskade von Nachtschmetterlingen

ist, wurden in dieser Arbeit mit *whole-cell patch-clamp* Ableitungen DAG-aktivierte Ströme in den ORNs des Tabakschwärmers *M. sexta* untersucht. Mit molekularbiologischen Methoden wurden außerdem TRP-ähnliche Ionenkanäle aus dem Gehirn- und aus dem Antennengewebe von Puppen und adulten Tieren von *M. sexta* kloniert.

Wie in der vorangegangenen Arbeit in *S. littoralis* konnte eine direkte Aktivierung von Kationenströmen durch DAG in etwa 65 % der kultivierten ORNs von *M. sexta* nachgewiesen werden. Bei dem ausgelösten Strom handelte es sich stets um einen linearen, unspezifischen Kationenstrom mit einem Umkehrpotential von ca. 0 mV. Wie schon bei dem in *S. littoralis* beschriebenen DAG-aktivierten Strom, wurde PKC für die Aktivierung des DAG-aktivierten Stromes von *M. sexta* nicht benötigt. Applikation von Lanthanum und pharmakologische Aktivierung von PKC durch Phorbolester führte zu einer Inhibierung des DAG-aktivierten Stromes. Dass der DAG-aktivierte Strom Ca^{2+} leitet, zeigte sich darin, dass Applikation eines Ca^{2+}/CaM-Antagonisten einen Anstieg der Stromamplitude auslöste. Im Gegensatz zu dem in *S. littoralis* charakterisierten DAG-aktivierten Strom hatte die extrazelluläre Ca^{2+}-Konzentration keinen Einfluss auf die Stromamplitude. Da die DAG-aktivierten Ströme ähnliche Eigenschaften wie Ströme durch TRP-Kanäle aufwiesen, wurde mittels RT-PCR überprüft, ob TRP-ähnliche Ionenkanäle im Gehirn und den Antennen von *M. sexta* exprimiert werden. Tatsächlich konnte ein 400 bp langes cDNA-Fragment (MsTRPLa) im Gehirn von männlichen und weiblichen adulten Tieren nachgewiesen werden, während ein vergleichsweise kurzes cDNA-Fragment (MsTRPLb; 276 bp) nur in den Antennen vorkam. Bei dem MsTRPLb-Fragment handelte es sich offenbar um eine Spleißvariante von MsTRPLa. Das MsTRPLa-Fragment zeigte eine deutliche Sequenzähnlichkeit mit der Porenregion und den umgebenden Transmembrandomänen S5 und S6 des TRPL-Kanals von *D. melanogaster*. Sequenzvergleiche des MsTRPLa-Fragments von *M. sexta* mit TRP-Kanälen aus Säugetieren ergaben die größte Übereinstimmung zu TRPC4-Kanälen. Das in den Antennen exprimierte MsTRPLb-Fragment kodiert keinen funktionsfähigen Ionenkanal, da die Poren-kodierende Sequenz scheinbar durch das Spleißen verloren ging. Dagegen kodiert das im Gehirn exprimierte MsTRPLa-Fragment eine funktionelle Pore, was in *Manganese quench*-Experimenten auch belegt werden konnte.

Unsere Studien über DAG-aktivierte Kationenströme zeigen, dass DAG in verschiedenen Arten von Nachtschmetterlingen ähnliche Ströme aktiviert. Die elektrophysiologischen Eigenschaften der DAG-aktivierten Ströme und die molekularen Eigenschaften der klonierten Ionenkanäle von *S. littoralis* und *M. sexta* deuten darauf hin, dass es sich bei den DAG-gesteuerten Ionenkanälen um TRP-verwandte Ionenkanäle handelt.

Kapitel III: Pharmakologische Untersuchungen von Proteinkinase C und cGMP-abhängigen Ionenkanälen in kultivierten olfaktorischen Rezeptorneuronen des Tabakschwärmers *Manduca sexta*.

Dolzer J, Krannich S, Stengl M. Pharmacological investigation of protein kinase C and cGMP-dependent ion channels in cultured olfactory receptor neurons of the hawkmoth *Manduca sexta*. *Chem Senses*, in press.

Vorangegangene Arbeiten zur olfaktorischen Transduktionkaskade in ORNs von *M. sexta* zeigten, dass die Konzentration von intrazellulärem Ca^{2+} und zyklischem Guanosinmonophosphat (cGMP) abhängig von der Dauer und Stärke eines Pheromonreizes ansteigt und PKC aktiviert wird. Diese Prozesse gehen

mit Mechanismen der Kurz- und Langzeitadaptation einher. In dieser Arbeit wurde in *inside-out patch-clamp* Ableitungen untersucht, ob in den ORNs von *M. sexta* Ionenkanäle vorkommen, die spezifisch über PKC oder cGMP reguliert werden.

Es konnten Ionenkanälen beschrieben werden, von denen einige PKC- bzw. cGMP-abhängig sind. Allerdings wurden viele dieser Ionenkanäle gleichzeitig oder unmittelbar aufeinanderfolgend aktiviert, weswegen es nicht immer möglich war, einzelne Ionenkanäle voneinander getrennt zu charakterisieren. Deshalb wurden die charakterisierten Ionenkanäle nach ihrer Leitfähigkeit in drei Gruppen unterteilt: Ionenkanäle mit geringer (2-20 pS), mittlerer (20-100 pS) oder großer Leitfähigkeit (> 100 pS). Die Ionenkanäle mit geringer Leitfähigkeit wurden nicht detailliert charakterisiert, da sie meist gleichzeitig mit Ionenkanälen mittlerer und großer Leitfähigkeit öffneten. In den wenigen Ableitungen, in denen die Kinetik der Ionenkanäle mit geringer Leitfähigkeit untersucht werden konnte, zeigte sich, dass diese Ionenkanäle für mehrere Sekunden geöffnet werden. Da die Ionenkanäle mit geringer Leitfähigkeit bei positivem Haltepotential Einwärtsströme leiteten und niemals in Anwesenheit von Ni^{2+} öffneten, sind sie wahrscheinlich Ca^{2+}-Kanäle. Bei den Ionenkanälen mit mittlerer Leitfähigkeit handelte es sich hauptsächlich um unspezifische Kationen- und K^{+}-Kanäle mit einem Umkehrpotential von ca. 0 mV und linearer oder rektifizierter Strom-Spannungs-Kennlinie (I-V). Diese Ionenkanäle konnten anhand ihrer Leitfähigkeit, I-V, Pharmakologie und Kinetik in mehrere Unterklassen unterteilt werden. Die Ionenkanäle mit großer Leitfähigkeit wurden nicht ausführlich charakterisiert, da es nicht möglich war, diese Ionenkanäle pharmakologisch zu identifizieren. Offensichtlich handelte es sich bei den Ionenkanälen mit großer Leitfähigkeit um Ca^{2+}-gesteuerte Cl^{-} -Kanäle oder unspezifische Kationenkanäle, die synchronisiert öffneten.

Viele der untersuchten Ionenkanäle öffneten oder schlossen PKC- und cGMP-abhängig. PKC öffnete Ionenkanäle mit mittleren Leitfähigkeiten (40, 60 oder 70 pS), während Ionenkanäle mit kleiner Leitfähigkeit (10 pS) oder großer Leitfähigkeit (>100 pS) geschlossen wurden. Applikation von cGMP führte zur Öffnung von Ionenkanälen mit mittleren und großen Leitfähigkeiten (55, 70 oder >100 pS), während Ionenkanäle mit mittleren Leitfähigkeiten (35 und 40 pS) geschlossen wurden. Diese Ergebnisse zeigen, dass PKC und cGMP verschiedene Ionenkanäle regulieren. Möglicherweise bietet diese differentielle Aktivierung von Ionenkanälen die Grundlage für unterschiedliche Adaptationsmechanismen bei der olfaktorischen Signalverarbeitung, wie z.B. Kurz- und Langzeitadaptation.

Kapitel IV: Zyklische Nukleotide aktivieren Ströme in kultivierten olfaktorischen Rezeptorneuronen des Tabakschwärmers *Manduca sexta*.

Krannich S, Stengl M. Cyclic nucleotide-activated currents in cultured olfactory receptor neurons of the hawkmoth *Manduca sexta*. *J Neurophysiol*, under review.

Vorangegangene Studien erlaubten nur eine sehr allgemeine Charakterisierung der zyklisch Nukleotid-abhängigen Ionenkanäle in den ORNs von *M. sexta*. In diesem Kapitel wurden zyklisch Nukleotid-abhängige Ströme näher charakterisiert. Im Unterschied zur vorangegangenen Arbeit wurden in dieser Arbeit *whole-cell patch-clamp* Ableitungen verwendet, bei denen keine einzelnen Ionenkanäle, sondern Ströme über die gesamte Zellmembran gemessen werden.

In etwa 81 % der kultivierten ORNs konnten Ionenströme nachgewiesen werden, die spezifisch von den zyklischen Nukleotiden Adenosinmonophosphat (cAMP) oder cGMP aktiviert wurden. Bei den charakterisierten Strömen handelte es sich stets um lineare, unspezifische Kationenströme mit einem Umkehrpotential von ca. 0 mV. Die cGMP-aktivierten Ströme zeigten eine stärkere Abhängigkeit von der extrazellulären Ca^{2+}-Konzentration und von Ca^{2+}/CaM, als die cAMP-aktivierten Ströme. Applikation von Lanthanum inhibierte oder potenzierte die cAMP- und cGMP-abhängigen Ströme, abhängig von der eingesetzten Konzentration. Die verwendeten Ca^{2+}-Kanal Blocker Ni^{2+} und Zn^{2+} inhibierten einen Teil der cAMP- und cGMP-abhängigen Ströme. Außerdem wurde erstmalig ein Strom ($I_{Ca(cAMP)}$) nachgewiesen, der von cAMP aktiviert und von Proteinkinasen moduliert wird. Die Kinetik dieses Stromes zeigte die typischen Merkmale eines spannungsabhängigen LVA Ca^{2+}-Stromes (*low voltage-activated Ca^{2+} current*). Die genaue Funktion dieses Stromes ist bislang unbekannt.

Insgesamt konnten mindestens drei verschiedene Unterklassen von zyklisch Nukleotid-aktivierten Ionenkanälen in den ORNs von *M. sexta* charakterisiert werden, von denen einer von cAMP- und zwei von cGMP gesteuert wurden. Da die beschriebenen Ionenkanäle von Ca^{2+} differentiell moduliert wurden, könnten sie in unterschiedliche Adaptationsmechanismen bei der olfaktorischen Signalverarbeitung eingebunden sein.

Introduction

List of Abbreviations	13
Introduction	15
The olfactory system of moths	16
The insect olfactory transduction pathway	17
The lipid second messenger pathway	18
The role of cyclic nucleotides in olfactory transduction	18
Ion channels involved in olfactory transduction pathways	19
- The transient receptor potential (TRP) channel family	19
- Cyclic nucleotide-gated (CNG) channels	20
Aims of the PhD thesis	21
The patch-clamp technique	22
References	23

List of Abbreviations

(8b)cAMP	(8-bromo) cyclic adenosine monophosphate
(8b)cGMP	(8-bromo) cyclic guanosine monophosphate
AC	adenylyl cyclase
CaCC	Ca^{2+}-activated Cl^- channel
CaM	Calmodulin
CAN	Ca^{2+}/CaM-activated channel
CNBD	cyclic nucleotide-binding domain
CNG(A/B)	cyclic nucleotide-gated channel (subunit A and B)
DAG	1,2-diacylglycerol
DGK	diacylglycerol kinase
DGL	diacylglycerol lipase
DOG	1,2-dioctanoyl-*sn*-glycerol
ER	endoplasmic reticulum
GPCR	G-protein-coupled receptor
HCN	hyperpolarization-activated cyclic nucleotide-modulated channel
Ih	hyperpolarization-activated current
IP_3(R)	inositol 1,4,5-triphosphate (receptor)
I-V	current-voltage relation
GC-D	guanylyl cyclase D
LVA	low voltage-activated current
PA	phosphatidic acid
PDE	phosphodiesterase
PIP_2	phosphatidylinositol 4,5-bisphosphate
PKA(C/G)	protein kinase A (protein kinase C or G)
PLC	phospholipase C
PMA	phorbol 12-myristate-13-acetate
PUFA	poly-unsaturated fatty acids
OBP	odorant-binding protein
OR	odorant receptor
ORN	olfactory receptor neuron
RT-PCR	reverse transcription - polymerase chain reaction
TRP(C)	(classical) transient receptor potential channel
W-7	N-(6-aminohexyl)-5-chloro-1-naphthalenesulfonamid

Introduction

The olfactory system plays a central role for the intra- and interspecific recognition and communication in vertebrates and invertebrates. All olfactory systems comprise specific olfactory organs, odorant receptors, and olfactory transduction pathways that allow the detection of odorants.

Particularly well-studied is the olfactory system of moths. Male moths can detect and analyze almost single molecules of the con-specific female sex-pheromone over distances of one km and more (Hildebrand 1995; Kaissling 2004). After detection of the pheromone, the pheromone stimulus is transformed into neural activity that is further processed in specific olfactory brain centers to elicit behavioral responses (Jacquin-Joly and Lucas 2005). Accordingly, previous studies focused on pheromone-dependent olfactory transduction pathways. Pheromone-independent olfactory transduction pathways, however, remained largely unexplored. In the first part of my PhD thesis, a novel olfactory transduction pathway in the moths *Spodoptera littoralis* (Boisduval) (Lepidoptera: Noctuidae; Fig. 1A) and *Manduca sexta* (Johannson) (Lepidoptera: Sphingidae; Fig. 1B) has been investigated that might be involved in pheromone-independent olfactory transduction pathways.

Since the moth olfactory system is permanently exposed to multiple odorants in the environment, it needs to filter out the relevant (sensitization) and suppress the irrelevant odorants (adaptation). Thus, in the second part of my PhD thesis, it was investigated whether transduction pathways in the olfactory system of *M. sexta* are involved in sensitization and adaptation.

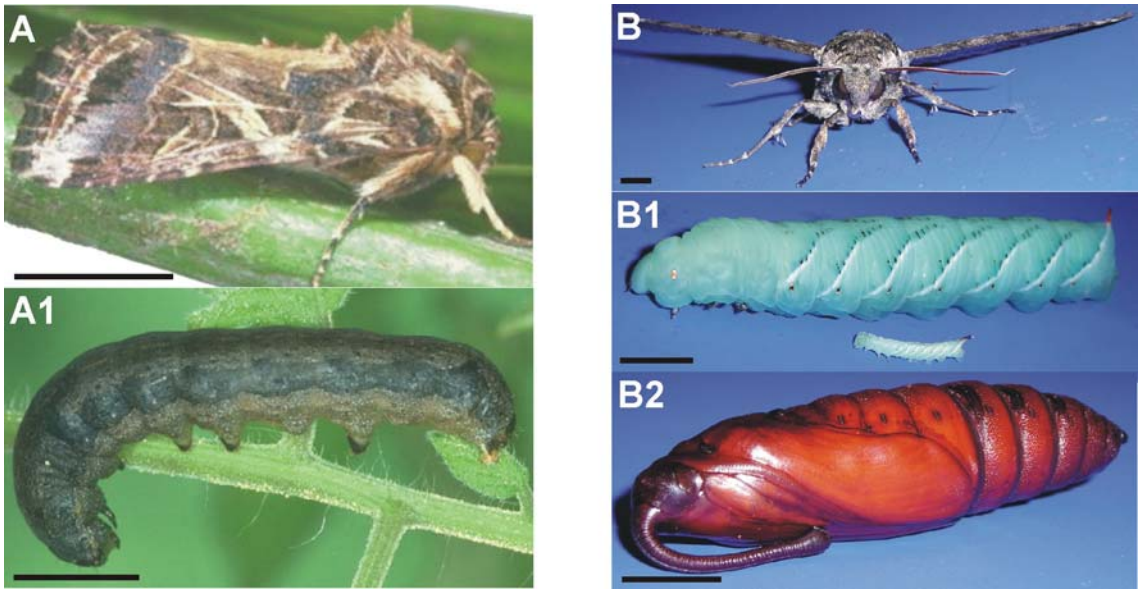

Figure 1 The moth (**A**) and larva (**A1**) of *Spodoptera littoralis* (Boisduval) (Lepidoptera: Noctuidae) (www.inra.fr/internet/Produits/HYPPZ/RAVAGEUR/6spolit.htm). The moth (**B**), the 1st and 4th instar larvae (**B1**), and pupa (**B2**) of *Manduca sexta* (Johannson) (Lepidoptera: Sphingidae). Scale bars 1 cm.

The olfactory system of moths

The two antennae are the principal olfactory organ of a moth. Each antenna consists of three segments, the basal scapus and pedicellus, and the flagellum. The flagellum forms the main part of the antenna and comprises a species-specific number of annuli. Each annulus carries multiple mechano- or chemosensory hair structures on its frontal and lateral side, the sensilla (Fig. 2A). The rear side of the annulus is covered with scales (Sanes and Hildebrand 1976, Lee and Strausfeld 1990).

The antenna of the male moth contains a large number of specialized olfactory sensilla, the sensilla trichoidea, which exclusively perceive the female pheromone blend. The sensilla trichoidea of *M. sexta* have a length of about 70 to 600 µm and are arranged in basket case-like structures (Fig. 2A; Lee and Strausfeld 1990). The cuticle of each sensillum trichoideum has many tiny pores through which the odorants enter the sensillum trichoideum. The lumen of each sensillum trichoideum contains the sensillum lymph and the dendrites of two bipolar olfactory receptor neurons (ORNs; Sanes and Hildebrand 1976; Ljungberg et al. 1993). At the ORN dendrites, the quality, quantity, and temporal pattern of odorants are converted into receptor potentials. Both ORNs are enclosed by three accessory cells - the trichogen, tormogen, and thecogen cell. Septate junctions form tight contacts between the accessory cells and the ORNs. The trichogen and tormogen cells secrete the cuticle and the sensillum lymph, while the thecogen cell encapsulates the somata of the two ORNs. Together, the three accessory cells separate

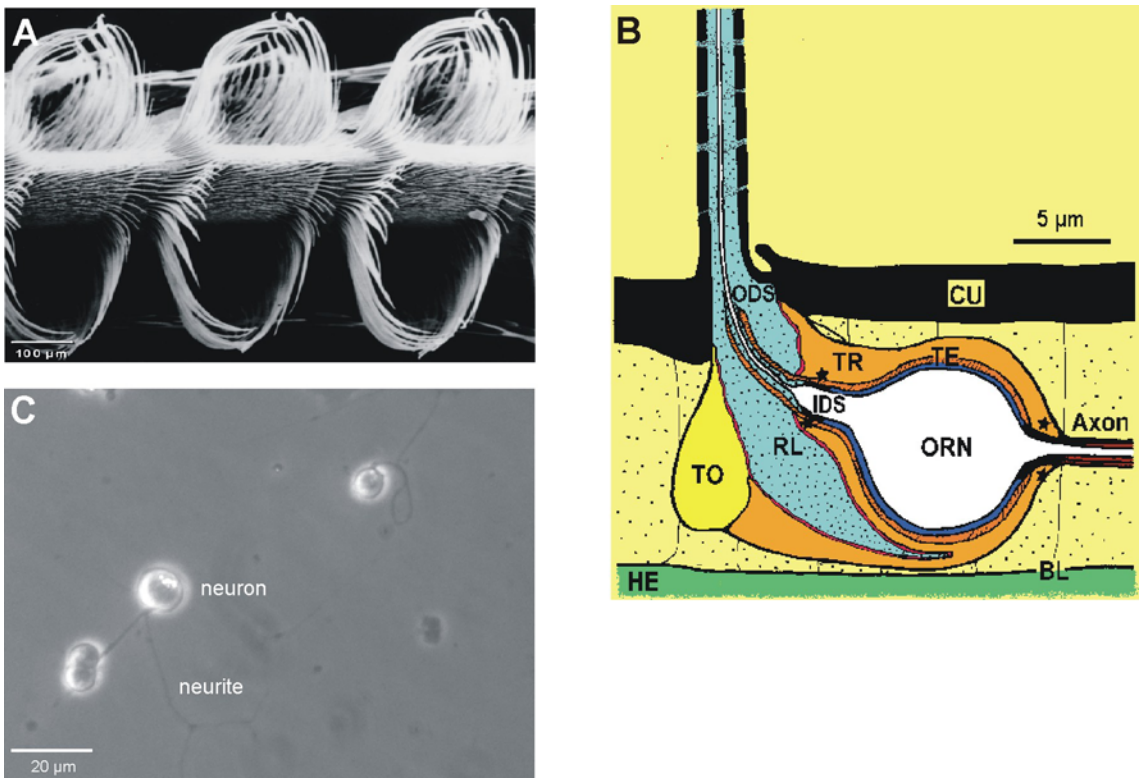

Figure 2 The olfactory system of moths. (**A**) Electron microscopic image of a male *M. sexta* antenna. The pheromone-sensitive sensilla trichoidea form basket case-like structures on the frontal and lateral side of the flagellum (Lee and Strausfeld 1990). (**B**) Two ORNs project into each sensillum trichoideum. BL: basal lamina, CU: cuticle, HE: hemolymph, IDS: inner dendritic segment, ODS: outer dendritic segment, ORN: olfactory receptor neuron, RL: receptor lymph cavity, TE: thecogen cell, TO: tormogen cell, TR: trichogen cell. The asterisks mark zones of septate junctions (after Keil 1989). (**C**) A 10 day-old primary cell culture of *M. sexta* antennae showing ORNs and their neurites.

the sensillum lymph from the hemolymph (Fig. 2B). As opposed to the hemolymph, the sensillum lymph contains a high concentration of odorant-binding proteins and K^+ (Kaissling 2004). The axons of the ORNs propagate the olfactory information to the primary olfactory center of the moth, the antennal lobes. In the antennal lobes, the olfactory information is further processed (Christensen and Hildebrand 2002).

The insect olfactory transduction pathway

Lipophilic odorant molecules, such as pheromones, cannot cross the aqueous sensillum lymph. Thus, odorant molecules have to bind to specific transport proteins, the pheromone- and general odorant-binding proteins, to traverse the sensillum lymph. These odorant-binding proteins (OBP) serve multiple functions, such as to solubilize, stabilize and concentrate odorant molecules (Kaissling 2004). It has been proposed that odorant molecules form complexes with OBPs to get transported to their olfactory receptors (OR) in the dendritic membrane of the ORN. Insect ORs belong to the class of G-protein-coupled receptors (GPCRs). GPCRs are characterized by the presence of seven transmembrane domains with an extracellular N-terminus (Fig. 4). Recent work showed that insect ORs have only weak sequence similarity to vertebrate GPCRs and possess an inverted seven transmembrane topology with an intracellular N-terminus (Fig. 3; Bargmann 2006).

Data from several groups suggest the following model of pheromone transduction in moths: Odorant molecules bind to ORs that interact with a G_q-protein. G-proteins are heterotrimeric proteins that consist of an α, β and γ subunit. After odorant binding, the α subunit of the G_q-protein activates phospholipase Cβ (PLCβ). The PLCβ hydrolyzes phosphatidylinositol 4,5-bisphosphate (PIP_2) into inositol 1,4,5-triphosphate (IP_3) and

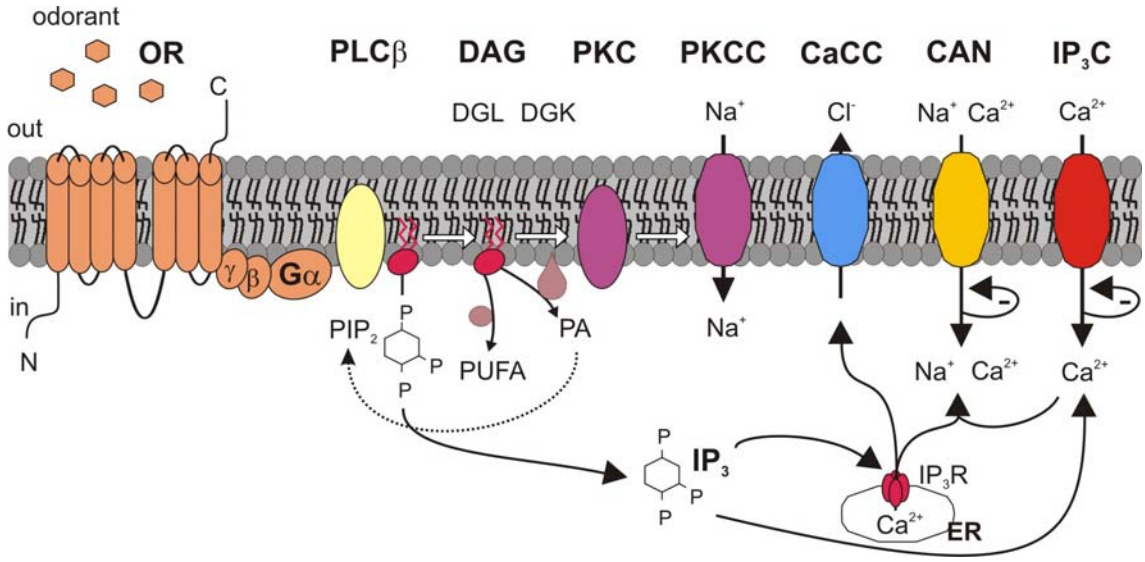

Figure 3 The IP_3 and DAG signaling pathway in insect ORNs. Odorants bind to G-protein-coupled odorant receptors (OR) that interact with phospholipase Cβ (PLCβ). PLCβ hydrolyzes phosphatidylinositol 4,5-bisphosphate (PIP_2) into inositol 1,4,5-triphosphate (IP_3) and diacylglycerol (DAG). IP_3 triggers transient Ca^{2+} influx through IP_3-dependent channels (IP_3C) in the cell membrane. In addition, IP_3 binds to IP_3 receptors (IP_3R) and releases Ca^{2+} from the endoplasmic reticulum (ER). The intracellular increase of Ca^{2+} in turn leads to the activation of Ca^{2+}/CaM-activated cation channels (CAN) and Ca^{2+}-activated Cl^- channels (CaCC). DAG activates protein kinase C (PKC), which then acts on PKC-dependent cation channels (PKCC). DAG is metabolized by either DAG lipase (DGL), which hydrolyzes DAG to poly-unsaturated fatty acids (PUFA), or by DAG kinase (DGK), which phosphorylates DAG to phosphatidic acid (PA). PA represents the first step in PIP_2 recycling.

1,2-diacylglycerol (DAG). The increase in IP_3 triggers a transient Ca^{2+} influx through IP_3-dependent Ca^{2+} channels in the cell membrane. Furthermore, IP_3 may bind to IP_3 receptors (IP_3R) in the endoplasmic reticulum and mediate Ca^{2+}-release from intracellular stores (Taylor et al. 2004). The Ca^{2+} increase in turn leads to the sequential activation of different Ca^{2+}-dependent channels and the depolarization of the ORN (Fig. 3; Ache and Zhainazarov 1995).

The lipid second messenger pathway

When PLCβ converts PIP_2 into IP_3, it simultaneously produces the glycerol derivative DAG (Fig. 3). Typically, the membrane-bound DAG and Ca^{2+} together activate cytosolic protein kinase C (PKC; Newton 2004). The PKC is then tethered to the plasma membrane. The activated PKC and other GPCR kinases phosphorylate the ORs and thereby terminate the odorant signal transduction pathway. Within seconds, DAG is metabolized and PKC returns to the cytosol (Becker and Hannun 2005). DAG can be metabolized by either DAG lipase (DGL), which hydrolyzes DAG to poly-unsaturated fatty acids (PUFA), or by DAG kinase (DGK), which phosphorylates DAG to phosphatidic acid (PA; Fig. 3). The conversion of DAG into PA is thought to be the main degradation pathway of DAG and at the same time represents the first step in PIP_2 recycling (Luo et al. 2004). DAG, its metabolites (PUFA), and/or the reduction of PIP_2 levels following PLCβ activation mediate the activation of transient receptor potential channels (see below).

The role of cyclic nucleotides in olfactory transduction

IP_3 and DAG are important signaling molecules in the olfactory transduction pathway, but are probably not involved in the sensitization or adaptation of the ORNs. Sensitization and adaptation are adjustments of sensitivity in response to adequate stimulation that change the dynamic range of an ORN without loss of resolution. Accordingly, sensitivity adjustments are the first steps in the processing of olfactory information. Previous studies in moths showed that pheromone stimuli induce slow and delayed increases in the intracellular cyclic guanosine monophosphate (cGMP) concentration in antennal homogenates (Ziegelberger et al. 1990; Boekhoff et al. 1993). This finding suggests that cGMP is not involved in the principal olfactory transduction pathway, but rather plays a role for long-term olfactory adaptation. The cGMP-rises appear to affect both protein kinase G (PKG; Fig. 4; Boekhoff et al. 1993) and cGMP-dependent delayed rectifier potassium channels (Zufall et al. 1991; Stengl et al. 1992). In moths, brief pheromone stimulation does not cause increases in the intracellular concentration of cyclic adenosine monophosphate (cAMP; Ziegelberger et al. 1990). Thus, cAMP is probably not involved in the moth pheromone transduction pathway.

In vertebrates, however, the principal olfactory transduction pathway includes cAMP (Kaupp and Seifert 2002). In vertebrate ORNs, odorant molecules usually bind to GPCRs that interact with a G_{olf}-protein. The α subunit of the G_{olf}-protein activates adenylyl cyclase III (ACIII) that then synthesizes cAMP (Fig. 4). A small subset of the vertebrate ORNs lack GPCRs, but instead expresses the ORN-specific guanylyl cyclase D (GC-D). The GC-D is a receptor-type GC that is possibly activated by peptide hormones. Activation of GC-D leads to an increase of the cGMP concentration in the ORNs (Fig. 4). Both cAMP and cGMP open cyclic nucleotide-gated (CNG) channels (see below) and, thereby, induce a rapid increase of the intracellular Ca^{2+} concentration. Ca^{2+} in turn leads to the activation of Ca^{2+}-dependent Cl^- channels and thus amplifies the depolarization. Furthermore, Ca^{2+} activates phosphodiesterases that hydrolyze

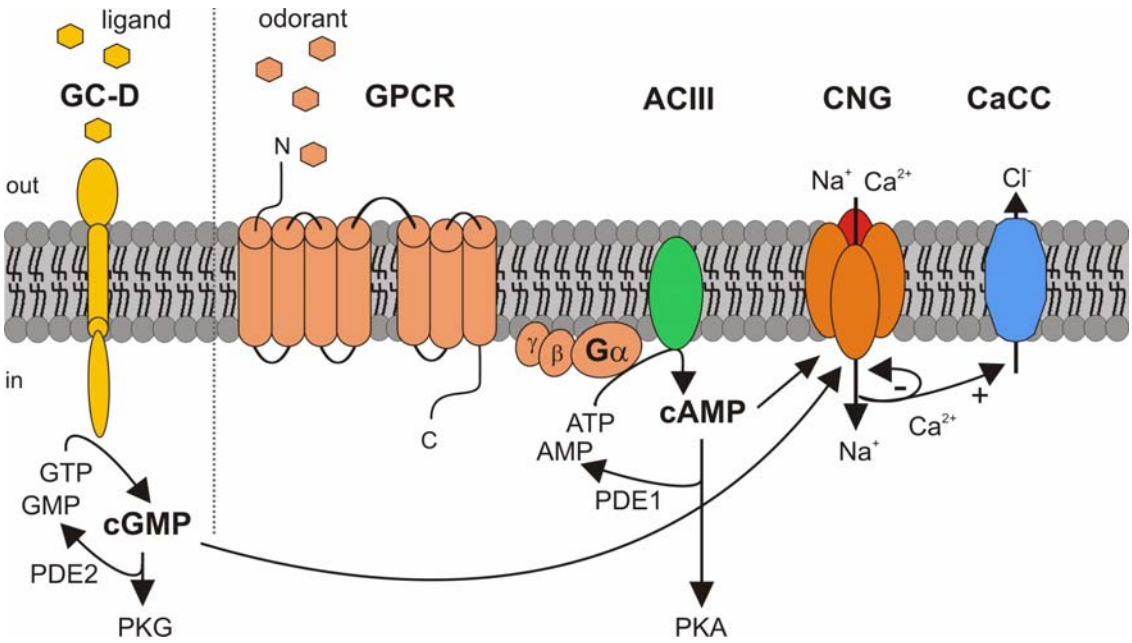

Figure 4 The cAMP- and cGMP signaling pathway in vertebrate ORNs. Odorants bind to G-protein-coupled odorant receptors (GPCR) that interact with adenylyl cyclase III (ACIII). ACIII activation leads to an increase of the cyclic adenosine monophosphate (cAMP) concentration. The ligand-mediated activation of receptor guanylyl cyclase D (GC-D) increases the cyclic guanosine monophosphate (cGMP) concentration. Both cAMP and cGMP in turn directly activate cyclic nucleotide-gated channels (CNG) and the respective protein kinases (PKA, PKG). The activation of CNG channels increases the intracellular Ca^{2+} concentration that subsequently mediates the activation of Ca^{2+}-activated Cl^- channels (CaCC). The Ca^{2+} increase stimulates the hydrolysis of cAMP by CaM-dependent phosphodiesterase (PDE1), and cGMP by cGMP-regulated phosphodiesterase (PDE2). Both pathways are present in different subsets of vertebrate ORNs (indicated by the dashed line).

cAMP and cGMP and thereby terminate the odorant signal transduction pathway (Fig. 4; Kaupp and Seifert 2002).

Ion channels involved in olfactory transduction pathways

Lipid second messengers and cyclic nucleotides act on specific ion channels that differ in their gating mechanism (opening and closing), voltage dependence, ion permeability, conductance, and regulation. Certain ion channels are directly activated by voltage-changes or ligand-binding, while others are indirectly activated by second messengers (Hille 2001). In the following, two families of voltage- and ligand-gated ion channels are described in more detail that are activated either by lipid second messengers such as DAG or by the cyclic nucleotides cAMP and cGMP.

The transient receptor potential (TRP) channel family

Recent studies indicated that lipid messenger such as DAG or its metabolites (PUFA) act on TRP channels (Hardie 2003). TRP channels were initially identified in the *Drosophila melanogaster* phototransduction pathway (dTRP and TRPL). On the basis of sequence similarity to dTRP and TRPL, a large number of TRP channel subfamilies have been identified in vertebrates and invertebrates. The best-studied subfamily includes the classical TRP (TRPC) channels. Based on sequence homology and functional similarity, the seven members of the TRPC channel family can be divided into four subgroups:

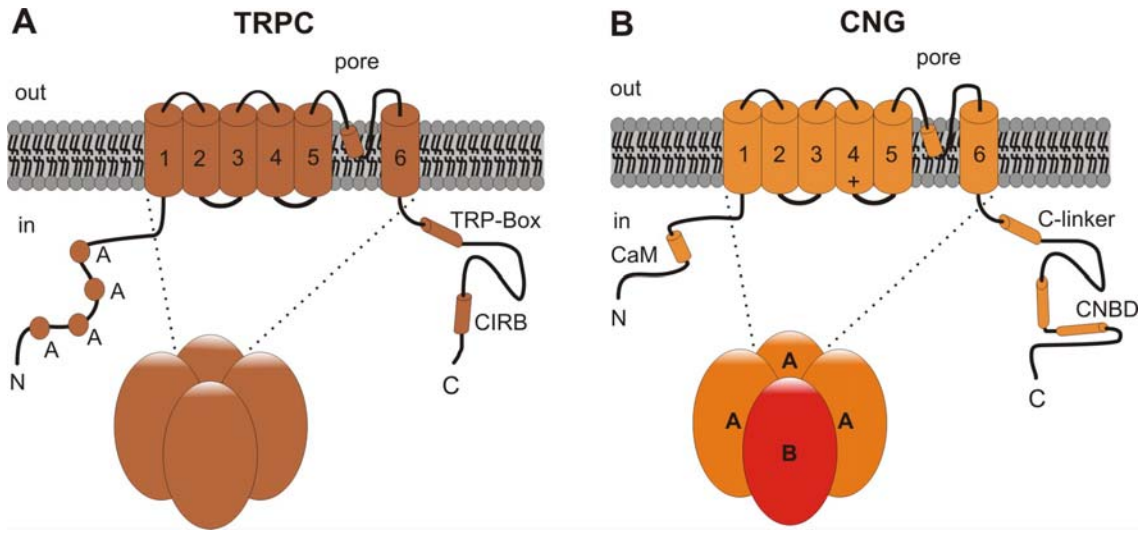

Figure 5 Ion channel structure. (**A**) TRP channels are homo- or heterotetrameric channels. Each TRP channel subunit consists of six transmembrane-spanning segments (1-6). The pore region is located between segments 5 and 6. Both the N- and C-termini localize to the cytoplasmic side of the membrane. The N-terminus contains ankyrin-like repeats (A). The C-terminus contains a region (CIRB) that binds CaM and IP_3R, as well as a conserved region of unknown function called TRP-Box. (**B**) Olfactory CNG channels are heterotetrameric channels composed of three A subunits (CNGA) and a B subunit (CNGB). All of these subunits consist of six transmembrane-spanning segments (1-6). The pore region is located between segments 5 and 6. Segment 4 comprises a charged sequence motif (+). Both the N- and C-termini localize to the cytoplasmic side of the membrane. The primary subunits CNGA2 and A4 contain a CaM-binding side near the N-terminus. All CNG channel subunits contain a cyclic nucleotide-binding domain (CNBD) and a C-linker at the C-terminus.

TRPC1, TRPC2, TRPC4/5, and TRPC3/6/7 (Minke and Cook 2002). TRPC2 (Lucas et al. 2003) and TRPC3/6/7 (Hofmann et al. 1999; Okada et al. 1999) are known to directly depend on DAG. At least TRPC2 localizes to the vertebrate olfactory system (Lucas et al. 2003).

TRP channel subunits form tetramers with a cation-permeable pore (Fig. 5A; Minke and Cook 2002). Each TRP tetramer is composed of either equal subunits (homotetramer, e.g. TRPC4) or different subunits from two or more related subgroup members (heterotetramer, e.g. TRPC4 and TRPC5). Each TRP channel subunit has six transmembrane segments with the pore region between the transmembrane segments 5 and 6, and intracellular C- and N-termini. The N-terminus contains three to four ankyrin-like repeats that are necessary for protein-protein interactions. The C-terminus contains the TRP-Box, a conserved region of unknown function. Terminal to the TRP-Box, all TRPC channel subunits have a calmodulin (CaM) and IP_3R binding domain (CIRB; Fig. 5A). Studies on the CIRB domain suggested that Ca^{2+}, CaM, and IP_3R play a complex and competitive role in the regulation of the basal activity of TRPC channels. The exact role of IP_3R is still unknown (Trebak et al. 2003). TRP channels are structurally related to the superfamily of voltage-gated K^+-channels, although they lack a voltage sensor in the transmembrane segment 4. Functionally, all TRP channels are categorized as non-selective cation channels with diverse ion permeability, but some TRP channels are highly selective for Ca^{2+} (Minke and Cook 2002).

Cyclic nucleotide-gated (CNG) channels

Several studies have characterized CNG channels in the vertebrate olfactory system. Olfactory CNG channels are directly activated by the cyclic nucleotides cAMP or cGMP, and conduct monovalent cations and Ca^{2+}. The Ca^{2+} influx through CNG channels probably causes a negative feedback via Ca^{2+}/CaM and, therefore, mediates adaptation (Kaupp and Seifert 2002).

All CNG channels form heterotetrameric complexes composed of three A subunits (CNGA1 to CNGA4) and a B subunit (CNGB1 or CNGB3). Olfactory CNG channels are composed of two principal CNGA2 subunits, a modulatory CNGA4 subunit, and a modulatory CNGB1b subunit (Fig. 5B; Bradley et al. 2001). Each CNG channel subunit consists of six transmembrane segments with a pore region between the transmembrane segments 5 and 6, and intracellular N- and C-termini. The C-terminus contains the C-linker region that mediates the binding of cyclic nucleotides to the gating machinery inside the pore. Terminal to the C-linker localizes the cyclic nucleotide-binding domain (CNBD). The CNBD determines the ligand sensitivity of the CNG channel. The N-terminus of the CNGA2 subunit contains a CaM-binding domain that interacts with the CNBD region on the C-terminus (principal subunit). The CNGA4 and CNGB1b subunits contain an IQ-motif that also binds CaM, and thus modulates the kinetic of Ca^{2+}/CaM-mediated inhibition (modulatory subunit). All CNG channels have a voltage sensor in the transmembrane segment 4 and are structurally related to the superfamily of voltage-gated K^+-channels, but their voltage-dependency is weak (Kaupp and Seifert 2002).

There are only few studies that have characterized insect olfactory CNG channels. Insect CNG channels have been found in the olfactory systems of *Drosophila melanogaster* (Baumann et al. 1994; Miyazu et al. 2000), *Apis mellifera* (Gisselmann et al. 2003), and *Heliothis virescens* (Krieger et al. 1999). Apart from the *D. melanogaster* CNG channels, the identified insect CNG channels belong to the subfamily of hyperpolarization-activated cyclic nucleotide-modulated (HCN) channels. As other CNG channels, HCN channels are directly activated by cAMP and cGMP, but open at hyperpolarizing and close at depolarizing potentials. HCN channels conduct a mixed current of monovalent cations, but prefer K^+ over Na^+. Divalent cations slightly permeate, but do not block HCN channels. The current through HCN channels is usually termed hyperpolarization-activated current (I_h) and contributes to the resting potential of neurons (Robinson and Siegelbaum 2003).

Aims of the PhD thesis

In moth ORNs, IP_3 appears to be the principal second messenger of the olfactory transduction pathway. However, previous *in vitro* (Zufall and Hatt 1991) and *in vivo* (Maida et al. 2000; Pophof and van der Goes van Naters 2002) studies suggested that DAG might also gate ion channels in moth ORNs. DAG is presumed to activate ion channels via interaction with PKC. Accordingly, in pheromone-sensitive ORNs of the moth *Antheraea polyphemus*, the PKC concentration increased upon pheromone application, and this increase appeared to be triggered by DAG (Maida et al. 2000). In the ORNs of *M. sexta*, PKC was shown to activate a Ca^{2+}-independent cation current (Stengl 1993). In vertebrates and *D. melanogaster*, however, DAG was shown to directly mediate the activation of TRP channels.

- Thus, the first aim of my PhD thesis was to investigate whether DAG activates ion channels in cultured moth ORNs directly or indirectly via PKC (Chapter 1, 2), and whether DAG activates ion channels that belong to the TRP channel family (Chapter 2).

Besides IP_3 and DAG, cyclic nucleotides may also process olfactory information. Previous biochemical (Ziegelberger et al. 1990; Boekhoff et al. 1993) and electrophysiological (Redkozubov 2000; Flecke et al. 2006) studies in moths suggested that cGMP is not involved in the principal olfactory transduction pathway. Accordingly, cGMP rather appears to play a role for long-term olfactory adaptation. Because pheromone stimulation did not elicit an increase of the cAMP concentration, cAMP is probably not involved in moth olfactory transduction. In vertebrates and invertebrates, both cAMP and cGMP were shown to directly activate ion channels that belong to the CNG channel family.

- Thus, the second aim of my PhD thesis was to investigate whether both cAMP and cGMP directly activate ion channels in cultured moth ORNs, and whether these channels correspond to CNG channels (Chapter 3, 4).

The patch-clamp technique

In the moth antennae, the ORNs are surrounded by accessory cells and, therefore, are not amenable to intracellular recordings. To record the activity of ion channels involved in olfactory transduction pathways, the ORNs were isolated in a long-term primary cell culture system (Fig. 2C; Stengl and Hildebrand 1990; Lucas and Nagnan Le-Meillour 1997). Then, the ion channels of single ORNs were characterized with the patch-clamp technique (Fig. 6; Hamill et al. 1981). The patch-clamp technique was developed by Neher and Sakmann who received the Nobel Prize in physiology or medicine for their work (1992). The method allows to control the membrane potential across a small membrane patch to measure the ionic current necessary to maintain the membrane potential. By patch-clamp recordings, it was possible to identify and characterize several types of ion channels in cultured moth ORNs (Zufall et al. 1991; Stengl et al. 1992; Stengl 1993, 1994; Lucas and Nagnan Le-Meillour 1997).

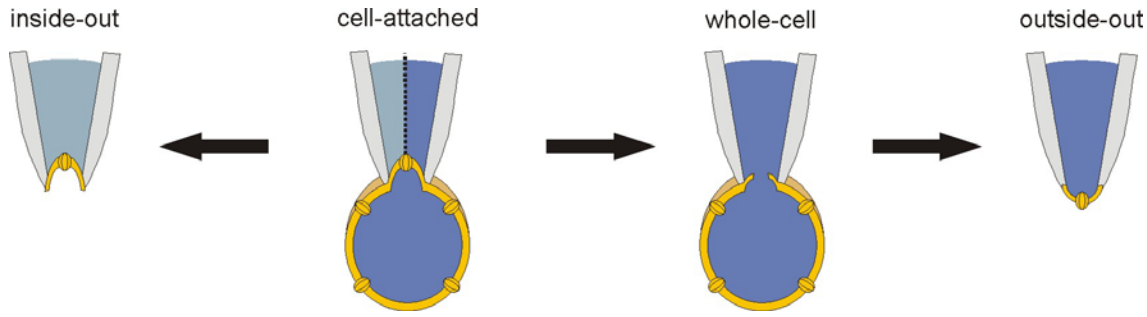

Figure 6 Patch-clamp configurations. When a firepolished glass electrode is sealed to the cell membrane, single channels can be recorded (**cell-attached configuration**). Subsequent retraction of the electrode excises the membrane patch (**inside-out configuration**). The cytoplasmic part of the patch faces the bath solution and single channels can be recorded. In the cell-attached configuration, it is also possible to apply gentle suction and thus destroy the patch under the electrode (**whole-cell configuration**). The inside of the cell now faces the electrode solution and the currents through the entire cell membrane are measured. Subsequent retraction of the electrode results in a small patch (**outside-out configuration**). The inside of the cell still faces the electrode solution and single channels can be recorded.

References

Wherever applicable, the number of citations was limited to available reviews. For more detailed citations see chapters and appendices.

Ache BW, Zhainazarov A (1995). Dual second-messenger pathways in olfactory transduction. *Curr Opin Neurobiol* 5:461-466.

Bargmann CI (2006). Comparative chemosensation from receptors to ecology. *Nature* 444: 295-301.

Baumann A, Frings S, Godde M, Seifert R, Kaupp UB (1994). Primary structure and functional expression of a *Drosophila* cyclic nucleotide-gated channel present in eyes and antennae. *EMBO J* 13: 5040-5050.

Becker KP, Hannun YA (2005). Protein kinase C and phospholipase D: intimate interactions in intracellular signalling. *CMLS* 62: 1448-1461.

Boekhoff I, Seifert E, Goggerle S, Lindemann M, Kruger BW, Breer H (1993). Pheromone-induced second-messenger signaling in insect antennae. *Insect Biochem Mol Biol* 23: 757-762.

Bradley J, Reuter D, Frings S (2001). Facilitation of calmodulin-mediated odor adaptation by cAMP-gated channel subunits. *Science* 294: 2176-2178.

Christensen TA, Hildebrand JG (2002). Pheromonal and host-oder processing in the insect antennal lobe: how different? *Curr Opin Neurobiol* 12: 393-399.

Gisselmann G, Warnstedt M, Gamerschlag B, Bormann A, Marx T, Neuhaus EM, Stoertkuhl K, Wetzel CH, Hatt H (2003). Characterization of recombinant and native Ih-channels from *Apis mellifera*. *Insect Biochem Mol Biol* 33: 1123-1134.

Hamill OP, Marty A, Neher E, Sakmann B, Sigworth FJ (1981). Improved patch-clamp techniques for high-resolution current recording from cells and cell-free membrane patches. *Pflugers Arch*, 391(2), 85-100.

Hardie RC (2003). Regulation of TRP channels via lipid second messengers. *Annu Rev Physiol* 65:735-759.

Hildebrand JG (1995). Analysis of chemical signals by nervous systems. *Proc Natl Acad Sci USA* 92: 67-74.

Hille B (2001). Ion channels of excitable membranes. 3rd edition, Sinauer, Sunderland, USA, pp. 663-723.

Hofmann T, Obukhov AG, Schaefer M, Harteneck C, Gudermann T, Schultz G (1999). Direct activation of human TRPC6 and TRPC3 channels by diacylglycerol. *Nature* 397: 259-263.

Jacquin-Joly E, Lucas P (2005). Pheromone reception and transduction: mammals and insects illustrate converging mechanisms across phyla. *Curr Topics in Neurochem* 4: 75-105.

Kaissling KE (2004). Physiology of pheromone reception in insects (an example of moths). *ANIR* 6: 73-91.

Kaupp UB, Seifert R (2002). Cyclic nucleotide-gated ion channels. *Physiol Rev* 82: 769-824.

Keil TA (1989). Fine structure of the pheromone-sensitive sensilla on the antenna of the hawkmoth, *Manduca sexta*. *Tiss Cell* 21: 139-151.

Krieger J, Strobel J, Vogl A, Hanke W, Breer H (1999). Identification of a cyclic nucleotide- and voltage-activated ion channel from insect antennae. *Insect Biochem Mol Biol* 29: 255-267.

Lee JK, Strausfeld N (1990). Structure, distribution and number of surface sensilla and their receptor cells on the olfactory appendage of the male moth *Manduca sexta*. *J Neurocytol* 19: 519-538.

Ljungberg H, Anderson P, Hansson BS (1993). Physiology and morphology of the pheromone-specific sensilla on the antennae of the male and female *Spodoptera littoralis* (Lepidoptera: Noctuidae). *J Insect Physiol* 39: 253-260.

Lucas P, Nagnan-Le Meillour P (1997). Primary culture of antennal cells of *Mamestra brassicae*: morphology of cell types and evidence for biosynthesis of pheromone-binding proteins *in vitro*. *Cell Tiss Res* 289: 375-382.

Lucas P, Ukhanov K, Leinders-Zufall T, Zufall F (2003). A diacylglycerol-gated cation channel in vomeronasal neuron dendrites is impaired in TRPC2 mutant mice: mechanism of pheromone transduction. *Neuron* 40: 551-561.

Luo B, Regier DS, Prescott SM, Topham MK (2004). Diacylglycerol kinases. *Cell Signal* 16: 983-989.

Maida R, Redkozubov A, Ziegelberger G (2000). Identification of PLC beta and PKC in pheromone receptor neurons of *Antheraea polyphemus*. *Neuroreport* 11, 1773-1776.

Minke B, Cook B (2002). TRP channel proteins and signal transduction. *Physiol Rev* 82: 429-472.

Miyazu M, Tanimura T, Sokabe M (2000). Molecular cloning and characterization of a putative cyclic nucleotide-gated channel from *Drosophila melanogaster*. *Insect Mol Biol* 9: 283-292.

Newton AC (2004). Diacylglycerol's affair with protein kinase C turns 25. *Trends Pharmacol Sci* 25: 175-177.

Okada T, Inoue R, Yamazaki K, Maeda A, Kurosaki T, Yamakuni T, Tanaka I, Shimizu S, Ikenaka K, Imoto K, Mori Y (1999). Molecular and functional characterization of a novel mouse transient receptor potential protein homologue TRP7. Ca(2+)-permeable cation channel that is constitutively activated and enhanced by stimulation of G protein-coupled receptor. *J Biol Chem* 274: 27359-27370.

Pophof B, Van der Goes van Naters W (2002). Activation and inhibition of the transduction process in silkmoth olfactory receptor neurons. *Chem. Senses* 27, 435-443.

Robinson RB, Siegelbaum SA (2003). Hyperpolarization-activated cation currents: From molecules to physiological function. *Annu. Rev. Physiol.* 65, 453-480.

Sanes JR, Hildebrand JG (1976). Structure and development of antennae in a moth, *Manduca sexta*. *Dev Biol* 51: 282-299.

Stengl M (1993). Intracellular-messenger-mediated cation channels in cultured olfactory receptor neurons. *J Exp Biol* 178: 125-147.

Stengl M (1994). Inositol-trisphosphate-dependent calcium currents precede cation currents in insect olfactory receptor neurons *in vitro*. *J Comp Physiol [A]* 174: 187-194.

Stengl M, Hildebrand JG (1990). Insect olfactory receptor neurons *in vitro*: Morphological and immunocytochemical characterization of male-specific antennal receptor cell from developing antennae of male *Manduca sexta*. *J Neurosci* 10: 837-847.

Stengl M, Zufall F, Hatt H, Hildebrand JG (1992). Olfactory receptor neurons from antennae of developing male *Manduca sexta* respond to components of the species-specific sex pheromone *in vitro*. *J Neurosci* 12: 2523-2531.

Taylor CW, da Fonseca PCA, Morris EP (2004). IP_3 receptors: the search for structure. *Trends in Biochem Sci* 29: 210-219.

Trebak M, Vazquez G, Bird GStJ, Putney JW (2003). The TRPC3/6/7 subfamily of cation channels. *Cell Calcium* 33: 451-461.

Ziegelberger G, van den Berg MJ, Kaissling KE, Klumpp S, Schultz JE (1990). Cyclic GMP levels and guanylate cyclase activity in pheromone-sensitive antennae of the silkmoths *Antheraea polyphemus* and *Bombyx mori*. *J Neurosci* 10: 1217-1225.

Zufall F, Hatt H (1991). Dual activation of a sex pheromone-dependent ion channel from insect olfactory dendrites by protein kinase C activators and cyclic GMP. *Proc. Natl. Acad Sci USA* 88, 8520-8524.

Zufall F, Stengl M, Franke C, Hildebrand JG, Hatt H (1991). Ionic currents of cultured olfactory receptor neurons from antennae of male *Manduca sexta*. *J Neurosci* 11: 956-965.

I. Diacylglycerol activates cation channels in moth olfactory receptor neurons.

Pézier A, Papaefthymiou C, Krannich S, Acquistapace A, Stengl M, Lucas P.

J Neurophysiol, under review.

ABSTRACT	27
INTRODUCTION	27
MATERIALS AND METHODS	28
Insects	28
Cell culture	28
Solutions and reagents	29
Patch-clamp experiments	29
RESULTS	30
DOG activates a current in ORNs	30
DOG-gated channels are cationic	30
Ca^{2+}-calmodulin modulates the amplitude of the DOG-activated current	32
DOG activates a current independently of PKC	32
A DAG kinase inhibitor activates a current with similar properties to the DOG-activated current	35
DISCUSSION	36
Moth ORNs express DAG-gated channels	36
Ca^{2+}-CaM down-regulates the opening of DAG-gated channels	37
DGK regulates the concentration of endogenous DAG	37
Potential role of DAG in the transduction cascade	38
Does the insect DAG-gated channel belong to the TRPC family?	39
ACKNOWLEDGEMENTS	39
GRANTS	39
REFERENCES	39

Diacylglycerol activates cation channels in olfactory receptor neurons

Adeline Pézier[1], Chrisovalantis Papaefthimiou[1], Steffi Krannich[1], Adrien Aquistapace[1], Monika Stengl[2], and Philippe Lucas[1]

[1]INRA, UMR1272 Physiologie de l'Insecte: Signalisation et Communication, Route de Saint Cyr, Versailles Cedex F-78026, France

[2]Biology, Animal Physiology, Philipps-University of Marburg, Karl-von-Frisch-Straße 8, Marburg D-35032, Germany

Correspondence to be sent to: Philippe Lucas, INRA, UMR1272 Physiologie de l'Insecte: Signalisation et Communication, Route de Saint Cyr, Versailles Cedex F-78026, France, e-mail: plucas@versailles.inra.fr

Abstract

The molecular mechanisms that underlie olfactory transduction remain a central question in insects. Sex pheromones activate insect olfactory receptor neurons (ORNs) through phosphoinositide signaling, resulting in the production of diacylglycerol (DAG) and inositol-1,4,5-trisphosphate. In this paper, we report a novel cationic current that is activated by the lipid messenger DAG in cultured ORNs from the Noctuid moth *Spodoptera littoralis*. The activation of the DAG-gated channel does not require protein kinase C. Decrease of extracellular Ca^{2+} concentration or the presence of a calmodulin antagonist strongly increased the DAG-activated current amplitude indicating that the DAG-gated channel is negatively modulated by Ca^{2+}-calmodulin. The inhibition of DAG degradation using a DAG kinase (DGK) inhibitor produced a sustained activation of a current that shared the properties of the DAG-activated current. On the basis of our results, we propose that DAG or one of its metabolites is involved in the olfactory transduction in the moth *S. littoralis* and that a DGK regulates the concentration of endogenously generated DAG. The DAG-activated cation channel is a potential member of the superfamily of canonical transient receptor potential channels.

Keywords: DAG-gated current, olfactory transduction, patch-clamp, olfactory receptor neuron, insect.

Introduction

Insects evolved olfactory systems of remarkable sensitivity and discriminatory power to process chemical cues carrying critically important information about their environment. Olfactory receptor neurons (ORNs) convert the information about the quality, quantity and temporal pattern of the detected odor stimuli into action potential trains propagating to the antennal lobes where the olfactory information is integrated (Hansson and Anton 2000). Although the physiology of pheromone-responding ORNs from male moths has been extensively studied and constitutes a model in invertebrate olfaction (Kaissling 2004), the molecular mechanisms underlying the transduction of odorants in insects remain to be fully elucidated.

The chemo-electrical signal transduction cascade is mediated by G-protein-coupled receptors (Clyne et al. 1999; Gao and Chess 1999; Krieger et al. 2002; Vosshall et al. 1999). Biochemical (Boekhoff

et al. 1990a; Boekhoff et al. 1990b; Breer et al. 1990), immunocytochemical (Laue et al. 1997; Laue and Steinbrecht 1997), molecular (Jacquin-Joly et al. 2002) and genetic investigations (Riesgo-Escovar et al. 1995) demonstrated that the binding of odorant molecules to olfactory receptors activates a G-protein of the Gq family, coupled to phospholipase C β (PLCβ) activation. PLCβ hydrolyses phosphatidylinositol 4,5-bisphosphate (PIP_2), a membrane phospholipid, into inositol 1,4,5-trisphosphate (IP_3) and 1,2-diacylglycerol (DAG). Several observations support the idea that IP_3 is a second messenger of insect olfactory transduction. IP_3-receptors, which are Ca^{2+}-channels, were immunolocalized in dendritic membranes of *Bombyx mori* ORNs (Laue and Steinbrecht 1997). IP_3 perfusion and odorant stimulation activated similar ionic currents in ORNs from the locust *Locusta migratoria* (Wegener et al. 1997) and the moth *Manduca sexta* (Stengl 1993; Stengl et al. 1992). Finally, in *M. sexta*, IP_3 was found to open Ca^{2+} channels, inducing an increase in the intracellular Ca^{2+} concentration that opens Ca^{2+}-dependent nonselective cationic channels (Stengl 1994).

In contrast to IP_3, the role of DAG in insect olfactory transduction has not been studied in detail. Monosensillar recordings from the moths *Antheraea polyphemus* and *B. mori* demonstrated that *in vivo* DAG stimulates the firing activity of ORNs (Maida et al. 2000; Pophof and Van der Goes Van Naters 2002). Moreover, inside-out recordings performed on patches excised from the outer dendrite of *A. polyphemus* ORNs suggested that DAG may be involved in the gating of ion channels (Zufall and Hatt 1991). In these studies, DAG was used as a membrane-permeable protein kinase C (PKC) activator and its effects were only discussed in this context. However, accumulating evidence has pointed at the role of the lipid environment in the regulation of many ion channels (Hilgemann 2004). After the discovery of the transient receptor potential (TRP) superfamily of ion channels (Hardie and Minke 1992), a number of studies on recombinant or native TRP channels reported their direct activation by DAG (Hardie 2003; Hofmann et al. 1999; Lucas et al. 2003; Okada et al. 1999; Shlykov and Sanborn 2004; Trebak et al. 2003; Venkatachalam et al. 2003).

The aim of this work was to identify the role of DAG in insect pheromone-responding ORNs. With whole-cell patch-clamp recordings from cultures of moth ORNs we characterized the biophysical and pharmacological properties of a novel DAG-gated cationic channel. Our data suggest that DAG is involved in the insect olfactory transduction cascade and that the DAG-activated channel expressed in insect ORNs is a new member of the growing family of TRP channels.

Materials and Methods

Insects

Spodoptera littoralis (Lepidoptera, Noctuidae) were reared on a semi-artificial diet (Poitout et al. 1972). Larvae were maintained at 21-24°C under long-day photoperiod (L:D 16:8 h). Pupae were selected within 12 h after pupation and were kept at 20°C until their antennal flagella were dissected.

Cell culture

Primary cell cultures of antennal ORNs were prepared from 3-day-old male pupae following the protocol previously reported (Lucas and Nagnan-Le Meillour 1997). Briefly, 20 to 30 antennal flagella were dissected under sterile conditions in a 3+2 medium (3 parts of Leibovitz's L15 medium + 2 parts of Grace's medium conditioned with yeastolate and lactalbumine hydrolysate). Flagella were incubated for 5 minutes in 1 mg/mL EGTA in Hank's Ca^{2+}- and Mg^{2+}-free balanced salt solution (HBSS), rinsed in HBSS and dissociated in L-cystein

activated papain (1 mg/mL) for 10 to 12 minutes. Flagella were rinsed in HBSS and triturated in 3+2 medium with a fire-polished Pasteur pipette. Dispersed cells were plated on 35 mm Falcon dishes. After 30 to 60 minutes the culture medium was replaced with 150 µL of a 3+2 medium supplemented with 5 % fetal calf serum and with Grace medium conditioned on the embryonic cell line MRLL-CH1 (Eide et al. 1975). Antennal cells were cultured with the hanging column technique at 20°C in a humid atmosphere. Half of the culture medium was replaced with fresh medium every 5 to 7 days.

Solutions and reagents

The standard NaCl-based bath solution for whole-cell recordings contained (in mM): 156 NaCl, 4 KCl, 6 $CaCl_2$, 5 Glucose and 10 HEPES, pH adjusted to 7.2 with NaOH and osmolarity adjusted to 360 mosmol/L with mannitol. In the Na^+-free bath solution, Na^+ and K^+ ions were substituted for 160 mM choline. The Cl^--free bath solution was made by replacing NaCl and KCl with 160 mM $NaCH_3SO_3$. In some experiments, the free Ca^{2+} concentration of the bath solution was buffered to 10^{-5} M (using HEDTA) or to 10^{-7} M (using EGTA). The pipette solution contained (in mM): 155 CsCl, 1 $CaCl_2$, 11 EGTA, 10 HEPES, pH 7.2 (CsOH) and adjusted to 330 mosmol/L with mannitol. The free Ca^{2+} concentration of the pipette solution was 17.8 nM as calculated with WebmaxC v.2.20 (http://www.stanford.edu/~cpatton/webmaxcS.htm). For inside-out recordings, the bath and pipette solution contained (in mM) 150 NaCl, 10 HEPES and 1 EGTA. In some experiments, Na^+ was isoosmotically replaced with $NMDG^+$ in the bath solution.

All drugs and chemicals were obtained from Sigma (France), except for the culture media (Invitrogen) and chelerythrine (Alomone). The DAG analog 1,2-dioctanoyl-sn-glycerol (DOG), R59949, staurosporine, phorbol 12-myristate 13-acetate (PMA) and U73122 were dissolved in dimethyl sulfoxide (DMSO). N-(6-aminohexyl)-5-chloro-1-naphthalenesulfonamide (W-7), H7 and chelerythrine were prepared in water. All aliquots were stored at -20°C. For drug application, the final DMSO concentration was less than 0.1 % and had no effect on electrophysiological properties of ORNs. DOG was focally pressure ejected on the recorded neuron. Other drugs were directly added to the bath solution. When PKC inhibitors (staurosporine, H7 and chelerythrine) were tested, cells were incubated for 20 to 30 minutes with one PKC inhibitor before patching an ORN and applying DOG. Solutions prepared from chemicals dissolved in DMSO were sonicated before addition to the bath solution.

Patch-clamp experiments

Whole-cell and inside-out patch-clamp recordings were performed on ORNs grown in culture for 10-25 days. ORNs were identified in the culture according to their morphology and electrophysiological properties, as described earlier (Lucas and Shimahara 2002). Cells were viewed at 600× magnification on an Olympus IX-70 inverted microscope. Inside out patches were excised from the soma. Patch pipettes were pulled from thick borosilicate glass capillaries (WPI, G150-10). Their tip resistance was 5 to 7 MΩ. The reference electrode was connected to the bath through an agar bridge. Currents were recorded using an Axopatch 200B amplifier (Molecular Device Corp., USA). Command potential sequences, data acquisitions and analyses were performed under pClamp 9. For whole cell recordings, ORNs were clamped at -60 mV and ramp protocols from +80 to -100 mV within 500 ms were applied to establish current-voltage (I-V) relationships. Currents recorded during voltage protocols were sampled at 20 kHz through a Digidata 1322A (Molecular Device Corp.,

USA). A Minidigi acquisition device (Molecular Device Corp., USA) was used during the entire experiment to sample at 500 Hz, on 2 channels, the recorded currents and the monitoring of drug application with a picospritzer. Since the Ca^{2+}-dependent K^+ current could not be totally blocked by replacing K^+ with Cs^+ in the pipette solution, a delay of at least 5 minutes was allowed after breaking into whole-cell configuration, for the Ca^{2+}-dependent K^+ current to stabilize before recording currents and/or adding any drug. The figures show representative traces uncorrected for leak currents. All results are expressed as means ± S.D. A 2-way analysis of variance (ANOVA) was used for statistical comparisons. A *P* value less than 0.05 was considered significant.

Results

DOG activates a current in ORNs

We applied puffs of the DAG analog, DOG, to neurons recorded in the whole-cell patch-clamp configuration to test whether DAG activates a current in insect ORNs. After application of 100 µM DOG puffs ranging from 200 ms to 30 s, 47 % of the recorded cells (55 out of 116) showed a current in response to DOG. A characteristic response to a 200-ms puff of DOG is shown in Fig. 1A. Inward currents developed with a delay of hundreds of ms up to tens of seconds. In most cases, the current did not develop gradually but instead appeared suddenly, sometimes in the form of transient bursts of current, and developed in steps as shown in the insert of Fig. 1A. The DOG-activated current usually reached a plateau. The current amplitude at the plateau averaged -136 ± 19 pA (*n* = 16) at -60 mV in standard bath solution. In ramp protocols, DOG-activated currents had a linear I-V relationship (Fig. 1B). Application of 1 mM La^{3+} blocked 90.4 ± 9.1 % of the current (*n* = 34), 0.5 mM La^{3+} blocked 95.3 ± 9.6 % (*n* = 10) and 0.1 mM La^{3+} blocked 95.4 % of the current (*n* = 2).

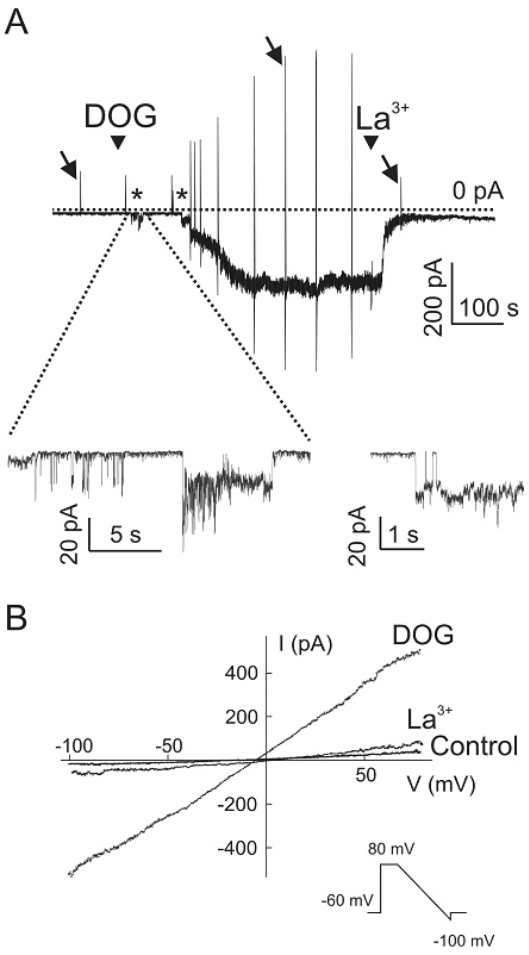

Figure 1 1,2-dioctanoyl-sn-glycerol (DOG), an analog of DAG, activates a current in moth ORNs. **(A)** After a 200-ms puff application of 100 µM DOG, a slow inward current developed. Membrane potential was -60 mV. The DOG-activated current was almost completely blocked by the application of 1 mM La^{3+}. Arrowheads indicate the time of application of DOG and La^{3+} in the bath solution. At regular intervals, voltage ramp protocols were applied. Arrows indicate currents recorded during ramp protocols that were used to establish I-V relationships shown in (B). * indicate two sections of the recording that were enlarged to illustrate the flickering activation of the DOG-activated current. **(B)** I-V relationships established from voltage ramp protocols triggered before DOG application, after DOG application, and after La^{3+} application.

DOG-gated channels are cationic

To determine the permeability of channels activated by DOG, we compared the DOG-activated current in different extracellular

solutions. When recordings were performed in standard NaCl-based bath solution, the reversal potential of the DOG-activated current averaged 0.0 ± 0.7 mV (*n* = 18) and its I-V relationship was always linear (Fig. 2A). When all anions in the bath solution were replaced with methane sulfonate (Cl^--free bath solution), I-V relationships of the DOG-gated current remained linear and the mean reversal potential remained close to 0 mV (0.7 ± 0.5 mV, *n* = 9) (Fig. 2B). Thus Cl^- ions do not support the DOG-activated current. Then, the extracellular monovalent cations were replaced with choline (Na^+-free bath solution). Due to the low survival of ORNs in Na^+-free bath solution in nominally free Ca^{2+} condition, the Ca^{2+} concentration was maintained at 6 mM. In this bath solution, the current recorded after DOG application exhibited a strong outward rectification with a reversal potential of -14.3 ± 1.6 mV (*n* = 3) (Fig. 2C). Modifications of the I-V relationship of the DAG-activated current in Na^+-free bath solution compared to standard bath solution indicated that DAG-activated channels are permeable to monovalent cations. Interestingly, in Na^+-free bath solution the outward current was blocked at potentials less positive than 30 mV,

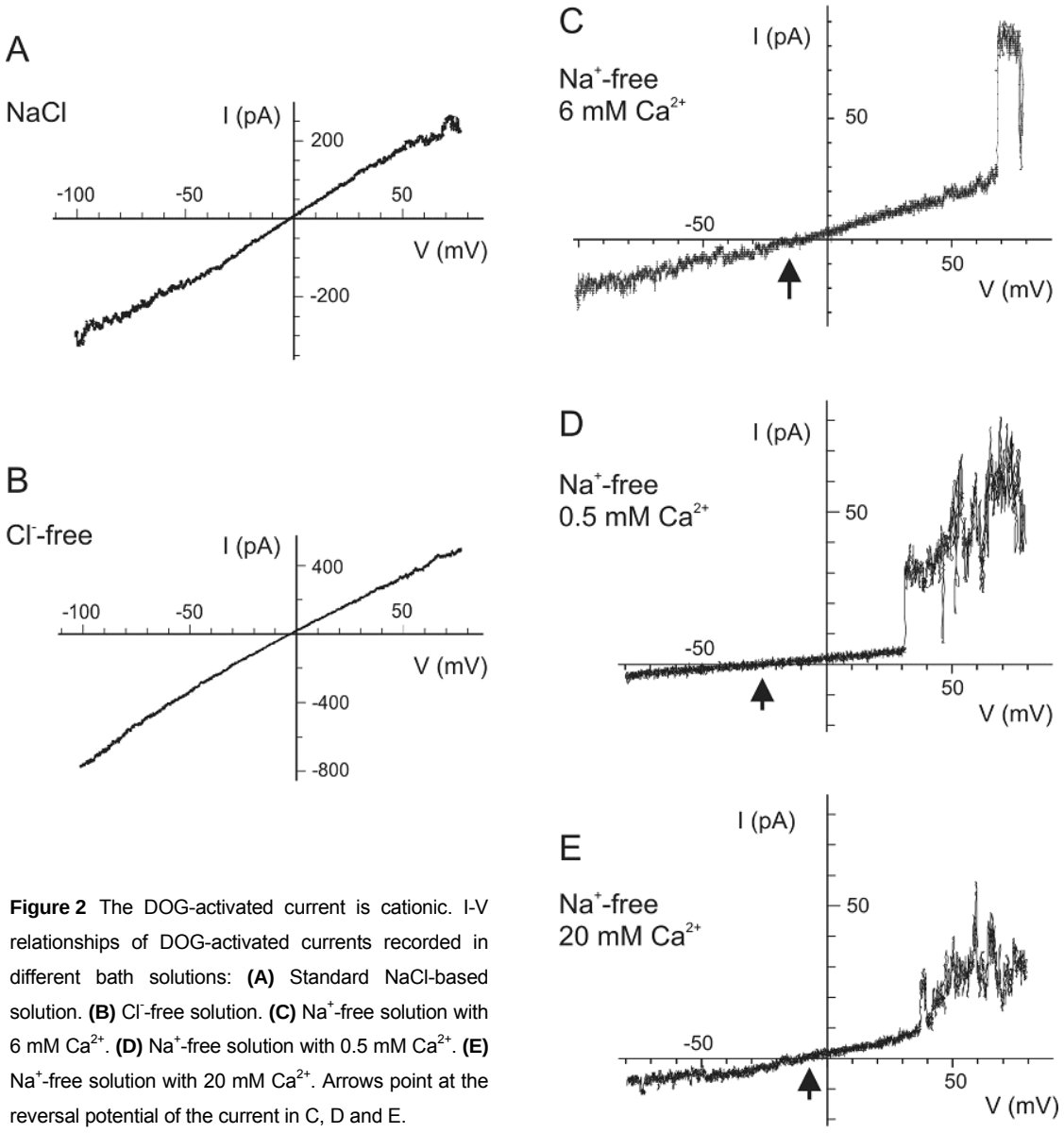

Figure 2 The DOG-activated current is cationic. I-V relationships of DOG-activated currents recorded in different bath solutions: **(A)** Standard NaCl-based solution. **(B)** Cl^--free solution. **(C)** Na^+-free solution with 6 mM Ca^{2+}. **(D)** Na^+-free solution with 0.5 mM Ca^{2+}. **(E)** Na^+-free solution with 20 mM Ca^{2+}. Arrows point at the reversal potential of the current in C, D and E.

suggesting that in absence of extracellular monovalent cations DAG-gated channels are blocked by external Ca^{2+}.

To determine whether DAG-gated channels are also permeable to Ca^{2+}, we varied the external concentration of Ca^{2+} in Na^{+}-free bath solution. Recordings started in the bath solution containing 0.5 mM Ca^{2+} and then, the bath solution was exchanged to the one containing 20 mM Ca^{2+}. In these conditions, the DOG-activated current showed a strong outward rectification (n = 3) and no clear inward current was observed even at 20 mM Ca^{2+} (Fig. 2D-E). However, the shift in the reversal potential from -30.0 ± 1.0 mV (n = 3) in 0.5 mM Ca^{2+} to -11.0 ± 2.6 mV (n = 3) in 20 mM Ca^{2+} suggested that DAG-gated channels are slightly permeable to Ca^{2+}.

Ca^{2+}-calmodulin modulates the amplitude of the DOG-activated current

To examine whether the DAG-activated current depends on Ca^{2+}, the responses to DOG were compared in NaCl-based bath solutions differing in their free Ca^{2+} concentration (Fig. 3). The peak amplitude of the inward current elicited by 100 µM DOG stimulations averaged 136 ± 19 pA (n = 16) in 6×10^{-3} M Ca^{2+}. When the Ca^{2+} concentration was adjusted to 10^{-5} M the amplitude of the activated current (417 ± 105 pA; n = 9) was significantly higher (P < 0.05) and the amplitude reached 596 ± 128 pA (n = 9; P < 0.01) in 10^{-7} M Ca^{2+}. The negative correlation between the amplitude of the DOG-activated current and the extracellular Ca^{2+}-concentration is supported also by high non parametric correlation coefficient (R= -0,5718, P=0,0004, n = 34).

Then, we investigated whether Ca^{2+} regulates the opening of DOG-gated channels from the intracellular side of the membrane. Since the Ca^{2+} sensitivity of many cationic channels is mediated by Ca^{2+}-calmodulin (Ca-CaM) (Saimi and Kung 2002), the CaM antagonist, W-7 (50 µM), was applied on ORNs after DOG stimulation. In standard bath solution, W-7 alone did not elicit any current (n = 5). When applied after DOG, W-7 significantly increased the amplitude of the DOG-activated current (Fig. 4A-B) from 406 ± 168 pA to 1009 ± 126 pA (n = 3; P < 0.01). The noise level was decreased after the perfusion with W-7, suggesting that most or all DOG-gated channels remained in the open state after the addition of W-7. The current elicited after application of DOG and W-7 had the same properties as the DOG-activated current: this current had an almost linear I-V relationship (Fig. 4C), a reversal potential close to 0 mV (-0.4 ± 0.3 mV; n = 3) and was blocked by La^{3+}.

DOG activates a current independently of PKC

To investigate whether or not DOG activates a current via PKC activation, we tested the effects of three different PKC blockers, chelerythrine (10 µM), H7 (10 µM) and staurosporine (2 µM), on the

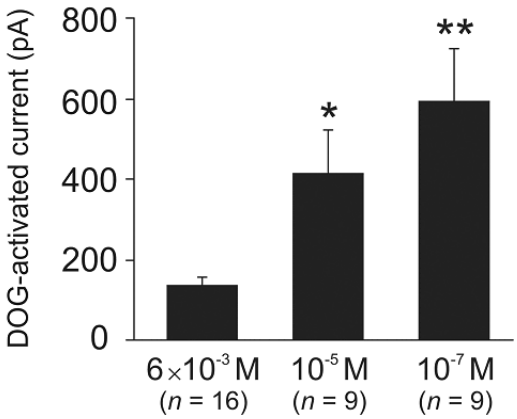

Figure 3 The amplitude of the DOG-activated current depends on the concentration of extracellular Ca^{2+}. Mean amplitude of the inward current activated after the application of a pulse of DOG (100 µM) on ORNs kept in a bath solution containing 6×10^{-3} M Ca^{2+}, 10^{-5} M Ca^{2+} or 10^{-7} M Ca^{2+}. Error bars indicate standard deviation. Stars indicate that the mean amplitudes of current measured in 10^{-5} M and 10^{-7} M Ca^{2+} were significantly different from the current measured in 6.10^{-3} M Ca^{2+} (* P < 0.05; ** P < 0.01).

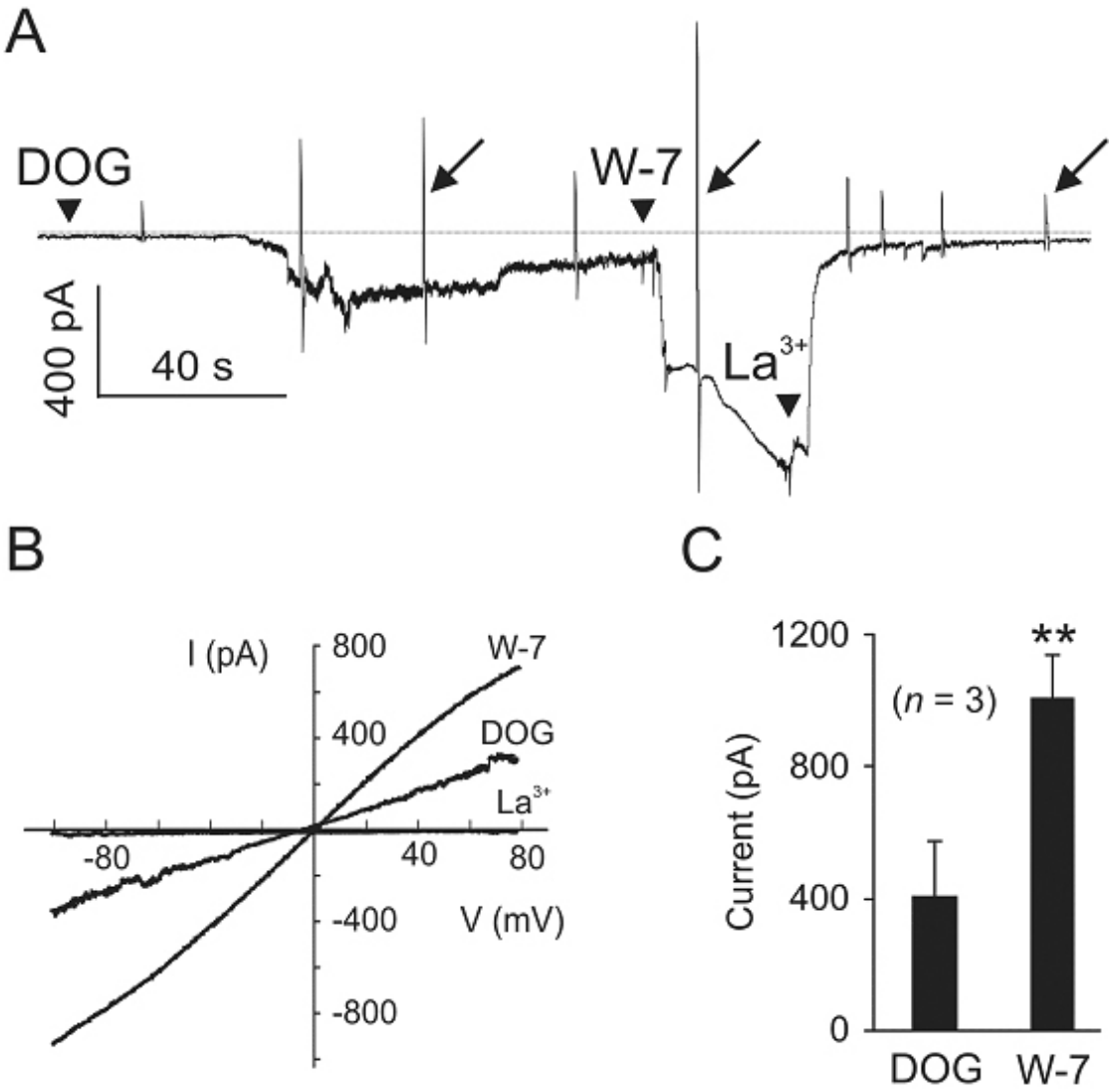

Figure 4 The DOG-activated current is down-regulated by Ca^{2+}-CaM. **(A)** The amplitude of the DOG-activated current was strongly increased after application of 50 µM of the CaM antagonist W-7. Application of 1 mM La^{3+} completely blocked this current. Recordings were performed in standard bath solution. Arrowheads indicate the time of application in the bath solution of DOG, W-7 and La^{3+}. Voltage ramp protocols were applied. Arrows indicate currents recorded during ramp protocols used to establish I-V relationships shown in B. **(B)** I-V relationships of the current shown in (A) after application of DOG, W-7 and La^{3+}. **(C)** Mean amplitude of the DOG-activated current before and after application of W-7. Error bars indicate standard deviation (n = 3). The difference between current amplitudes was significant (P < 0.01, paired t-test).

activation of currents by DOG. Responses of ORNs to 100 µM DOG were recorded after a pre-incubation with one of these blockers for at least 20 minutes. None of these PKC blockers prevented the activation of a La^{3+}-blockable inward current by DOG (Fig. 5 A-B). The mean amplitude of the DOG-activated current was 107 ± 48 pA (n = 3 out of 3 ORNs) in the presence of chelerythrine, 78 ± 13 pA (n = 4 out of 7 ORNs) in the presence of staurosporine and 252 ± 97 pA (n = 3 out of 4 ORNs) in the presence of H-7. Altogether, in the presence of a PKC blocker, DOG activated a current in 71 % of the ORNs (n = 10 out of 14).

In addition to blockers of PKC, the effect of a PKC activator, PMA, was also tested. Recordings were performed in the presence of 1 mM Mg-ATP in the recording electrode and PMA (100 µM) was

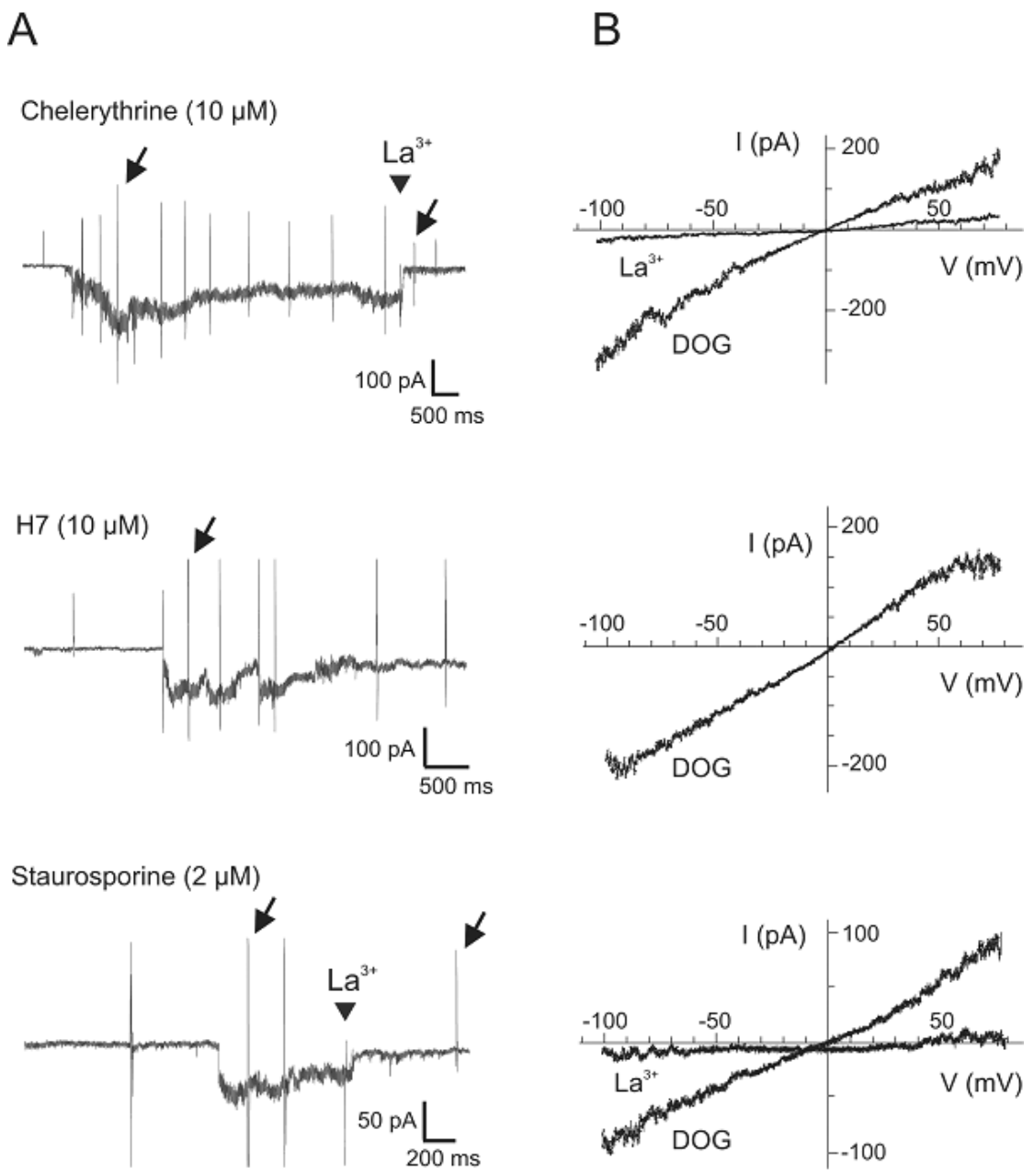

Figure 5 DAG can activate an inward current in the presence of PKC blockers. **(A)** Currents activated after stimulation with 100 µM DOG in the presence of 10 µM chelerythine, 10 µM H7 or 2 µM staurosporine. When La^{3+} was applied (arrowhead) the current was inhibited. Arrows indicate the currents recorded during ramp protocols used to establish I-V relationships shown in B. **(B)** I-V relationships established from currents shown in A before and after application of 1 mM La^{3+}.

pressure ejected on the recorded ORN. In absence of DOG application, no current (*n* = 3) was found to be activated by the PKC activator.

To confirm that DAG activates channels independently of PKC, DAG-activated currents were recorded in the inside-out configuration. In symmetrical NaCl-based solutions, the application of DOG on the excised patch activated a current with a linear I-V relationship and a reversal potential close to 0 mV (-2.8 ± 9.0 mV; *n* = 6) (Fig. 6). When the bath solution was replaced with a NMDG-based solution, the outward component of the DOG-activated current was strongly reduced and the reversal potential was shifted to 61.5 ± 24.3 mV; *n* = 6). Thus, DOG activated a cationic current in excised patches.

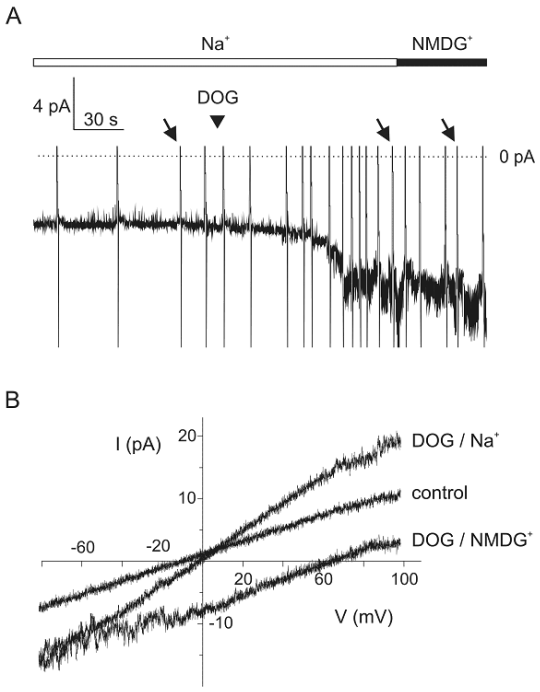

Figure 6 DAG activates a cationic current in excised patches. **(A)** Current recorded from a patch excised in the inside-out configuration and kept at -60 mV. After application of DOG (arrowhead) the intensity of current flowing through the patch of membrane increased. The bath solution was switched from a Na^+-based solution (white bar) to a $NMDG^+$-based solution (black bar). Ramp protocols from +100 to -80 mV were applied regularly to establish I-V relationships. Arrows indicate currents recorded during ramp protocols that were used to establish I-V relationships shown in (B). **(B)** I-V relationships established from currents shown in A before DOG application, and after the activation of the DOG-activated current in Na^+-based solution and in $NMDG^+$-based solution.

A DAG kinase inhibitor activated a current with similar properties to the DOG-activated current

The mechanism involved in the regulation of DAG concentration was then studied. DAG can be metabolized differently: a DAG lipase can hydrolyze a fatty acid chain of DAG to generate a monoacylglycerol and a free fatty acid (Meves 1994). DAG can be transformed to phosphatidylcholine or phosphatidylethanolamine by the addition of CDP-choline or ethanolamine. DAG kinases (DGK) can phosphorylate DAG to produce phosphatidic acid (Raghu et al. 2000; van Blitterswijk and Houssa 2000). The conversion of DAG to phosphatidic acid is considered to be the major route for DAG degradation (Luo et al. 2004).

A specific blocker of DGK, R59949 (20 μM), was employed to determine whether this enzyme is involved in turning off the DAG signaling in insect ORNs. R59949 is an inhibitor of the type I, Ca^{2+}-activated DGK (van Blitterswijk and Houssa 2000). It was added to ORNs in the presence of 1 mM Mg-ATP in the patch pipette solution because ATP contributes to PIP_2 regeneration. In 5 out of 12 ORNs, the application of R59949 elicited a sustained activation of a current that reached 55 ± 44 pA (n = 5) at -60 mV within the 4 minutes following drug application. The delay for current activation was 66 ± 84 s. The current that developed after incubation with R59949 shared the properties of the DOG-activated current (Fig. 7 A-B). This

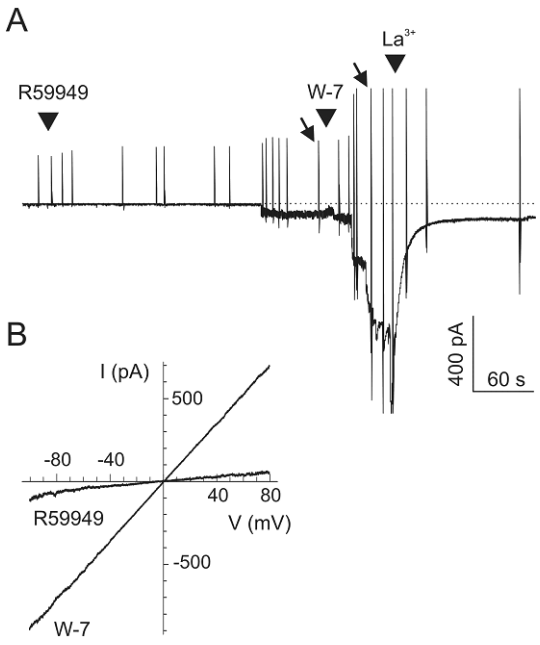

Figure 7 A DAG kinase (DGK) regulates DAG concentration in ORNs. **(A)** Application of the DGK inhibitor R59949 (20 μM) produces a sustained inward current in ORNs. Membrane potential was -60 mV. Arrowheads indicate the time of application in the bath solution of R59949, W-7 and La^{3+}. Arrows indicate currents recorded during ramp protocols used to establish I-V relationships shown in B. **(B)** I-V relationships established from currents shown in A after application of R59949 (20 μM) and after application of W-7 (50 μM).

R59949-activated current had a linear I-V relationship, with a reversal potential close to 0 mV (-5.1 ± 4.0 mV; *n* = 5), its amplitude was strongly increased in the presence of W-7 (*n* = 2) and it was blocked by application of 1 mM La^{3+} (*n* = 4). In control experiments, no current was recorded in the presence of 1 mM ATP (*n* = 6).

In most recordings, a small inward current and some noise, reflecting most probably channel openings, were observed spontaneously. The application of La^{3+} (1 mM) was found to rapidly reduce the current amplitude and noise activity (*n* = 5) (Fig. 8A). To test whether this activity originates from a basal PLC activity, we tested the effect of the PLC blocker U73122. The application of 10 µM U73122 (*n* = 6) induced a rapid reduction of the amplitude of the current and reduced the noise (Fig. 8B).

Discussion

Moth ORNs express DAG-gated channels

Treatment of ORNs *in vitro* with exogenous DAG (100 µM DOG) induced the activation of a cationic current in almost half (47 %) of the recorded ORNs. The DOG-activated currents usually did not develop progressively but instead activated in steps, suggesting that DAG-gated channels are clustered or somehow coupled, similar to retinal transient receptor potential (TRP) channels of *Drosophila melanogaster* that can be

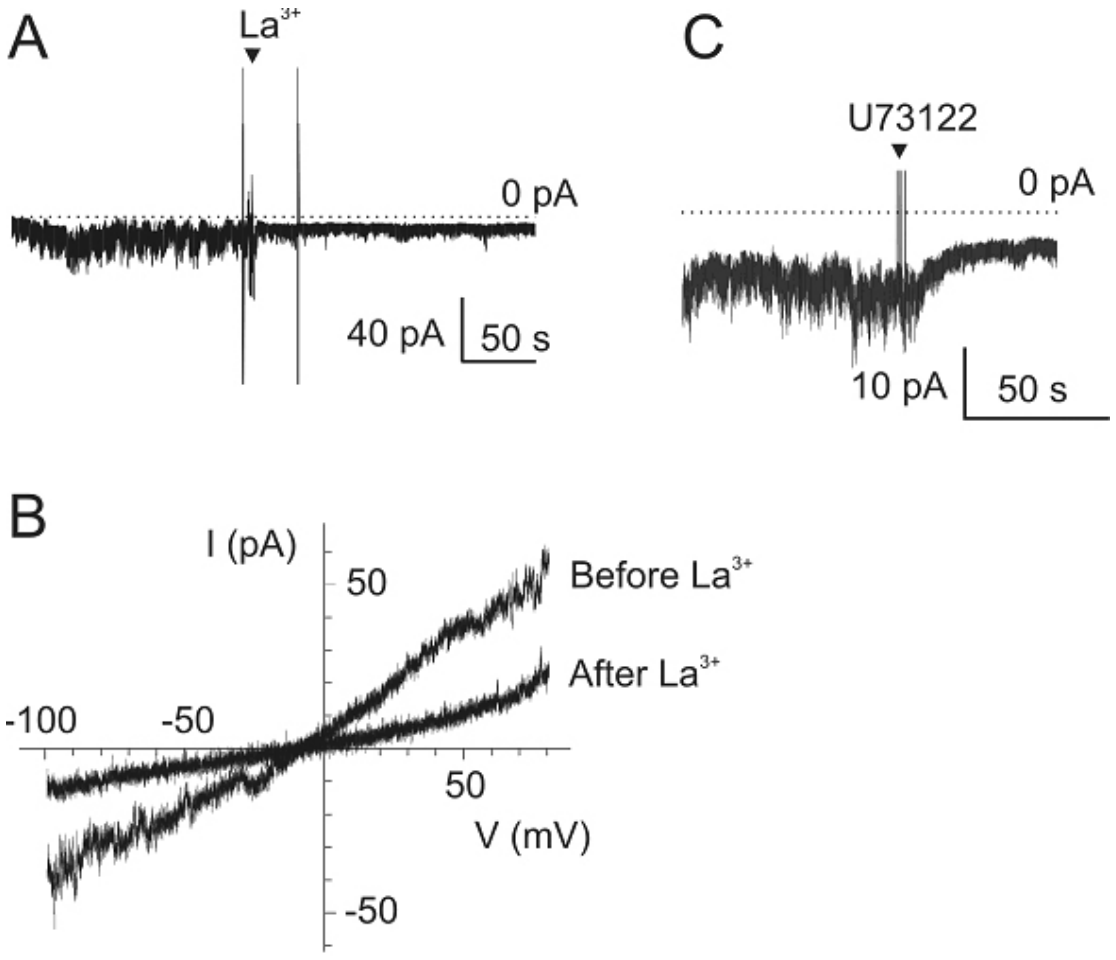

Figure 8 Spontaneous channel openings in ORNs are La^{3+}-blockable and may originate from second messenger-gated channels due to a basal PLC activity. **(A)** La^{3+} (1 mM) blocks a small-amplitude spontaneous current. **(B)** The spontaneous La^{3+}-blockable current has a linear I-V relationship and a reversal potential close to 0 mV. **(C)** The PLC blocker, U73122 (10 µM), blocks the spontaneous current.

gated coordinately (Haab et al. 2000).

Previous effects of DAG analogs on the electrical activity of moth pheromone-responding ORNs were hypothesized to be PKC-mediated (Pophof and Van Der Goes Van Naters 2002; Zufall and Hatt 1991). Moreover, a 6-fold increase in PKC-activity was measured in antennal homogenates of male moths after pheromone stimulation (Maida et al. 2000). However, we found that the DAG-activated currents were not blocked by the three PKC inhibitors we tested, chelerytrine, H7, staurosporine, and no current was activated by the PKC activator, PMA, alone. Therefore, DAG can activate cationic channels in insect ORNs independently of PKC, as already demonstrated in other systems (Hofmann et al. 1999; Lucas et al. 2003; Shlykov and Sanborn 2004; Tesfai et al. 2001). The effect of DAG can also be attributed to one of its metabolites known to be polyunsaturated fatty acids such as arachidonic, linolenic and linoleic acids as described in other systems (Broad et al. 1999; Chyb et al. 1999; Spehr et al. 2002). The activation of a cationic current in the inside-out configuration suggests that in moth ORNs, it is DAG and not its downstream metabolites that activates cationic channels.

Ca^{2+}-CaM down-regulates the opening of DAG-gated channels

The amplitude of the DOG-activated current depended on the concentration of extracellular Ca^{2+}. The regulation of many channels involved in Ca^{2+} signaling is mediated by CaM (Saimi and Kung 2002; Zhu 2005). CaM has been localized in the dendrites of ORNs (Laue and Steinbrecht 1997). Therefore, we wanted to know whether the dependence of the DAG-activated current to Ca^{2+} occurs by the interaction with CaM. In this aim, we tested the effects of a CaM antagonist, W-7, on responses to DOG. Perfusion of W-7 strongly increased the amplitude of the DOG-activated current and reduced the noise level. This observation suggests that in the presence of the CaM antagonist cationic channels remained in the open state and, therefore, CaM is involved in the modulation of the DOG-activated current. We propose that Ca^{2+} entering ORNs through DOG-gated channels is involved in a down-regulation of these channels via its interaction with CaM, allowing a phasic activation of the DAG-activated current following odor stimuli.

DGK regulates the concentration of endogenous DAG

Spontaneous channel openings that were observed from most ORNs disappeared after application of the PLC inhibitor U-73122, which blocks the production of DAG, or after the application of La^{3+}, which blocks the opening of DAG-gated channels. One possible interpretation of these results can be that DAG-gated channels are activated in resting ORNs by endogenous DAG resulting from a basal PLC activity. Such a constitutive PLC activity was described in mouse vomeronasal sensory (VNO) neurons (Lucas et al. 2003). Therefore, to determine whether endogenous DAG can activate a current, ORNs were perfused with an inhibitor of the enzyme DGK, which is involved in DAG degradation (Raghu et al. 2000; van Blitterswijk and Houssa 2000). Blockage of the DGK activity induced the development of a sustained current with the properties of the current activated by exogenous DAG. These results indicate that ORNs contain a DGK that metabolizes the endogenous DAG. This observation is in good agreement with the antennal expression of a DGK as revealed from the analysis of an EST antennal library and its expression at the base of olfactory sensilla (Chouquet et al. 2007). Our results suggest that there is a production of DAG in the basal state and that inhibition of DAG breakdown increased the concentration of DAG, leading to the activation of DAG-gated channels. Similarly, in

the *Drosophila* DGK mutant, *rdgA*, the light-sensitive TRP and TRPL channels are constitutively active in photoreceptors (Raghu et al. 2000).

Potential role of DAG in the transduction cascade

In *S. littoralis,* receptor potentials were recorded *in vivo* in response to pheromone stimuli after reducing extracellular sensillar Ca^{2+} concentration to 20 nM (Pézier et al. 2007), demonstrating that, at least at the pheromone concentration used in that study, depolarizing currents are not strictly dependent on the IP_3-dependent Ca^{2+} entry. This observation supports the hypothesis that other sensory channels can also play a key role in ORN depolarization, and DAG-gated cationic channels are good candidates. Such a key role of DAG in signal transduction was demonstrated in pheromone transduction in mammals and in phototransduction in insects, two other PLC-dependent transduction pathways. The primary electrical response of mice VNO neurons to pheromones depends on DAG through the activation of DAG-gated TRPC2 channels (Lucas et al. 2003). In *Drosophila* photoreceptors, the light sensitive current is activated by a lipid messenger such as DAG or its metabolites (polyunsaturated fatty acids) (Hardie 2003).

The activation of PLC leads not only to the production of DAG but also to an equimolar synthesis of IP_3. In *M. sexta* ORNs, IP_3 was found to elicit a Ca^{2+} entry (Stengl 1994), which activates Ca^{2+}-dependent currents (Stengl 1993) similar to pheromone-dependant currents (Stengl et al. 1992). Therefore, the question arises about the respective roles of IP_3 and DAG in insect olfactory transduction. Different transduction pathways can coexist within ORNs (Boekhoff et al. 1994; Delay and Dionne 2002). In lobster ORNs, the IP_3 and cAMP transduction pathways can coexist within the same ORN (Hatt and Ache 1994), being involved in the transduction of different odors and inducing ORN excitation and inhibitory, respectively. However, in contrast to cAMP and IP_3 that depend on the activation of different enzymes and thus can be produced independently, DAG and IP_3 are generated at the same time after PLC activation. This implies that the DAG and the IP_3 pathways can only be involved in the transduction of different odors, like for instance pheromone compounds and general odorants, if the channels they activate are not co-expressed within the same ORNs.

If DAG- and IP_3-activated channels co-localize within ORNs, interactions between the DAG and the IP_3 cascades can be expected. Such interaction was observed in rabbit portal vein myocytes where IP_3 and DAG act in synergy to mediate the activation of TRPC6-like channels by noradrenaline (Albert and Large 2003). Likewise, DAG alone does not fully account for the activation of human TRPC6 channels and other receptor-mediated events act synergistically with DAG to stimulate channel activity (Estacion et al. 2004).

Moth pheromone-sensitive ORNs are characterized by the extremely wide dynamic range from threshold to saturation of the receptor potential recorded in response to pheromone stimuli of constant duration and graded intensities, which is of about 8 decades (Dolzer et al. 2003; Kaissling 2001; Zack 1979). The two types of second messenger- (DAG and IP_3) gated channels may contribute to this wide dynamic range of the receptor potential (Rospars et al. 2007). In that hypothesis, DAG opens cationic channels directly and generates a quick and major depolarization, and IP_3 induces a Ca^{2+} entry and/or a store-operated Ca^{2+} release which opens channels that amplify the depolarization for high odorant concentration. Future experiments will address the following questions: do DAG- and IP_3-gated channels co-localize within the same ORNs? Do

DAG and IP_3 activate channels synergistically? Do IP_3 and DAG account for the wide dynamic range of the receptor potential of moth ORNs?

Does the insect DAG-gated channel belong to the TRPC family?

The transient receptor potential (TRP) superfamily comprises a large group of related channels that have emerged as cellular sensors of various internal and external cues both in vertebrate and invertebrates (Clapham 2003). Many TRP channels play important roles in sensory physiology. The DAG-gated channel we showed to be expressed in moth ORNs share similarities with TRP channels. TRP channels are cationic channels (Clapham et al. 2001), multiple calmodulin binding sites were identified on TRP channels (Zhu 2005) and La^{3+} is considered as a non-specific blocker of these proteins (Halaszovich et al. 2000).

TRP channels are conserved throughout animal phylogeny and, based on amino acid sequence comparisons, they are subdivided into 7 subfamilies (Montell et al. 2002). DAG-gated channels have higher similarity with TRP canonical (TRPC) channels, which are most highly related to the original fly TRP channels (Niemeyer et al. 1996). Generally, the activation of TRPC channels is triggered by the stimulation of phospholipase C (Clapham et al. 2001; Montell 2005). In addition to TRP channels identified from *Drosophila* photoreceptors (Hardie 2003; Hardie and Minke 1992), DAG-gated channels expressed by insect ORNs share similarities with DAG-gated TRPC channels of the types TRPC2 (Lucas et al. 2003), TRPC5 (Lee et al. 2003), and TRPC3/6/7 (Dietrich et al. 2005; Hofmann et al. 1999; Trebak et al. 2003; Venkatachalam et al. 2003) identified from vertebrate cells. These DAG-gated channels are Ca^{2+} permeable non-specific cationic channels and thus contribute to the increase in intracellular Ca^{2+} concentration that follows adequate simulation of the cells. Expression of TRP channels in adult olfactory organs was only reported so far in *D. melanogaster* (Honda et al. 2005) and in *M. sexta* (Ackermann et al. 2004). However, TRP channels have not yet been shown to be involved in insect olfaction except in adaptation processes in *Drosophila* (Störtkuhl et al. 1999), but in that case TRP channels were not expressed in the adult antennae and were proposed to be involved in olfactory system development. DAG-gated channels expressed in insect ORNs are prime candidates to belong to the TRP family of cation channels.

Acknowledgements

We are very grateful to Jean-Marc Nichols for rearing moths and to Didier Trotier and Jean-Pierre Rospars for fruitful discussions. Present address of Steffi Krannich: Biology, Animal Physiology, Philipps-University of Marburg, Karl-von-Frisch Straße, D-35032 Marburg, Germany. Present address of Chrisovalantis Papaefthimiou: Laboratory of Animal Physiology, School of Biology, Aristotle University, GR-54124 Thessaloniki, Greece.

Grants

This work was supported by the French Agence Nationale de la Recherche (Aromalim ANR-05-PNRA-002-07).

References

Ackermann F, Chubanov V, Copenhaver P, Gudermann T, and Stengl M. TRP/TRP-like channel proteins in the antenna of *Manduca sexta*. TRP channels as new pharmacological targets. 25th symposium at Rauischholzhausen castle, Germany, 2004.

Albert AP and Large WA. Synergism between inositol phosphates and diacylglycerol on native TRPC6-like channels in rabbit portal vein myocytes. *J Physiol* 552: 789-795, 2003.

Boekhoff I, Michel WC, Breer H, and Ache BW. Single odors differentially stimulate dual second messenger pathways in lobster olfactory receptor cells. *J Neurosci* 14: 3304-3309, 1994.

Boekhoff I, Raming K, and Breer H. Pheromone-induced stimulation of inositol-triphosphate formation in insect antennae is mediated by G-proteins. *J Comp Physiol A* 160: 99-103, 1990a.

Boekhoff I, Strotmann J, Raming K, Tareilus E, and Breer H.

Odorant-sensitive phospholipase C in insect antennae. *Cell Signal* 2: 49-56, 1990b.

Breer H, Boeckhoff I, and Tareilus E. Rapid kinetics of second messenger formation in olfactory transduction. *Nature* 345: 65-68, 1990.

Broad LM, Cannon TR, and Taylor CW. A non-capacitative pathway activated by arachidonic acid is the major Ca^{2+} entry mechanism in rat A7r5 smooth muscle cells stimulated with low concentrations of vasopressin. *J Physiol* 517.1: 121-134, 1999.

Chouquet B, Bozzolan F, Solvar M, Duportets L, Jacquin-Joly E, Lucas P, and Debernard S. Molecular cloning and expression patterns of olfactory diacylglycerol kinase from *Spodoptera littoralis*. *10th ESITO meeting*, Roscoff, 2007.

Chyb S, Raghu P, and Hardie RC. Polyunsaturated fatty acids activate the *Drosophila* light-sensitive channels TRP and TRPL. *Nature* 397: 255-259., 1999.

Clapham DE. TRP channels as cellular sensors. *Nature* 426: 517-524, 2003.

Clapham DE, Runnels LW, and Strubing C. The TRP ion channel family. *Nat Rev Neurosci* 2: 387-396, 2001.

Clyne PJ, Warr CG, Freeman MR, Lessing D, Kim J, and Carlson JR. A novel family of divergent seven-transmembrane proteins: candidate odorant receptors in *Drosophila*. *Neuron* 22: 327-338, 1999.

Delay RJ and Dionne VE. Two second messengers mediate amino acid responses in olfactory sensory neurons of the salamander, *Necturus maculosus*. *Chem Senses* 27: 673-680, 2002.

Dietrich A, Kalwa H, Rost BR, and Gudermann T. The diacylgylcerol-sensitive TRPC3/6/7 subfamily of cation channels: functional characterization and physiological relevance. *Pflugers Arch* 451: 72-80, 2005.

Dolzer J, Fischer K, and Stengl M. Adaptation in pheromone-sensitive trichoid sensilla of the hawkmoth *Manduca sexta*. *J Exp Biol* 206: 1575-1588, 2003.

Eide PE, Caldwell JM, and Marks EP. Establishment of two cell lines from embryonic tissue of the tobacco hornworm, *Manduca sexta* (L). *In Vitro* 11: 395-399, 1975.

Estacion M, Li S, Sinkins WG, Gosling M, Bahra P, Poll C, Westwick J, and Schilling WP. Activation of human TRPC6 channels by receptor stimulation. *J Biol Chem* 279: 22047-22056, 2004.

Gao Q and Chess A. Identification of candidate *Drosophila* olfactory receptors from genomic DNA sequence. *Genomics* 60: 31-39, 1999.

Haab JE, Vergara C, Bacigalupo J, and O'Day PM. Coordinated gating of TRP-dependent channels in rhabdomeral membranes from *Drosophila* retinas. *J Neurosci* 20: 7193-7198, 2000.

Halaszovich CR, Zitt C, Jungling E, and Luckhoff A. Inhibition of TRP3 channels by lanthanides. Block from the cytosolic side of the plasma membrane. *J Biol Chem* 275: 37423-37428., 2000.

Hansson BS and Anton S. Function and morphology of the antennal lobe: new developments. *Annu Rev Entomol* 45: 203-231, 2000.

Hardie RC. Regulation of TRP channels via lipid second messengers. *Annu Rev Physiol* 65: 735-759, 2003.

Hardie RC and Minke B. The trp gene is essential for a light-activated Ca^{2+} channel in *Drosophila* photoreceptors. *Neuron* 8: 643-651, 1992.

Hatt H and Ache BW. Cyclic nucleotide- and inositol phosphate-gated ion channels in lobster olfactory receptor neurons. *Proc Natl Acad Sci USA* 91: 6264-6268, 1994.

Hilgemann DW. Biochemistry. Oily barbarians breach ion channel gates. *Science* 304: 223-224, 2004.

Hofmann T, Obukhov AG, Schaefer M, Harteneck C, Gudermann T, and Schultz G. Direct activation of human TRPC6 and TRPC3 channels by diacylglycerol. *Nature* 397: 259-263, 1999.

Honda T, Amy NL, and Warr CG. Identification and characterisation of genes involved in olfactory signal transduction in *Drosophila*. *8th annual meeting of AACSS (Australasian Association for Chemosensory Science)*, Heron Island, Australia, 2005.

Jacquin-Joly E, Francois MC, Burnet M, Lucas P, Bourrat F, and Maida R. Expression pattern in the antennae of a newly isolated lepidopteran Gq protein alpha subunit cDNA. *Eur J Biochem* 269: 2133-2142., 2002.

Kaissling K-E. Olfactory perireceptor and receptor events in moths: a kinetic model. *Chem Senses* 26: 125-150, 2001.

Kaissling K-E. Physiology of pheromone reception in insects (an example of moths). *ANIR* 6: 73-91, 2004.

Krieger J, Raming K, Dewer YM, Bette S, Conzelmann S, and Breer H. A divergent gene family encoding candidate olfactory receptors of the moth *Heliothis virescens*. *Eur J Neurosci* 16: 619–628, 2002.

Laue M, Maida R, and Redkozubov A. G-protein activation, identification and immunolocalization in pheromone-sensitive sensilla trichodea of moths. *Cell Tissue Res* 288: 149-158, 1997.

Laue M and Steinbrecht RA. Topochemistry of moth olfactory sensilla. *Int J insect Morphol Embryol* 26: 217-228, 1997.

Lee YM, Kim BJ, Kim HJ, Yang DK, Zhu MX, Lee KP, So K, and Kim W. TRPC5 as a candidate for the nonselective cation channel activated by muscarinic stimulation in murine stomach. *Am J Physiol* 284: G604–G616, 2003.

Lucas P and Nagnan-Le Meillour P. Primary culture of antennal cells of *Mamestra brassicae*: morphology of cell types and evidence for biosynthesis of pheromone-binding proteins *in vitro*. *Cell Tissue Res* 289: 375-382, 1997.

Lucas P and Shimahara T. Voltage- and calcium-activated currents in cultured olfactory receptor neurons of male *Mamestra brassicae* (Lepidoptera). *Chem Senses* 27: 599-610, 2002.

Lucas P, Ukhanov K, Leinders-Zufall T, and Zufall F. A

diacylglycerol-gated cation channel in vomeronasal neuron dendrites is impaired in TRPC2 mutant mice: mechanism of pheromone transduction. *Neuron* 40: 551-561, 2003.

Luo B, Regier DS, Prescott SM, and Topham MK. Diacylglycerol kinases. *Cell Signal* 16: 983-989, 2004.

Maida R, Redkozubov A, and Ziegelberger G. Identification of PLC beta and PKC in pheromone receptor neurons of *Antheraea polyphemus*. *Neuroreport* 11: 1773-1776, 2000.

Meves H. Modulation of ion channels by arachidonic acid. *Prog Neurobiol* 43: 175–186, 1994.

Montell C. Drosophila TRP channels. *Pflügers Arch* 451: 19-28, 2005.

Montell C, Birnbaumer L, Flockerzi V, Bindels RJ, Bruford EA, Caterina MJ, Clapham DE, Harteneck C, Heller S, Julius D, Kojima I, Mori Y, Penner R, Prawitt D, Scharenberg AM, Schultz G, Shimizu N, and Zhu MX. A unified nomenclature for the superfamily of TRP cation channels. *Mol Cell* 9: 229-231, 2002.

Niemeyer BA, Suzuki E, Scott K, Jalink K, and Zuker CS. The *Drosophila* light-activated conductance is composed of the two channels TRP and TRPL. *Cell* 85: 651-659, 1996.

Okada T, Inoue R, Yamazaki K, Maeda A, Kurosaki T, Yamakuni T, Tanaka I, Shimizu S, Ikenaka K, Imoto K, and Mori Y. Molecular and functional characterization of a novel mouse transient receptor potential protein homologue TRP7. Ca^{2+}-permeable cation channel that is constitutively activated and enhanced by stimulation of G protein-coupled receptor. *J Biol Chem* 274, 1999.

Pézier A, Acquistapace A, Renou M, Rospars J-P, and Lucas P. Ca^{2+} stabilizes the membrane potential of moth olfactory receptor neurons at rest and is essential for their fast repolarization. *Chem Senses* 32: 305-317, 2007.

Poitout S, Bues R, and Le Rumeur C. Elevage sur milieu artificiel simple de deux noctuelles parasites du coton *Earias insulana* et *Spodoptera littoralis*. *Entomol exp appl* 15: 341-350, 1972.

Pophof B and Van Der Goes Van Naters W. Activation and inhibition of the transduction process in silkmoth olfactory receptor neurons. *Chem Senses* 27: 435-443, 2002.

Raghu P, Usher K, Jonas S, Chyb S, Polyanovsky A, and Hardie RC. Constitutive activity of the light-sensitive channels TRP and TRPL in the *Drosophila* diacylglycerol kinase mutant, rdgA. *Neuron* 26: 169-179, 2000.

Riesgo-Escovar J, Raha D, and Carlson JR. Requirement for a phospholipase C in odor response: overlap between olfaction and vision in *Drosophila*. *Proc Natl Acad Sci USA* 92: 2864-2868, 1995.

Rospars J-P, Gu Y, and Lucas P. An integrated view of sexual pheromone transduction in moths. *10th ESITO meeting*, Roscoff, 2007.

Saimi Y and Kung C. Calmodulin as an ion channel subunit. *Annu Rev Physiol* 64: 289-311, 2002.

Shlykov SG and Sanborn BM. Stimulation of intracellular Ca^{2+} oscillations by diacylglycerol in human myometrial cells. *Cell Calcium* 36: 157-164, 2004.

Spehr M, Hatt H, and Wetzel CH. Arachidonic acid plays a role in rat vomeronasal signal transduction. *J Neurosci* 22: 8429-8437, 2002.

Stengl M. Inositol-triphosphate-dependent calcium currents precede cation currents in insect olfactory receptor neurons *in vitro*. *J comp Physiol* 174: 187-194, 1994.

Stengl M. Intracellular-messenger-mediated cation channels in cultured olfactory receptor neurons. *J exp Biol* 178: 125-147, 1993.

Stengl M, Zufall F, Hatt H, and Hildebrand JG. Olfactory receptor neurons from antennae of developing male *Manduca sexta* respond to components of the species-specific sex pheromone *in vitro*. *J Neurosci* 12: 2523-2531, 1992.

Störtkuhl KF, Hovemann BT, and Carlson JR. Olfactory Adaptation Depends on the Trp Ca^{2+} Channel in *Drosophila*. *J Neurosci* 19: 4839-4846, 1999.

Tesfai Y, Brereton HM, and Barritt GJ. A diacylglycerol-activated Ca^{2+} channel in PC12 cells (an adrenal chromaffin cell line) correlates with expression of the TRP-6 (transient receptor potential) protein. *Biochem J* 358: 717-726, 2001.

Trebak M, Vazquez G, Bird GS, and Putney JW, Jr. The TRPC3/6/7 subfamily of cation channels. *Cell Calcium* 33: 451-461, 2003.

van Blitterswijk WJ and Houssa B. Properties and functions of diacylglycerol kinases. *Cell Signal* 12: 595-605, 2000.

Venkatachalam K, Zheng F, and Gill DL. Regulation of canonical transient receptor potential (TRPC) channel function by diacylglycerol and protein kinase C. *J Biol Chem* 278: 29031-29040, 2003.

Vosshall LB, Amrein H, Morozov PS, Rzhetsky A, and Axel R. A spatial map of olfactory receptor expression in the *Drosophila* antenna. *Cell* 96: 725-736, 1999.

Wegener JW, Hanke W, and Breer H. Second messenger-controlled membrane conductance in locust (*Locusta migratoria*) olfactory neurons. *J Insect Physiol* 43: 595-605, 1997.

Zack C. Sensory adaptation in the sex pheromone receptor cells of Saturniid moths (Doctorat de l'Université Ludwig-Maximilians, Munich). Munich, 1979.

Zhu MX. Multiple roles of calmodulin and other Ca^{2+}-binding proteins in the functional regulation of TRP channels. *Pflugers Arch* 451: 105-115, 2005.

Zufall F and Hatt H. Dual activation of a sex pheromone-dependent ion channel from insect olfactory dendrites by protein kinase C activators and cyclic GMP. *Proc Natl Acad Sci USA* 88: 8520-8524, 1991.

II. Diacylglycerol-dependent currents and TRP-like channels in the hawkmoth *Manduca sexta*.

Krannich S, Ackermann F, Chubanov V, Gudermann T, Stengl M.

ABSTRACT	45
INTRODUCTION	45
MATERIALS AND METHODS	47
Cell cultures	47
Solutions and reagents for electrophysiology	47
Patch-clamp technique and data analysis	48
cDNA synthesis and RT-PCR	48
Construction of a chimeric TRP channel protein for manganese influx measurements	49
RESULTS	50
DOG activates a current in moth ORNs	50
DOG activates a cation current in different extracellular Ca^{2+} solutions	50
DOG activates a current modulated by Ca^{2+}/CaM	51
DOG activates a current independently of PKC	51
DOG activates a current inhibited by PKC	52
Two alternatively spliced TRP-like channel mRNAs are expressed in *M. sexta*	52
MsTRPLa encodes a functional TRP-like channel pore	53
DISCUSSION	54
DAG directly activates currents in moth ORNs	54
DAG probably acts on TRP-like channels	54
Ca^{2+}-dependency of DAG-dependent currents	56
PKC modulates DAG-dependent currents	56
Conclusions	57
ACKNOWLEDGEMENTS	57
REFERENCES	57

Diacylglycerol-dependent currents and TRP-like channels in the hawkmoth *Manduca sexta*

Steffi Krannich[1,2], Frauke Ackermann[1,3], Vladimir Chubanov[3], Thomas Gudermann[3], and Monika Stengl[1,2]

[1]Biology, Animal Physiology, Philipps-University of Marburg, Karl-von-Frisch-Straße 8, Marburg D-35032, Germany

[2]Institute of Biology, Animal Physiology, University of Kassel, Heinrich-Plett-Straße 40, Kassel D-34132, Germany

[3]Department of Pharmacology and Toxicology, Philipps-University of Marburg, Karl-von-Frisch-Straße, Marburg D-35032, Germany

Correspondence to be sent to: Monika Stengl, Biology, Animal Physiology, Philipps-University of Marburg, Karl-von-Frisch-Straße 8, Marburg D-35032, Germany, e-mail: stengl@staff.uni-marburg.de

Abstract

In insects, odorants were thought to activate G-protein coupled receptors that activate phospholipase C at the beginning of the olfactory transduction cascade. The activation of phospholipase C leads to the equimolar production of inositol 1,4,5-triphosphate and diacylglycerol (DAG). While inositol 1,4,5-triphosphate is known to play a major role in insect olfactory transduction, the role of DAG is still unknown. Here, we used whole-cell patch-clamp recordings to characterize DAG-dependent currents in cultured olfactory receptor neurons of the hawkmoth *Manduca sexta*. The membrane-permeable DAG analogue DOG directly activated currents without interaction with protein kinase C. The DAG-dependent currents carried monovalent cations and Ca^{2+}, were modulated by Ca^{2+}/calmodulin, and were inhibited by lanthanum and protein kinase C. Thus, the electrophysiological properties of the moth DAG-dependent currents resembled those of currents through transient receptor potential (TRP) channels. RT-PCR experiments identified mRNA transcripts with high sequence similarity to the *Drosophila melanogaster* TRP-like channel mRNA in the brain and antennae of *Manduca sexta*. Thus, the putative moth DAG-gated channels likely represent TRP channels. Our results suggest a decisive role of DAG in the moth olfactory transduction cascade probably via activation of TRP channels.

Keywords: DAG-dependent current, insect olfactory transduction, patch-clamp, olfactory receptor neurons, TRP channels.

Introduction

Odors play a central role for intra- and interspecific recognition and communication in insects. Male moths, for example, can detect and analyze almost single molecules of the female sex pheromone (Kaissling and Priesner 1970). Accordingly, pheromone detection in moths is one of the best-studied models of how olfactory systems transduce and process odor information

(Hildebrand 1995; Hansson 2002; Kaissling 2004).

Previous biochemical (Breer et al. 1990; Boekhoff et al. 1990; Laue et al. 1997), electrophysiological (Zufall and Hatt 1991; Zufall et al. 1991; Stengl et al. 1992; Stengl 1993, 1994; Wegener et al. 1997), and molecular genetic studies (Riesgo-Escovar et al. 1995; Jacquin-Joly et al. 2002) extensively characterized the initial steps of the insect olfactory transduction cascade. Upon activation of olfactory receptors by odorants, phospholipase C hydrolyzes phosphatidylinositol 4,5-bisphosphate (PIP_2) to equimolar concentrations of inositol 1,4,5-triphosphate (IP_3) and 1,2-diacylglycerol (DAG). While IP_3 has been shown to play a role in the pheromone-dependent olfactory transduction pathway (Boekhoff et al. 1990; Stengl 1993, 1994; Wegener et al. 1997), the role of DAG remained largely unknown.

Presumably, membrane-bound DAG and Ca^{2+} together activate ion channels via interaction with protein kinase C (PKC). Within seconds, PKC returns to the cytosol while DAG is metabolized by either DAG lipase (DGL) to poly-unsaturated fatty acids (PUFA), or by DAG kinase (DGK) to phosphatidic acid (PA; Ha and Exton 1993). The conversion of DAG into PA is considered to be the main degradation pathway of DAG and at the same time is the first step in PIP_2 recycling (Luo et al. 2004). Recent studies indicate that DAG, its metabolites (PUFA), and/or the reduction of PIP_2 levels upon PLCβ activation mediate the activation of transient receptor potential (TRP) channels (Hardie 2003; Vazquez et al. 2004).

TRP channels constitute a large and diverse family of non-selective cation channels, which occur in a variety of organisms, tissues and cell types. TRP channels form homo- or heterotetrameric complexes composed of four subunits. Each subunit is comprises of six transmembrane domains, with the channel pore between the transmembrane domains 5 and 6. At the C-terminus, TRP channels contain a putative Ca^{2+}/calmodulin (CaM) binding site (Minke and Cook 2002; Clapham 2003; Venkatachalam and Montell 2007).

DAG-dependent TRP channels - dTRP and TRP-like (TRPL) - have been firstly characterized in the phototransduction pathway of *Drosophila melanogaster* (Hardie and Minke 1992; Niemeyer 1996; Hardie 2003). However, dTRP also localizes to the olfactory system of *D. melanogaster* (Stortkuhl et al. 1999; Honda et al. 2005). Based upon sequence similarity to dTRP and TRPL, several TRP channel subfamilies have been identified in vertebrates and invertebrates (Minke and Cook 2002; Venkatachalam and Montell 2007). One subfamily is that of vertebrate canonical TRP (TRPC) channels (Vazquez et al. 2004). Among the seven TRPC channels, TRPC2 (Lucas et al. 2003), TRPC3 (Hofmann et al. 1999; Trebak et al. 2003; Venkatachalam et al. 2003), TRPC5 (Lee et al. 2003), TRPC6 (Hofmann et al. 1999), and TRPC7 (Okada et al. 1999) are directly activated by DAG. At least TRPC2 localizes to the olfactory system (Liman et al. 1999; Menco et al. 2001). All DAG-gated TRP channels are Ca^{2+} permeable non-selective cation channels that are inhibited by lanthanum (Hardie 2003; Clapham et al. 2005).

In the olfactory system of moths, DAG is likely to activate ion channels (Zufall and Hatt 1991; Maida et al. 2000; Pophof and van der Goes van Naters 2002). Recent findings of Pézier and colleagues (unpublished) indicate that DAG directly activates a cation current in olfactory receptor neurons (ORNs) of *Spodoptera littoralis*. The corresponding putative DAG-gated channel showed similar electrophysiological properties as TRP channels. Here, we set out to identify and characterize DAG-dependent TRP-like channels in the ORNs of *Manduca sexta*.

Materials and Methods

Cell cultures

Cell culture media and chemicals were purchased from PAA (Cölbe, Germany), Gibco (Karslruhe, Germany), and Sigma (Taufkirchen, Germany). Dissociation of cells was performed as previously described (Stengl and Hildebrand 1990). Briefly, antennae of male *M. sexta* pupae were dissected in Hanks Balanced Salt Solution containing 1 % penicillin-streptomycin solution (HBSS/PS). Antennae were incubated for 5 min at room temperature in HBSS/PS containing 1.3 mM EGTA, rinsed in HBSS, and successively dissociated in two batches for 5 and 3 min at 37°C in HBSS/PS containing 24 mM papain. Dissociation was stopped with Leibovitz L-15 medium supplemented with 10 % fetal bovine serum. Then, the cell suspension was centrifuged for 5 min at 90 -110 rcf. Cells were resuspended in HBSS/PS and plated on glass-bottom culture dishes coated with concanavalin A and poly-L-lysine. After 30 min, cell culture medium was added. Within 24 h after dispersion, the cell culture medium was completely replaced.

HEK 293 cells were grown at 37°C in monolayer culture in humidified air atmosphere with 5 % CO_2 using Minimal Essential Medium supplemented with 2 mM L-glutamine, 10 % fetal bovine serum, and 1 % penicillin-streptomycin solution.

Solutions and reagents for electrophysiology

Solutions contained reagents at doses commonly used for patch-clamp recordings (Zufall et al. 1991; Stengl 1993, 1994). All solutions were adjusted to pH 7.1-7.2 and 370-380 mOsm for extracellular solutions, and 340 mOsm for pipette solution, respectively. Standard extracellular solution contained in mM: NaCl 156; KCl 4; $CaCl_2$ 6; glucose 5 and HEPES 10. To block voltage-dependent sodium currents, all extracellular solutions were supplemented with 10^{-8} M tetrodotoxin. To investigate if currents depend on the extracellular Ca^{2+} concentration, Ca^{2+} in the extracellular solution was either increased to 20 mM, or reduced to 10^{-5} and 10^{-7} M (buffered with EGTA). The ionic composition of the patch pipette solution was identical in all experiments and contained in mM: CsCl 160; $CaCl_2$ 1; EGTA 11 and HEPES 10. Cesium was used to prevent potassium-dependent outward currents.

The membrane-permeable DAG analogue 1,2-dioctanoyl-*sn*-glycerol (DOG), the PKC activator 12-myristate-13-acetate (PMA), and the protein kinase inhibitor staurosporine were dissolved in dimethyl sulfoxid (DMSO). DMSO-containing solutions were sonicated to facilitate homogenous dilution of the compounds. Final DMSO concentration was kept under 0.1 % because this concentration did not influence the response characteristics of ORNs. The Ca^{2+}/CaM antagonist N-(6-aminohexyl)-5-chloro-1-naphthalenesulfonamid (W-7) and the non-specific inhibitor of Ca^{2+}-permeable cation channels lanthanum (La^{3+}) were dissolved in ddH_2O. At the beginning of each experiment, extracellular solution was pipetted onto the cells as a control. After a delay of ~2 min, DOG was applied by puff application with a PicoSpritzer (General Valve, Fairfield, New Jersey, USA; application volume <10 nl for 0.2 - 20 sec) or pipetted onto the recorded ORNs at a concentration of 100 µM (Pézier et al. unpublished). Other reagents such as W-7 (10 µM; Krannich and Stengl unpublished), PMA (250 nM; Stengl 1993), or La^{3+} (10 to 500 µM) were pipetted into the extracellular solution. To investigate the effects of the protein kinase inhibitors staurosporine (1 µM) or H7 (10 µM; Stengl 1993) on DAG-activated currents, ORNs were pre-incubated with the respective protein kinase inhibitor for 15 to 30 min before breaking into whole-cell and application of DOG.

Patch-clamp technique and data analysis

Patch-clamp recordings were performed in whole-cell configuration (Hamill et al. 1981). Cultured 10 to 25 day-old ORNs were used for electrophysiology and identified on the basis of their morphology (Stengl and Hildebrand 1990). ORNs were monitored at 600x on an inverted microscope (Axioscope 135; Zeiss, Göttingen, Germany) equipped with phase-contrast optics. Patch electrodes were pulled from thick borosilicate glass capillaries (GC150T-10; Clark Electromedical Instruments, Reading, UK) with a micropipette puller (Sutter P97; Sutter, Novato, CA, USA). The tip resistance was 2 to 8 MΩ. Junction potential was nullified prior to seal formation, and capacitance and series resistance of the patch pipette were compensated. After breaking into whole-cell configuration and a subsequent delay of ~2 min for the stabilization of outward currents, the experiment was started. ORNs were clamped at -60 mV and three consecutive voltage ramp protocols from -100 mV to +100 mV, with 500 ms each, were applied to establish current-voltage (I-V) relations.

Data acquisition was carried out with an Axopatch 1D amplifier using a Digidata 1200B interface (Molecular Devices Corp., Union City, CA, USA). Data acquisition and analyses were performed with pClamp (version 8 to 9; Molecular Devices Corp.). Currents which were recorded during voltage protocols were sampled at 20 kHz and low-pass filtered at 2 kHz. A MiniDigi acquisition device (MiniDigi1A; Molecular Devices Corp.) was used to continuously sample currents at 1 kHz and to record the time of drug application on a second acquisition channel. Figures show representative traces that were corrected for leak currents. Mean current amplitudes were determined at -100 mV. All data were presented as mean ± SEM. Statistical significance (p-value of < 0.05) was evaluated with two-tailed Student's t-test.

cDNA synthesis and RT-PCR

To isolate total RNA, 15 frozen antennae or whole brains of pupae or adult *M. sexta* were homogenized in liquid nitrogen. Then, total RNA was extracted with "Trifast reagent" (Peqlab, Erlangen, Germany) and transcribed into cDNA using the "Revert Aid first-strand cDNA synthesis Kit" (MBI Fermentas, St-Leon Rot, Germany). To amplify cDNAs encoding TRP-like channel proteins of *M. sexta*, several primer pairs (Tab. 1) were designed against conserved regions of TRP channels of *D. melanogaster*, *Anopheles gambia,* and *Caliphora vicians.* Only the following primer pair, which was directed against the C-terminus of the *M. sexta* TRPL homolog allowed amplification of a TRP-like fragment: 5´-TCGCGGATCTGGAGAAAAGGAA-3´ (MsTRPL forward) and 5´-TGGCATAGGAGTTGGACATCA TAGC-3´ (MsTRPL reverse). This primer pair was designed in collaboration with PF Copenhaver (Dept. Cell and Developmental Biology, Oregon Health Science University, Portland, USA). The PCR reactions were performed in a total volume of 50 µl, containing 2 µl cDNA, 100 pM of the respective primers, 0.4 mM dNTPs, 1.5 mM $MgCl_2$, and 1.25 U Taq polymerase. After an initial heating at 94°C for 5 min, 35 cycles followed with denaturation at 94°C for 45 s, annealing at 56°C for 45 s, and extension at 70°C for 50 s. To fill gaps in the PCR products, all probes were finally heated at 70°C for 10 min. Then, 10 µl of each PCR product were analyzed on 1.5 % agarose gels. PCR fragments in the expected size were gel-extracted and ligated into the pcDNA3.1/V5-His-TOPO vector (Invitrogen, Karlsruhe, Germany). The resulting vectors were transfected into DH5α *E. coli*. After cultivation, plasmid DNA was prepared with the "NucleoBond Plasmid Purification Kit" (Macherey-Nagel, Düren,

Table 1 Primer pairs designed against different conserved regions of TRP channels.

primer	primer sequence
degenerative *Dm.Ag.Cv*_TRP_ct forward	5`-GTCTCATTGGGCCGCATGATTATCGA-`3
degenerative *Dm.Ag.Cv*_TRP_ct reverse	5`-CCATCCTCAAAATAGCTCATCCAC-`3
degenerative *Dm.Ag.Cv*_TRP_nt forward	5`-ATATGTGGAGGCTGTGGAGG-`3
degenerative *Dm.Ag.Cv*_TRP_nt reverse	5`-ACACACTCATCGCAACCGCA-`3
degenerative *Dm.Ag.Cv*_TRPa forward 1	5`-AAATGCGGTTGCGATGAGTGTGT-`3
degenerative *Dm.Ag.Cv*_TRPa forward 2	5`-AAATGCGGCTGCGATGAGTGT-`3
degenerative *Dm.Ag.Cv*_TRPa reverse	5`-ACACCAAAGTATAGATGAAGAAGAA-`3
degenerative *Dm.Ag.Cv*_TRPb forward	5`-GTCTCATTGGGCCGCATGATAATCG
degenerative *Dm.Ag.Cv*_TRPb reverse	5`-CCATCCTCGAAGTAGCTCATCCACA-`3
*Ms*TRPL forward	5`-TCGCGGATCTGGAGAAAAGGAA-`3
*Ms*TRPL reverse	5`-TGGCATAGGAGTTGGACATCATAGC-`3

Dm = *Drosophila melanogaster*, *Ag* = *Anopheles gambia*, *Cv* = *Caliphora vicians*, *Ms* = *Manduca sexta*. Only the *M. sexta* primer pair resulted in TRP-like PCR products.

Germany), restricted with XhoI and HindIII, and completely sequenced. As positive controls, we amplified 500 bp of the ubiquitously expressed actin gene in the brain [5`-GGCCGTGCTCTCCCTGTA-3` (forward) and 5`-TGTCGACGTCGCACTTCAT-3` (reverse)] and 500 bp of the epinephrin receptor gene [5`-GCGCAATGCCAACCGAATCTAC-3` (forward) and 5`-CCTCACCGGGGGCTATCTCTGC-3` (reverse)] in the antennae of *M. sexta*.

Construction of a chimeric TRP channel protein for manganese influx measurements

Since the PCR fragment encoded only a part of the putative *M. sexta* TRPL channel (transmembrane domain 5, pore, and transmembrane domain 6), a chimeric TRPL channel protein was constructed. The corresponding cDNA encoded the N- and C-termini of the human TRPC6 (hTRPC6) channel and the span of the transmembrane domain 5, pore, and transmembrane domain 6 of the amplified MsTRPLa fragment. Defined restriction sites were inserted to the 3' and 5' end of MsTRPLa by PCR, and the resulting MsTRPLa fragment was inserted in the range of transmembrane domain 5, pore, and transmembrane domain 6 of the htrpc6 gene. Then, a cDNA encoding yellow fluorescent protein (YFP) was inserted at the C-terminus of the hTRPC6/MsTRPLa fusion construct to visualize the corresponding fusion protein in cultured cells. HEK 293 cells were co-transfected with the YFP-tagged chimeric hTRPC6/MsTRPLa channel protein and the histamine receptor, which interacts with the TRPC6 channel (Jung et al. 2003). The transfected cells were identified by YFP fluorescence, and loaded with 5 µM Fura-2 acetoxymethylester (Fura-2; Calbiochem, Bad Soden, Germany) dissolved in HBS (150 mM NaCl, 5.4 mM KCl, 2 mM $CaCl_2$, 1 mM $MgCl_2$, 5 mM HEPES, 10 mM glucose, pH 7.4) in the dark for 40 min at room temperature. Then, cells were washed with HBS and imaging at 360 nm was started. To activate the histamine receptor and the corresponding YFP-tagged chimeric hTRPC6/MsTRPLa channel, HBS was exchanged for HBS containing 100 mM $MnCl_2$ and 50 mM histamine. After 1 min of stimulation, the Mn^{2+} influx through the chimeric hTRPC6/MsTRPLa channel was determined as percentage of the initial Fura-2 fluorescence at 360 nm (isobestic point of Fura-2). As Mn^{2+} has a similar permeability as Ca^{2+} through plasma membrane Ca^{2+} channels, the quench of the Fura-2 fluorescence at 360 nm allows estimation of Mn^{2+} entry (Tutdibi et al. 1999).

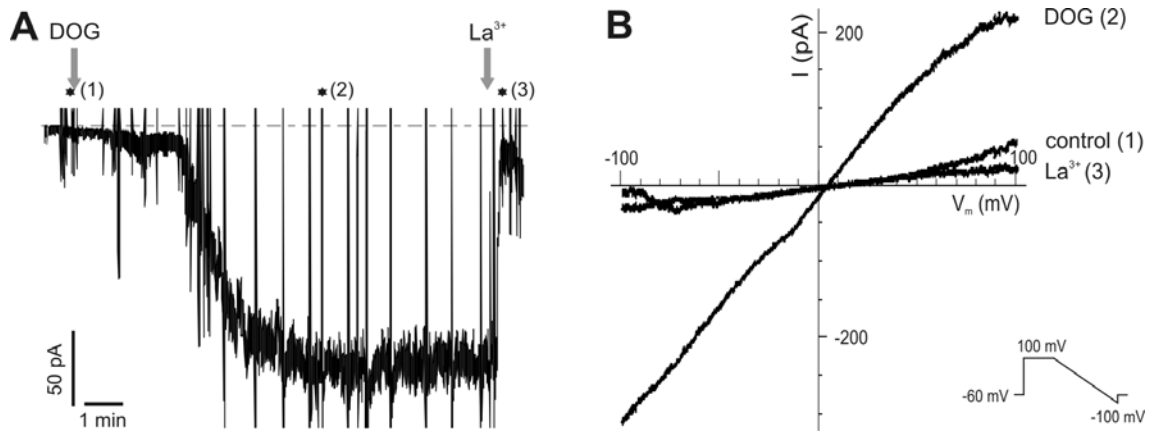

Figure 1 Whole-cell patch-clamp recordings of cultured *M. sexta* ORNs. (**A**) Application of 100 µM DOG (arrow), an analogue of DAG, activated a slow inward current at -60 mV membrane potential. This current was inhibited by 500 µM La^{3+} (arrow). Dashed line indicates 0 pA level. Large transient interruptions of the inward current are voltage ramp protocols. Asterisks and numbers indicate voltage ramp protocols used to establish I-V relations at the beginning of the experiment (control; 1), after DOG- (2), and after La^{3+}-application (3). Corresponding I-V relations are shown in (**B**).

Results

DOG activates a current in moth ORNs

To characterize DAG-dependent currents, we stimulated *M. sexta* ORNs (*n* = 82) in whole-cell patch-clamp recordings with the membrane-permeable DAG analogue DOG. DOG (100 µM) was mainly applied in puffs or pipetted into the extracellular solution. Since no obvious differences between both application procedures were found, we pooled the data.

DOG-application induced a continuously increasing inward current with a delay of 74 ± 7 sec in 59 (72 %) of the 82 stimulated *M. sexta* ORNs. The amplitude of the inward current generally reached a plateau and did not decline over the course of the recording (Fig. 1A). In standard extracellular solution, 26 of 40 ORNs (65 %) responded to DOG (Tab. 2). The DOG-activated current had a linear I-V relation (Fig. 1B), a mean reversal potential of 1.6 ± 1.6 mV, and a mean amplitude of 237 ± 53 pA. Subsequent application of La^{3+} (Tab. 2), a non-specific blocker of Ca^{2+}permeable cation channels, significantly inhibited 77.1 ± 3.4 % of the DOG-activated current in 24 of 26 ORNs ($p < 0.01$; Fig. 1A, B). La^{3+} inhibited the ORNs irrespective of the applied concentration: 500 µM La^{3+} (*n* = 7 of 7 ORNs), 250 µM La^{3+} (*n* = 8 of 9 ORNs), 100 µM La^{3+} (*n* = 7 of 7 ORNs), and 10 µM La^{3+} (*n* = 2 of 3 ORNs). The remaining La^{3+}-independent outwardly rectified current had a mean reversal potential of 7 ± 4.2 mV that did not significantly differ from the DOG-activated current.

DOG activates a cation current in different extracellular Ca^{2+} solutions

To examine whether DOG-activated currents depend on the extracellular Ca^{2+} concentration, Ca^{2+} in the extracellular solution was either increased to 20 mM, or reduced to 10^{-5} or 10^{-7} M (Tab. 2; Fig. 2). DOG induced linear currents in each of the extracellular solutions. Subsequent La^{3+}-application inhibited these currents. In extracellular solution containing 20 mM Ca^{2+}, the DOG-activated current had a mean amplitude of 802 ± 262 pA and a mean reversal potential of 4.7 ± 2.6 mV (*n* = 7 of 9 ORNs). Similarly, in extracellular solution containing 10^{-5} M Ca^{2+}, the DOG-activated current had a mean amplitude of 609 ± 174 pA and a mean reversal potential of 5.5 ± 3.5 mV (*n* = 7 ORNs). In extracellular solution

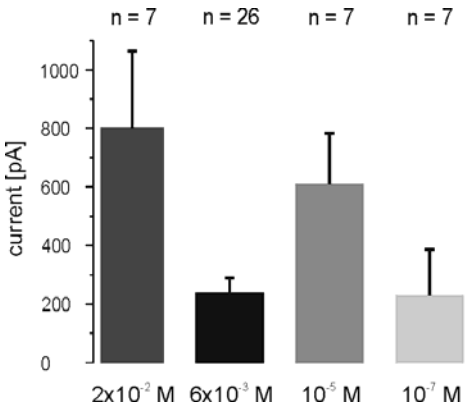

Figure 2 DOG-activated currents appeared not to depend on the extracellular Ca^{2+} concentration. Mean amplitude of DOG-activated (100 µM) inward currents at -100 mV in ORNs kept in extracellular solution containing 2 x 10^{-2} M, 6 x 10^{-3} M, 10^{-5} M, and 10^{-7} M Ca^{2+}. The mean amplitudes did not significantly differ. Error bars represent SEM.

containing 10^{-7} M Ca^{2+}, the DOG-activated current had a mean amplitude of 229 ± 157 pA and a mean reversal potential of 3.1 ± 5.2 mV (*n* = 7 of 9 ORNs). Thus, the mean amplitudes or reversal potentials of the DOG-activated currents did not significantly differ in the different extracellular solutions.

DOG activates a current modulated by Ca^{2+}/CaM

CaM binds intracellular Ca^{2+}, and hence inactivates Ca^{2+} permeable channels. To investigate whether Ca^{2+}/CaM inhibits DOG-activated currents, the CaM antagonist W-7 was applied. Application of W-7 (10 µM) alone did not elicit any current response (*n* = 3 ORNs), but significantly increased the DOG-activated current ($p < 0.01$; Tab. 2). Application of W-7 induced a ~2-fold increase of the DOG-activated current (*n* = 13 of 17 ORNs; Fig. 3B). Apart from the increase of current amplitude, the properties of the DOG-activated current remained unchanged. The La^{3+}-inhibited currents still showed a linear I-V relation (Fig. 3A) and a mean reversal potential of 3.9 ± 1.9 mV.

DOG activates a current independently of PKC

To examine whether DOG-activated currents depend on PKC, ORNs were pre-incubated with the protein kinase inhibitors staurosporine (1 µM) or H7 (10 µM) for at least 15 min and then stimulated with DOG. Both protein kinase inhibitors did not prevent DOG-activated currents (Tab. 2). In the presence of staurosporine, 3 of 8 ORNs showed a current response to DOG. The linear current (Fig. 4A) had a mean reversal potential of 5.7 ± 2.7 mV and a mean amplitude of 150 ± 53 pA. In the presence of H7, 6 of 9 ORNs showed a current response to DOG. The linear current (Fig. 4B) had a mean reversal potential of -2.1 ± 8.7 mV and a mean amplitude of 76 ± 18 pA, which significantly differed from the mean

Table 2 Pharmacological properties of the DOG-activated current.

	n	activation (%)	rectification	reversal potential (mV)	mean amplitude (pA)
6 mM Ca	40	65	linear	1.6 ± 1.6	237 ± 53
+ staurosporine	8	38	linear	5.7 ± 2.7	150 ± 53
+ H7	9	67	linear	-2.1 ± 8.7	76 ± 18
20 mM Ca	9	78	linear	4.7 ± 2.6	802 ± 262
10^{-5} M Ca	7	100	linear	5.5 ± 3.5	609 ± 174
10^{-7} M Ca	9	78	linear	3.1 ± 5.2	229 ± 157
++ W-7	17	77	linear	3.9 ± 1.9	364 ± 85
	n	**inhibition (%)**	**rectification**	**reversal potential (mV)**	**current inhibition (%)**
++ PMA	8	88	linear	3.6 ± 3.3	41.7 ± 7.9
++ La^{3+}	27	93	outward	7.0 ± 4.2	77.1 ± 3.4

n = number of ORNs recorded, + incubation with protein kinase inhibitor in 6 mM Ca, ++ pipetted into extracellular solution. See Materials and Methods for solutions. Values represent mean ± SEM.

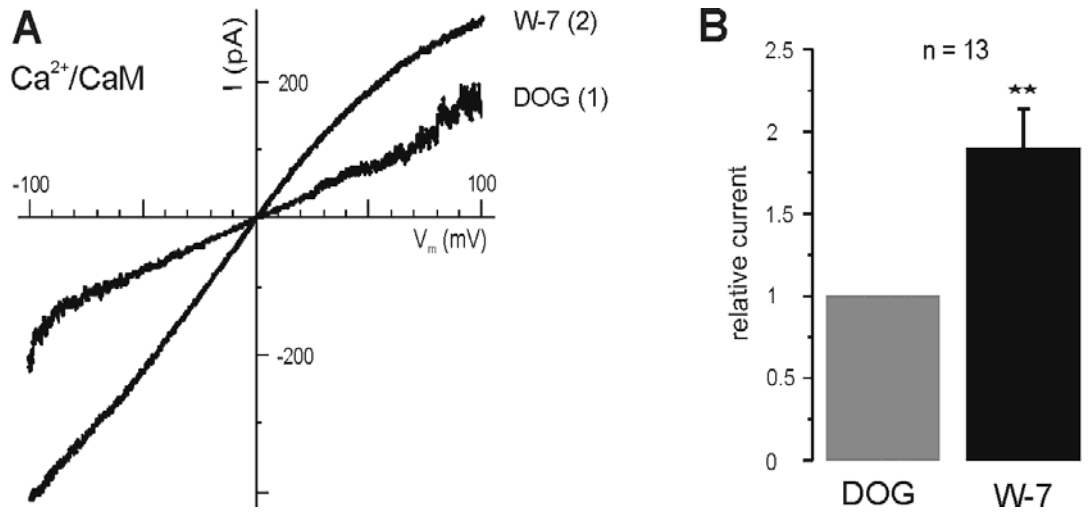

Figure 3 DOG-activated currents were decreased by Ca^{2+}/CaM. (**A**) I-V relation showing the increase of the DOG-activated current (1) upon application of 10 µM W-7 (2), a CaM antagonist. (**B**) Relative increase of the DOG-activated current after W-7-application. The difference between the relative current amplitudes was significant ($p > 0.01$). Error bars represent SEM.

amplitude recorded in standard extracellular solution without protein kinase inhibitors ($p < 0.01$). Subsequent La^{3+}-application inhibited the DOG-activated currents. When ORNs were initially stimulated with DOG, and then 10 µM H7 was applied, the DOG-activated current remained unchanged (n = 3 ORNs; data not shown).

DOG activates a current inhibited by PKC

To investigate whether PKC modulates DOG-activated currents, ORNs were stimulated with DOG, and then the PKC activator PMA was applied. Application of 250 nM PMA (Tab. 2) significantly inhibited 41.7 ± 7.9 % of the DOG-activated current ($p < 0.01$; n = 7 of 8 ORNs). Subsequent La^{3+}-application further inhibited 70.8 ± 6.6 % of the remaining current (n = 4 ORNs; Fig. 4C). In the presence of the protein kinase inhibitor H7, PMA-application did not effect the DOG-activated current (n = 3 ORNs; data not shown).

Two alternatively spliced TRP-like channel mRNAs are expressed in *M. sexta*

To investigate whether TRP-like channel mRNAs are expressed in *M. sexta*, RT-PCR experiments were performed with a primer pair directed against the putative C-terminus of the *M. sexta* TRPL homolog. Two different cDNA fragments with sequence similarity to TRP channel cDNAs could be detected in the antennae and brain of *M. sexta*. Both cDNA fragments showed the highest sequence similarity to *D. melanogaster* TRPL cDNA (82 %; Fig. 5), and thus were termed MsTRPLa and MsTRPLb. MsTRPLa had a length of 400 bp and was expressed in the adult brain, but not in the antennae (Fig. 6A). With respect to the *D. melanogaster* TRPL channel cDNA, MsTRPLa encodes the transmembrane domain 5, pore, and transmembrane domain 6. Compared to vertebrate TRP channels, MsTRPLa showed sequence similarity to the TRPC4/5 subgroup (29 %; Fig. 5). In contrast, MsTRPLb had a length of 276 bp and was exclusively expressed in the pupal and adult antennae of *M. sexta* (Fig. 6B, C). The expression level of the MsTRPLb mRNA in the antennae appeared to increase during pupal development (Fig. 6C). Sequence analyses suggest that MsTRPLb is a splice variant of MsTRPLa. Splicing apparently occurs at the end

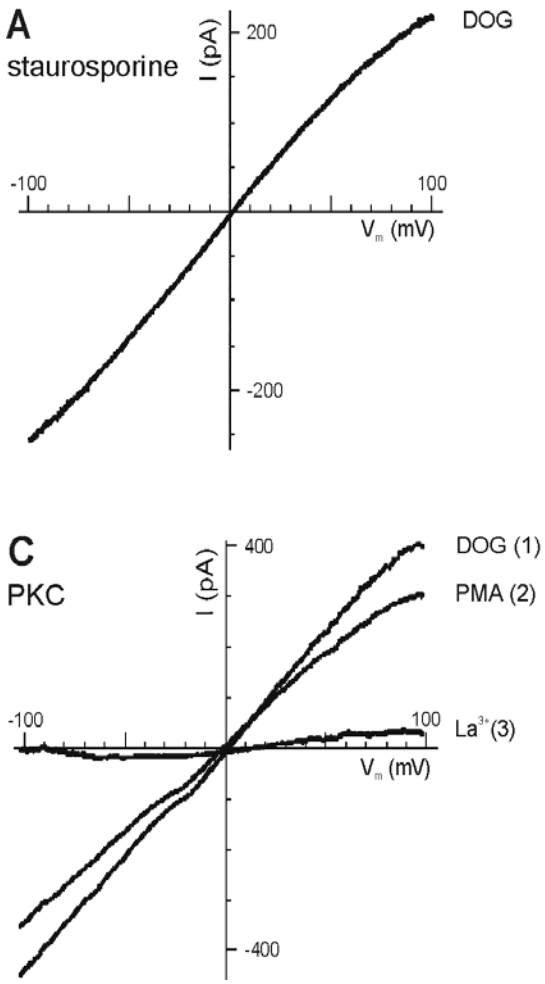

Figure 4 DOG activated currents in the presence of protein kinase inhibitors. I-V relations of DOG-activated currents (1) in the presence of 1 µM staurosporine (**A**) and 10 µM H7 (**B**). While staurosporine typically did not influence DOG-activated currents, H7 significantly reduced the respective currents. Subsequent La^{3+}-application (2) inhibited the DOG-activated currents. (**C**) The DOG-activated current (1) was decreased by 250 nM PMA (2), a PKC activator in standard extracellular solution. Subsequent La^{3+}-application (3) inhibited the remaining current.

of transmembrane domain 5 (Fig. 5) and results in a frame-shift and the generation of an early stop codon. The subsequent nonsense mRNA sequence had no sequence similarity to any available mRNA.

MsTRPLa encodes a functional TRP-like channel pore

To investigate whether the TRP-like channel fragment MsTRPLa encodes a functional channel protein, manganese influx measurements were performed with a chimeric channel protein composed of the MsTRPLa fragment and the N- and C-terminus of the hTRPC6 channel. The pore region of the hTRPC6 channel was replaced by the MsTRPLa sequence. Since the hTRPC6 channel can be activated by a G-protein coupled receptor, the YFP-tagged chimeric hTRPC6/MsTRPLa channel was co-transfected with a histamine receptor into HEK 293 cells. The chimeric hTRPC6/MsTRPLa channel localized to the plasma membrane like the hTRPC6 channel (data not shown). Fura-2 measurements showed that Mn^{2+} influx through the chimeric hTRPC6/MsTRPLa channel and the hTRPC6 channel significantly reduced the fluorescence in Fura-2-loaded HEK 293 cells ($p < 0.01$; Fig. 7); i.e. in hTPRC6-expressing cells by about 39 ± 8 % ($n = 12$) and in cells that expressed the chimeric hTPRC6/MsTRPLa channel by about 48 ± 5 % ($n = 111$; Fig. 7). The Mn^{2+}-induced decrease of fluorescence did not significantly differ between the cells expressing hTPRC6 channels and cells expressing the chimeric hTPRC6/MsTRPLa channels.

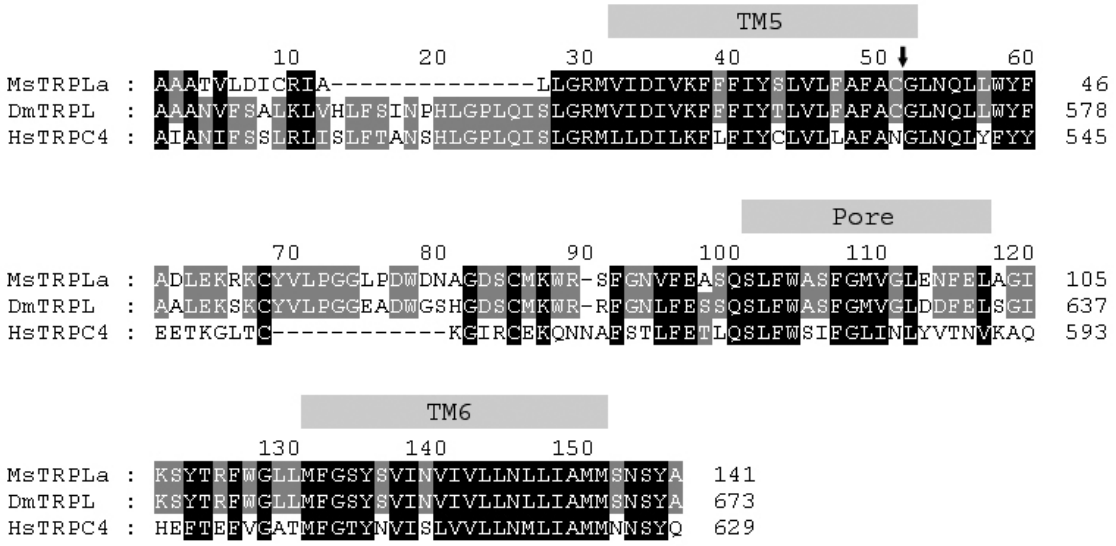

Figure 5 Sequence similarity between the putative MsTRPLa channel protein and *D. melanogaster* and vertebrate TRP channels. The putative MsTRPLa channel protein showed the highest sequence similarity to the *D. melanogaster* TRPL channel (DmTRPL). MsTRPLa also showed sequence similarity to the human TRPC4 channel (HsTRPC4). Grey boxes indicate the transmembrane domain 5 (TM5), pore, and transmembrane domain 6 (TM6) of TRP channels. Identical regions were shaded in black, conserved regions in grey, and regions without sequence similarity were white. The black arrow indicates the start of the sequence that is missing in the MsTRPLb protein.

Discussion

Here, we used whole-cell patch-clamp recordings to characterize DAG-dependent currents in cultured ORNs of *M. sexta*. We found that DAG activates a PKC-independent cation current that is modulated by Ca^{2+}/CaM. The DAG-dependent current was inhibited by La^{3+} and PKC. Thus, the electrophysiological properties of the putative DAG-gated channels correspond to those of TRP channels. Since mRNA transcripts with high sequence similarity to transcripts encoding *D. melanogaster* TRPL and vertebrate TRPC4 channels could be detected in the antennae and brain of *M. sexta* by RT-PCR, we assume that the putative moth DAG-gated channels belong to the TRP channel family.

DAG directly activates currents in moth ORNs

In the course of the olfactory transduction cascade, PLC produces equimolar concentrations of IP_3 and DAG. Previous studies suggested that DAG primarily activates PKC (Newton 2004). In ORNs of the moth *Antheraea polyphemus*, the PKC concentration 6-fold increased upon pheromone application, and this increase appeared to be triggered by DAG (Maida et al. 2000). In ORNs of *M. sexta*, PKC activated a Ca^{2+}-independent non-selective cation current (Stengl 1993). However, since protein kinase inhibitors did not prevent DAG-dependent currents in the ORNs of *S. littoralis* (Pézier et al. unpublished) and *M. sexta*, DAG also appears to directly activate ion channels in moth ORNs. Thus, like IP_3 (Boekhoff et al. 1990; Stengl 1993, 1994; Wegener et al. 1997), DAG is likely to play an essential role in the moth olfactory transduction cascade.

DAG probably acts on TRP-like channels

Our RT-PCR experiments suggest that two mRNA transcripts with high sequence similarity to the *D. melanogaster* TRPL channel mRNA are differentially expressed in the brain and antennae of *M. sexta*. Since the *D. melanogaster* TRPL

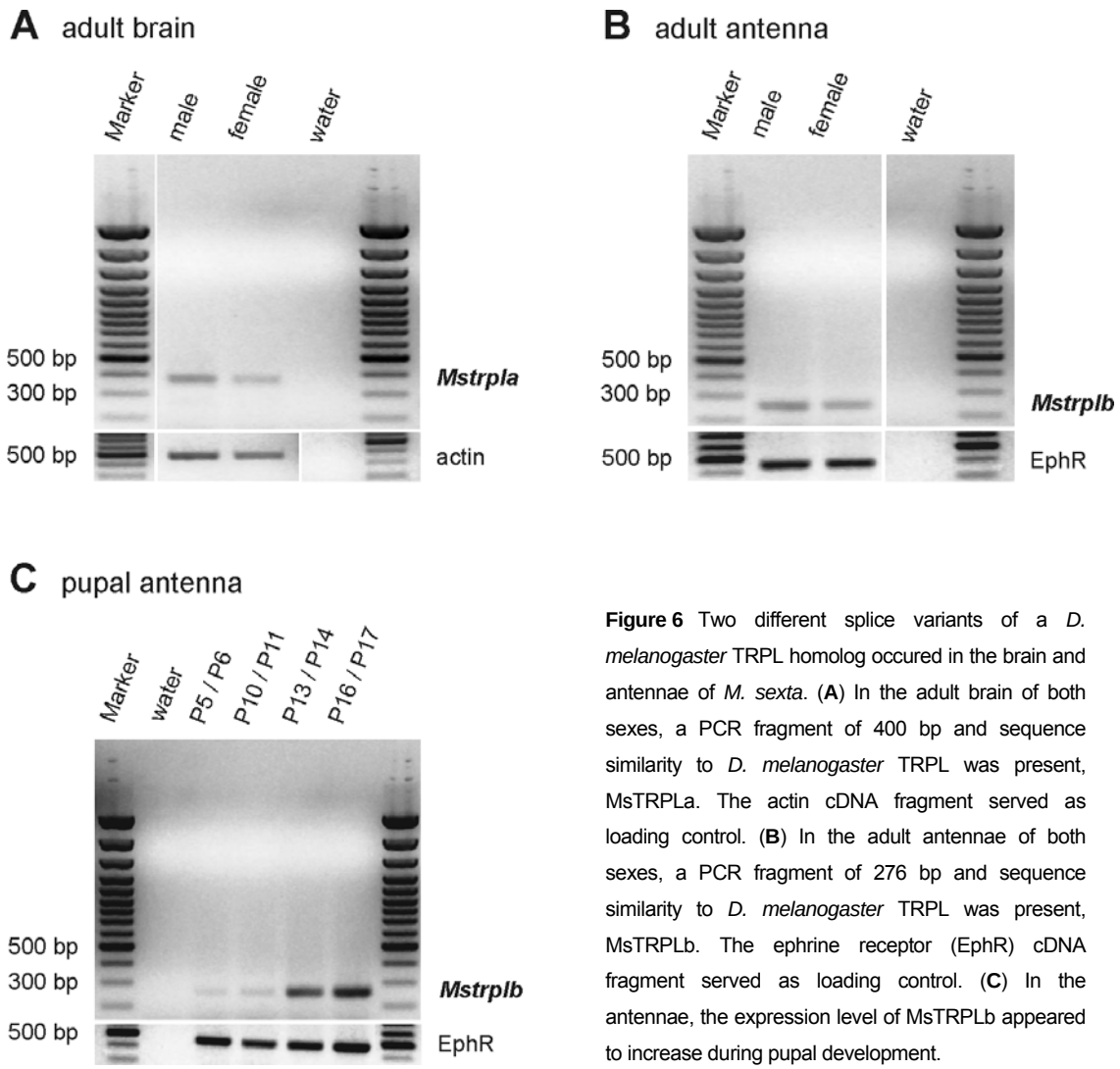

Figure 6 Two different splice variants of a *D. melanogaster* TRPL homolog occured in the brain and antennae of *M. sexta*. (**A**) In the adult brain of both sexes, a PCR fragment of 400 bp and sequence similarity to *D. melanogaster* TRPL was present, MsTRPLa. The actin cDNA fragment served as loading control. (**B**) In the adult antennae of both sexes, a PCR fragment of 276 bp and sequence similarity to *D. melanogaster* TRPL was present, MsTRPLb. The ephrine receptor (EphR) cDNA fragment served as loading control. (**C**) In the antennae, the expression level of MsTRPLb appeared to increase during pupal development.

channel is known to be directly activated by DAG and its metabolites PUFA (Chyb et al. 1999; Estacion et al. 2001), the putative moth DAG-gated channels appear to represent DAG-gated TRP channels. Therefore, the two mRNAs encoding putative moth DAG-gated channels were termed MsTRPLa and MsTRPLb. While MsTRPLa was expressed in the brain, but not in the antennae, MsTRPLb exclusively occured in the antennae. Manganese influx experiments demonstrated that MsTRPLa encodes a functional channel pore that conducts divalent cations. However, because the MsTRPLa protein also showed sequence similarity to the protein of the DAG-independent TRPC4 channel protein of vertebrates (Plant and Schaefer 2003), it is still unknown whether the encoded channel pore belongs to a DAG-gated channel. Since the cDNA fragment of MsTRPLa did not include regulatory sites, we could not test whether activation of the corresponding TRP-like channel depends on DAG. The MsTRPLb mRNA appears to be a splice variant of MsTRPLa, which lacks a functional channel pore and transmembrane domain 6. Splicing of MsTRPLa to MsTRPLb results in a frame-shift during translation and the introduction of an early stop codon in the protein sequence downstream of transmembrane domain 5. Thus, unlike MsTRPLa, MsTRPLb probably does not encode a functional TRP channel.

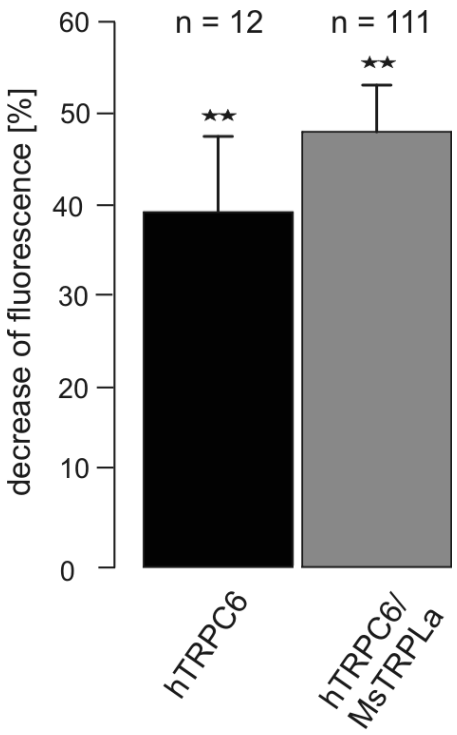

Figure 7 Manganese influx measurements on HEK 293 cells co-expressing the chimeric hTRPC6/MsTRPLa channel and the histamine receptor. In the presence of 100 mM $MnCl_2$, HEK 293 cells expressing either hTRPC6- or chimeric hTRPC6/MsTRPLa channels showed significantly reduced Fura-2 fluorescence at 360 nm upon application of 50 mM histamine ($p < 0.01$). Error bars represent SEM.

Ca^{2+}-dependency of DAG-dependent currents

Ion selectivity is an important functional feature of ion channels. TRP channels are generally classified as non-selective cation channels with diverse ion permeability, but some TRP channels are highly selective for Ca^{2+} (Minke and Cook 2002; Clapham 2005). However, the TRP-like putative DAG-gated channels in the ORNs of *M. sexta* appear to be not selective for Ca^{2+}. The amplitude of the corresponding DAG-dependent current did not significantly differ between extracellular solutions with low and high Ca^{2+} concentrations. In contrast, DAG-dependent currents in the ORNs of *S. littoralis* increased in extracellular solution with low Ca^{2+} concentration (Pézier et al. unpublished). Nevertheless, the putative DAG-gated channels in the ORNs of *M. sexta* appear to conduct Ca^{2+}, because the CaM antagonist W-7 significantly increased the amplitude of the DAG-dependent current. Thus, like TRP channels (Phillips et al. 1992; Warr and Kelly 1996; Zhu 2005), putative DAG-gated channels in *M. sexta* ORNs probably contain a Ca^{2+}/CaM binding site at the C-terminus and are negatively regulated by Ca^{2+}/CaM. The Ca^{2+}/CaM-dependent inhibition of the putative DAG-gated channels in the ORNs of *M. sexta* is weaker than that of the putative DAG-gated channels in the ORNs of *S. littoralis* (Pézier et al. unpublished). Accordingly, the putative DAG-gated channels in the ORNs of *M. sexta* appear to primarily conduct monovalent cations, and are only slightly permeable for Ca^{2+}.

PKC modulates DAG-dependent currents

The TRP/TRPL channels of *D. melanogaster* and also some vertebrate TRPC channels are activated by DAG and subsequently modulated by DAG-induced PKC (Huber et al. 1998; Okada et al. 1999; Zhang and Saffen 2001; Venkatachalam et al. 2003). Accordingly, PKC is presumed to act as a universal feedback control mechanism (Venkatachalam et al. 2003). Similar to the activation of *D. melanogaster* and vertebrate TRP channels, the activation of putative DAG-gated channels in *M. sexta* ORNs did not depend on PKC. Instead, PKC partly inhibited currents through putative DAG-gated channels. This corresponds to the finding that PKC inhibited vertebrate DAG-gated TRPC3/6/7 channels (Okada et al. 1999; Zhang and Saffen 2001; Venkatachalam et al. 2003). Since application of the protein kinase inhibitors staurosporine and H7 significantly reduced currents through putative DAG-gated channels, DAG also seems to activate PKC-dependent channels, which are known to occur in the ORNs of *M. sexta* (Stengl 1993). However, in contrast to

the Ca^{2+}-permeable putative DAG-gated channels, the PKC-dependent channels are independent to Ca^{2+} (Stengl 1993).

Conclusions

Our patch-clamp experiments showed that *M. sexta* ORNs express DAG-gated channels that are activated independently of PKC, and are modulated by Ca^{2+}/CaM. PKC and La^{3+} inhibited the putative moth DAG-gated channels. RT-PCR experiments showed that a TRP-like channel is expressed in the brain of *M. sexta*, which is most closely related to the *D. melanogaster* TRPL channel. Future experiments will analyze whether the ORNs of *M. sexta* contain DAG-gated TRP-like channels.

Acknowledgements

The authors would like to thank Cornelia Ellendt, Martina Kern, Basil el Jundi, and Stefanie Rulla for insect rearing, Philip F. Copenhaver for providing the *M. sexta* TRPL homolog primer pair, and Philippe Lucas for valuable discussions. This work was supported by DFG grant STE 531/13-1 to Monika Stengl.

References

Boekhoff I, Strotmann J, Raming K, Tareilus E, Breer H. Odorant-sensitive phospholipase C in insect antennae. *Cell Signal* 2: 49-56, 1990.

Breer H, Boekhoff I, Tareilus E. Rapid kinetics of second messenger formation in olfactory transduction. *Nature* 345: 65-68, 1990.

Chyb S, Raghu P, Hardie RC. Polyunsaturated fatty acids activate the *Drosophila* light-sensitive channels TRP and TRPL. *Nature* 397: 255-259, 1999.

Clapham DE. TRP channels as cellular sensors. *Nature* 426: 517-524, 2005.

Clapham DE, Julius D, Montell C, Schultz G. International Union of Pharmacology. XLIX. Nomenclature and structure-function relationships of transient receptor potential channels. *Pharmacol Rev* 57: 427-450, 2005.

Estacion M, Sinkins WG, Schilling WP. Regulation of the *Drosophila* transient receptor potential-like (TRPL) channels by phospholipase C-dependent mechanisms. *J Physiol* 530:1-19, 2001.

Ha KS, Exton JH. Differential translocation of protein kinase C isozymes by thrombin and platelet-derived growth factor. *J Biol Chem* 268: 10534-10539, 1993.

Hamill OP, Marty A, Neher E, Sakmann B, Sigworth FJ. Improved patch-clamp techniques for high-resolution current recording from cells and cell-free membrane patches. *Pflugers Arch* 391: 85-100, 1981.

Hansson BS. A bug's smell--research into insect olfaction. *Trends Neurosci* 25: 270-274, 2002.

Hardie RC. TRP channels in *Drosophila* photoreceptors: the lipid connection. *Cell Calcium* 33: 385-393, 2003.

Hardie RC, Minke B. The *trp* gene is essential for a light-activated Ca^{2+} channel in *Drosophila* photoreceptors. *Neuron* 8: 643-651, 1992.

Hildebrand JG. Analysis of chemical signals by nervous systems. *Proc Natl Acad Sci USA* 92: 67-74, 1995.

Hofmann T, Obukhov AG, Schaefer M, Harteneck C, Gudermann T, Schultz G. Direct activation of human TRPC6 and TRPC3 channels by diacyglycerol. *Nature* 397: 259-263, 1999.

Honda T, Amy NL, Warr CG. Identification and characterisation of genes involved in olfactory signal transduction in *Drosophila*. *8th annual meeting of AACSS (Australasian Association for Chemosensory Science)*, Heron Island, Australia, 2005.

Huber A, Sander P, Bahner M, Paulsen R. The TRP Ca^{2+} channel assembled in a signaling complex by the PDZ domain protein INAD is phosphorylated throughthe interaction with protein kinase C (ePKC). *FEBS Lett* 425: 317-322, 1998.

Jacquin-Joly E, Francois MC, Burnet M, Lucas P, Bourrat F, Maida R. Expression pattern in the antennae of a newly isolated lepidopteran Gq protein alpha subunit cDNA. *Eur J Biochem* 269, 2133-2142, 2002.

Jung S, Muhle A, Schaefer M, Strotmann R, Schultz G, Plant TD. Lanthanides potentiate TRPC5 currents by an action at extracellular sites close to the pore mouth. *J Biol Chem* 278: 3562-3571, 2003.

Kaissling KE. Physiology of pheromone reception in insects (an example of moths). *ANIR* 6: 73-91, 2004.

Kaissling KE, Priesner E. Smell threshold of the silkworm. *Naturwissenschaften* 57: 23-28, 1970.

Laue M, Maida R, Redkozubov A. G-protein activation, identification and immunolocalization in pheromone-sensitive sensilla trichoidea of moths. *Cell Tiss Res* 288: 149-158, 1997.

Lee YM, Kim BJ, Kim HJ, Yang DK, Zhu MX, Lee KP, So K, Kim W. TRPC5 as a candidate for the nonselective cation channel activated by muscarinic stimulation in murine stomach. *Am J Physiol* 284: G604–G616, 2003.

Liman ER, Corey DP, Dulac C. TRPC2: A candidate transduction channels for mammalian pheromone sensory signaling. *Proc Natl Acad Sci USA* 96: 5791-5796, 1999.

Lucas P, Ukhanov K, Leinders-Zufall T, Zufall F. A

diacylglycerol-gated cation channel in vomeronasal neuron dendrites is impaired in TRPC2 mutant mice: Mechanisms of pheromone transduction. *Neuron* 40: 551-561, 2003.

Maida R, Redkozubov A, Ziegelberger G. Identification of PLCβ and PKC in pheromone receptor neurons of *Antheraea polyphemus*. *Neuroreport* 11: 1773-1776, 2000.

Menco BPhM, Carr VMcM, Ezeh PI, Liman ER, Yankova MP. Ultrastructural localization of G-proteins and the channel protein TRPC2 to microvilli of rat vomeronasal receptor cells. *J Comp Neurol* 438: 468-489, 2001.

Minke B, Cook B. TRP channel proteins and signal transduction. *Physiol Rev* 82: 429-472, 2002.

Newton AC. Diacylglycerol's affair with protein kinase C turns 25. *Trends in Pharmacol Sci* 25: 175-177, 2004.

Niemeyer BA, Suzuki E, Scott K, Jalink K, Zuker CS. The *Drosophila* light-activated conductance is composed of the two channels TRP and TRPL. *Cell* 85: 651-659, 1996.

Okada T, Inoue R, Yamazaki K, Maeda A, Kurosaki T, Yamakuni T, Tanaka I, Shimizu S, Ikenaka K, Imoto K, Mori Y. Molecular and functional characterization of a novel mouse transient receptor potential protein homologue TRP7. *J Biol Chem* 274: 27359-27370, 1999.

Phillips AM, Bull A, Kelly LE. Identification of a *Drosophila* gene encoding a calmodulin-binding protein with homology to the *trp* transduction gene. *Neuron* 8: 631-642, 1992.

Plant TD, Schaefer M. TRPC4 and TRPC5: receptor-activated Ca^{2+}-permeable nonselective cation channels. *Cell Calcium* 33: 441-450, 2003.

Pophof B, Van der Goes van Naters W. Activation and inhibition of the transduction process in silkmoth olfactory receptor neurons. *Chem. Senses* 27: 435-443, 2002.

Stengl M. Intracellular-messenger-mediated cation channels in cultured olfactory receptor neurons. *J Exp Biol* 178: 125-147, 1993.

Stengl M. Inositol-trisphosphate-dependent calcium currents precede cation currents in insect olfactory receptor neurons in vitro. *J Comp Physiol [A]* 174: 187-194, 1994.

Stengl M, Hildebrand JG. Insect olfactory neurons in vitro: morphological and immunocytochemical characterization of male-specific antennal receptor cells from developing antennae of male *Manduca sexta*. *J Neurosci* 10: 837-847, 1990.

Stengl M, Zufall F, Hatt H, Hildebrand JG. Olfactory receptor neurons from antennae of developing male *Manduca sexta* respond to components of the species-specific sex pheromone in vitro. *J Neurosci* 12: 2523-2531, 1992.

Stortkuhl KF, Hovemann BT, Carlson JR. Olfactory adaptation depends on the Trp Ca^{2+} channel in *Drosophila*. *J Neurosci* 19: 4839-4846, 1999.

Trebak G, Bird GStJ, McKay RR, Birnbaumer L, Putney JW. Signaling mechanism for receptor-activated TRPC3 channels. *J Biol Chem* 278: 16244-16252, 2003.

Tutdibi O, Brinkmeier H, Rudel R, Fohr KJ. Increased calcium entry into dystrophin-deficient muscle fibres of MDX and ADR-MDX mice is reduced by ion channel blockers. *J Physiol* 515: 859-868, 1999.

Vazquez G, Wedel BJ, Aziz O, Trebak M, Putney JW. The mammalian TRPC cation channels. *Biochim Biophys Acta* 1742: 21-36, 2004.

Venkatachalam K, Zheng F, Gill DL. Regulation of canonical transient recpetor potential (TRPC) channel function by diacylglycerol and protein kinase C. *J Biol Chem* 278: 29031-29040, 2003.

Venkatachalam K, Montell C. TRP channels. *Annu Rev Biochem* 76: 387-417, 2007.

Warr CG, Kelly LE. Identification and characterization of two distinct calmodulin-binding sites in the TRPL ion-channel protein of *Drosophila melanogaster*. *Biochem J* 314: 497-503, 1996.

Wegener JW, Breer H, Hanke W. Second messenger-controlled membrane conductance in locust (*Locusta migratoria*) olfactory neurons. *J Insect Physiol* 43: 595-603, 1997.

Zhang L, Saffen D. Muscarinic acetylcholine receptor regulation of TRPC6 Ca^{2+} channel isoforms. *J Biol Chem* 276: 13331-13339, 2001.

Zhu MX. Multiple roles of calmodulin and other Ca^{2+}-binding proteins in the functional regulation of TRP channels. *Eur J Physiol* 451: 105-115, 2005.

Zufall F, Hatt H. Dual activation of a sex pheromone-dependent ion channel from insect olfactory dendrites by protein kinase C activators and cyclic GMP. *Proc Natl Acad Sci USA* 88: 8520-8524, 1991.

Zufall F, Stengl M, Franke C, Hildebrand JG, Hatt H. Ionic currents of cultured olfactory receptor neurons from antennae of male *Manduca sexta*. *J Neurosci* 11: 956-965, 1991.

III. Pharmacological investigation of protein kinase C- and cGMP-dependent ion channels in cultured olfactory receptor neurons of the hawkmoth *Manduca sexta*.

Dolzer J, Krannich S, Stengl M.

Chem Senses, in press.

ABSTRACT	61
INTRODUCTION	61
MATERIALS AND METHODS	63
Cell cultures	63
Solutions	63
Electrophysiology	64
Data analysis of single channel recordings	65
RESULTS	66
Ion channel classes observed after excision into high Ca^{2+}, in the presence or absence of PMA and/or 8bcGMP	67
Small-conductance ion channels (2 to 20 pS)	70
Medium-conductance ion channels (20 to 100 pS)	71
Large-conductance ion channels (>100 pS)	72
DISCUSSION	73
Second messenger-mediated ion channels	73
A hypothesis of sensitivity modulation in ORNs	75
ACKNOWLEDGEMENTS	76
REFERENCES	76

Pharmacological investigation of protein kinase C- and cGMP-dependent ion channels in cultured olfactory receptor neurons of the hawkmoth *Manduca sexta*

Jan Dolzer[1], Steffi Krannich[1,2] and Monika Stengl[1,2]

[1]Biology, Animal Physiology, Philipps-University of Marburg, Karl-von-Frisch-Straße 8, Marburg D-35032, Germany

[2]Institute of Biology, Animal Physiology, University of Kassel, Heinrich-Plett-Straße 40, Kassel D-34132, Germany

Correspondence to be sent to: Monika Stengl, Biology, Animal Physiology, Philipps-University of Marburg, Karl-von-Frisch-Straße 8, Marburg D-35032, Germany, e-mail: stengl@staff.uni-marburg.de

Abstract

In the hawkmoth *Manduca sexta*, pheromone stimuli of different strength and duration rise the intracellular Ca^{2+} concentration in olfactory receptor neurons. While second-long pheromone stimuli activate protein kinase C (PKC), which apparently underlies processes of short-term adaptation, minute-long pheromone stimuli elevate cGMP concentrations, which correlates with time courses of long-term adaptation. To identify ion channels involved in the sliding adjustment of olfactory sensitivity, inside-out patch-clamp recordings on cultured olfactory receptor neurons of *Manduca sexta* were performed to characterize Ca^{2+}-, PKC-, and cGMP-dependent ion channels.

Stepping to positive holding potentials in high intracellular Ca^{2+} elicits different Ca^{2+}-dependent ion channels, namely small-conductance channels (2 to 20 pS), medium-conductance channels (20 to 100 pS), and large-conductance channels (>100 pS). Ion channels of 40, 60 and 70 pS opened after PKC activation, while 10 and >100 pS channels were observed less frequently. Application of 8bcGMP opened 55 and 70 pS channels and increased the open probability of >100 pS channels, while even in the presence of phorbol ester 40 pS channels were inhibited. Thus, cGMP elevations activate a different set of ion channels as compared to PKC and suppress at least one PKC-dependent ion channel.

Keywords: Olfactory adaptation, *Manduca sexta,* insect olfactory transduction, ion channels, patch-clamp.

Introduction

Adaptation, the adjustment of sensitivity in response to adequate stimulation, enlarges the dynamic range of an olfactory receptor neuron (ORN) without loss of resolution, and provides the first stage of processing sensory information. In vertebrate ORNs, three different mechanisms of olfactory adaptation coexist: short-term adaptation, desensitization, and long-term adaptation. These three olfactory adaptation mechanisms vary in their time courses and pharmacological properties (Zufall and Leinders-Zufall 2000). The influx of Ca^{2+} through cyclic nucleotide-gated (CNG) channels and the Ca^{2+}-dependent modulation of CNG channels plays a

crucial role as a feedback signal in vertebrate olfactory adaptation (Zufall and Leinders-Zufall 2000; Matthews and Reisert 2003; Pifferi et al. 2006). In insects, most studies on olfactory adaptation mechanisms were accumulated in moths (Zack-Strausfeld and Kaissling 1986; Kaissling et al. 1986; Marion-Poll and Tobin 1992; Dolzer et al. 2003; Flecke et al. 2006). In *Manduca sexta*, our extracellular recordings revealed at least three different mechanisms of olfactory adaptation. One that decreases the amplitude and the initial slope of the sensillum potential, one that accelerates the repolarization phase, and one that decreases the action potential response even further than the parameters of the sensillum potential (Dolzer et al. 2003). Whether these different moth olfactory adaptation mechanisms correspond to the different mechanisms in vertebrates, and what types of ion channels are involved in moths remained elusive.

Previous patch-clamp studies in moth ORNs showed that pheromone stimulation activates a phospholipase C which elicits transient IP_3-dependent Ca^{2+} influx (Boekhoff et al. 1990; Stengl 1994; Wegener et al. 1997; Stengl et al. 1999). The transient influx of Ca^{2+} triggers a temporal sequence of Ca^{2+}-dependent currents (Stengl 1993). Within the first milliseconds of pheromone application a directly Ca^{2+}-dependent, Ca^{2+}-permeable inwardly rectified cation channel opened with a conductance of about 20 pS at 25 mV and 50 pS at -100 mV holding potential (Stengl et al. 1992; Stengl 1993). Because the lipophilic pheromone cannot be easily removed except after addition of pheromone binding protein or bovine serum albumine, pheromone was usually present for several seconds and minutes after application (Stengl et al. 1992; Stengl 1993). This led to further elevation of the intracellular Ca^{2+} concentration as measured via patch-clamp recordings (or via Ca^{2+}-imaging with FURA, Monika Stengl and Bernd Lindemann, unpublished). The intracellular Ca^{2+} increase finally blocked Ca^{2+}-dependent cation channels and caused activation of a protein kinase C (PKC). PKC activated TEA-blockable cation currents with apparently little Ca^{2+} conductance, caused further depolarization, but decreased the intracellular Ca^{2+} concentrations (Stengl 1993, 1994; Stengl et al. 1999). We, therefore, hypothesize that the duration of the pheromone stimulus, the corresponding increase of the intracellular Ca^{2+} concentration, and the resulting regulation of PKC activity determine pheromone-sensitivity of the antenna and might underlie mechanisms of short-term adaptation. Short-term adaptation in moths implies a fast decrease in pheromone-sensitivity and lasts less than 5 min, whereas long-term adaptation occurs more slowly and can last for several hours. Corresponding with time courses of long-term adaptation, pheromone stimuli induced minute-long rises in cGMP levels in moth antennae (Ziegelberger et al. 1990; Boekhoff et al. 1993; Redkozubov 2000). In *M. sexta*, minute-long pheromone stimulation resulted in cGMP rises in pheromone-sensitive ORNs and their respective supporting cells (Stengl et al. 2001) and adapts the action potential response but not the sensilla potential (Flecke et al. 2006). This suggests that Ca^{2+}-, PKC-, and cGMP-dependent processes might underlie mechanisms of olfactory short- and long-term adaptation in *M. sexta* and might orchestrate a sliding adjustment of odor sensitivity.

To further test this hypothesis, we initially characterized Ca^{2+}-, PKC-, and cGMP-dependent ion channels in cultured ORNs of *M. sexta.* Inside-out patches were excised into bath solutions with high (intracellular) Ca^{2+} to activate Ca^{2+}-dependent cation channels, previously shown to be pheromone-dependent

(Stengl 1993; 1994). Then, the Ca^{2+}-dependent ion channels were stimulated with the PKC activator phorbol ester (PMA, phorbol 12-myristate 13-acetate) and/or the membrane permeable cGMP analog 8-bromo cGMP (8bcGMP) to search for differential second messenger modulation. Application of PKC and cGMP activated different populations of cation channels. Furthermore, cGMP blocked at least one population of cation channels that opened PKC-dependently. Thus, our results are consistent with our hypothesis that different sets of second messenger-mediated ion channels are involved in the different mechanisms of olfactory adaptation, which depend on stimulus length and strength.

Materials and Methods

Unless indicated otherwise, all chemicals and biochemicals were obtained from Sigma (Deisenhofen, Germany), all cell culture media from Gibco (Karlsruhe, Germany). The salts for the electrophysiological salines were obtained from Merck (Frankfurt/M, Germany).

Cell cultures

Cell cultures were prepared according to Stengl and Hildebrand (1990). Briefly, male pupae were staged using external markers (Jindra et al. 1997). For dispersion, animals were anesthetized by cooling, and the antennae were dissected in Hank's Balanced Salt Solution with Penicillin/ Streptomycin (HBSS/PS). Antennal tubes were washed in HBSS/PS and incubated in HBSS/PS + 7 mM EGTA at 37°C for 5 min. The tissue was digested with papain (1 mg/ml in HBSS/PS) in two batches for 5 and 10 min at 37°C, respectively. The digestion was stopped by adding Leibovitz medium (L-15) supplemented with 10 % fetal bovine serum. Cells were centrifuged at 70 to 110 rcf for 5 to 8 min and the pellet was resuspended in HBSS/PS. The cells were plated out in glass-bottom culture dishes, which were coated with Concanavalin A and Poly-L-Lysin, and allowed to settle for 15 to 30 min before adding 1 ml of a 2:1 cell culture medium. The medium was replaced completely within 24 h after dispersion. Every 4 to 7 days part of the medium was replaced subsequently. The cell cultures were used for electrophysiology from 10 days up to 4 weeks after plating.

Solutions

All solutions were adjusted to pH 7.1-7.2. The osmolality was adjusted with mannitol to 370-390 mosmol for bath solutions and 330-350 mosmol for pipette solutions, respectively. During recordings cells were kept in 1 ml bath solution. Drugs were applied either by puff application with a PicoSpritzer (General Valve, Fairfield, New Jersey), or pipetted into the bath. Each recording was started under standard bath and high CsCl intracellular pipette conditions to activate sustained Ca^{2+}-dependent non-selective cation channels and to minimize K^+ channel activity. To recognize and stabilize Ca^{2+}-dependent inwardly rectified cation channels, the Ca^{2+} concentration in the patch pipette was buffered. Then, to further characterize Ca^{2+}-dependent ion channels, voltage step protocols were employed and bath solutions were exchanged. The change of solutions was monitored by about 0.1 % food dye (McCormick, Baltimore, Maryland) added to the bath solutions. Exchange of bath solutions took less than 30 s. The respective agents were applied to analyze whether ion channels were affected in opposite or synergistic ways by PKC or cGMP. Standard bath solution contained (in mM): NaCl 156; KCl 4; $CaCl_2$ 6; glucose 5; HEPES 10. To block voltage-dependent sodium channels 10^{-8} M tetrodotoxin (TTX) was added to all bath solutions. In order to determine Ca^{2+}-

dependence of ion channels, in few experiments the bath solution contained a reduced Ca^{2+} concentration (10^{-7} M). In order to separate different cationic channels, the bath solutions contained 6 mM nickel, 1 or 10 mM zinc, 20 mM tetraethylammonium (TEA), or 160 mM N-methyl-D-glucamin (NMDG). Bath solutions with reduced chloride concentration contained acetate- or D-gluconate salts (156 mM NaAc, 4 mM KAc, 6 mM $CaAc_2$, 10 mM Hepes, 5 mM glucose, 10^{-8} M TTX).

The standard pipette solution contained (in mM): CsCl 160; $CaCl_2$ 0.5; BAPTA 1 (EGTA 11) and HEPES 10. The Ca^{2+} concentration was buffered to mimic low extracellular Ca^{2+} conditions, which were shown to stabilize otherwise transient Ca^{2+}-dependent and pheromone-dependent currents (Stengl 1993, 1994). Furthermore, 20 mM TEA, 10 mM zinc or 6 mM Ca^{2+} were used in some experiments to isolate the interdependently activated ion channels. In analogy to bath solutions, pipette solutions with reduced chloride concentrations contained acetate- or D-gluconate salt.

The PKC activator phorbol ester (PMA, phorbol 12-myristate 13-acetate; n = 74) was applied by puff application onto the recorded ORNs at a concentration of 10 nM (application volume <10 nl of the respective stock solution, for 2 - 10 msec pulse duration). In 2 - 10 msec pulses, the membrane-permeable cGMP analog 8-bromo cGMP (8bcGMP) was applied at concentrations of 10 mM (n = 49), 100 µM (n = 15), 500 µM (n = 15), and 5 µM (n = 5) dissolved in extracellular solution. Furthermore, concentrations of 8bcGMP of 100 µM (n = 2) and 10 µM (n = 7) were pipetted into the bath solution. Because a detailed analysis of all application modes and concentrations did not reveal consistent differences they were pooled. All control applications were puff applications with standard bath solution. Because of the typically delayed action of 8bcGMP, activation within 5 min after drug- or control application was scored as application-dependent.

Since different types of ion channels always opened at the same time and could not be obtained in isolation, three different channel classes were formed depending on their conductance. Small-conductance channels showed a maximal conductance of 20 pS at all potentials tested. Medium-conductance channels expressed conductances of more than 20 pS up to less than 100 pS. Also, rectifying cation channels with conductances of less than 20 pS at some potentials but larger than 20 pS at other potentials were grouped to the medium-conductance channels. Ion channels of more than 100 pS conductance were classified as large-conductance channels.

Electrophysiology

For patch-clamp recordings the culture medium was removed. Cell cultures were washed with about 1 ml of bath solution, and the dish was placed in the recording setup with about the same volume of bath solution. The culture dishes were continuously perfused with bath solution at a low flow rate, using a gravity feed perfusion system equipped with 6 reservoirs and a Teflon rotary valve (Rheodyne, Rohnert Park, California). The cells were viewed with an inverted microscope (Axiovert 35 or 135, Zeiss, Göttingen, Germany) equipped with phase contrast optics and an additional heat filter (KG-1, Zeiss). ORNs were identified by their round or only slightly spindle-shaped soma of 5 to 10 µm diameter (Stengl and Hildebrand 1990). The patch-clamp headstage and the drug application pipette were mounted on electronic micromanipulators (Luigs & Neumann, Ratingen, Germany) attached to aluminum profiles (X-95, Newport, Irvine, California).

Inside-out patch-clamp recordings were performed according to standard procedures (Hamill et al. 1981). For all recordings shown, upward deflections from the closed level are outward movements of positive ions, downward deflections from the closed level are inward movement of positive ions. Since the cultured cells deteriorated quickly in bath solutions with low Ca^{2+} concentration, the cell cultures were usually kept in standard bath solutions (high Ca^{2+}). Inside-out patches were excised into bath solutions containing high Ca^{2+} to search for Ca^{2+} activated ion channels (Stengl 1993, 1994; Stengl et al. 1992, 1999). Inside-out configurations were verified at the beginning of the recording via application of voltage steps which should show fast transitions of currents, clear voltage control, and expected reversal potentials of previously characterized cation channels. Cell-attached recordings were not possible, because of electrode drift, which caused patch excision into the inside-out configuration.

Signals were amplified with an Axopatch 1D amplifier (Axon Instruments, Union City, California), passed through the built-in anti-aliasing filter at a cutoff frequency of 2 kHz, digitized in a Digidata 1200B digitizer (Axon Instruments) at a sampling rate of 10 or 20 kHz, and stored and analyzed using pCLAMP software (versions 6 to 8, Axon Instruments). In addition, the signals were continuously recorded on a strip chart recorder (EasyGraf, Gould, Valley View, Ohio) and stored on DAT (DTR-1202, Bio-Logic, Claix, France). When signals were digitized offline from the tape, they were either passed through the amplifier or through an external anti-aliasing filter (900C/9L8L, Frequency Devices, Haverhill, Massachusetts) and digitized at different sampling rates, depending on the filter setting.

Data analysis of single channel recordings

In single-channel recordings, single-unit currents were determined from amplitude histograms created with Fetchan 6 (pCLAMP). When the data had to be lowpass-filtered to improve the signal-to-noise ratio, either the analog 8-pole Bessel filter of the amplifier was used to condition signals during off-line digitization from the DAT tape, or the data were conditioned with the digital Gaussian filters implemented in Fetchan 6 or Clampfit 8. The cutoff frequencies were typically between 200 Hz and 1 kHz, but in rare cases cutoff frequencies as low as 50 Hz were also used. The amplitude histograms were fitted with Gaussian functions (2^{nd} to 6^{th} order) in pStat 6 with manual seeding of the initial values. The number of terms was determined manually, often by comparison of different models. Model comparison, implemented in pStat was not used. Although the measures that describe the Goodness of Fit put out by the software were recorded, the quality of the fits was almost exclusively judged by eye. The current-voltage (I-V) relations were determined by one of two methods, depending on the experiment. When a single or few copies of only one channel type were active for a longer period, the holding potential was stepped to different values, and the single-unit currents were determined for each potential. Potentials are given as potential across the membrane. Since typically many copies of one channel type, or different channels were open or exhibited transitions, voltage step protocols with step duration of 100 ms were applied. To exclude effects of voltage-dependent activation or inactivation, two types of step protocols were applied successively. First the holding potential was stepped from negative (typically -120 mV) to positive (max 100 mV) potentials across the membrane in 20 mV increments. Then the potential was stepped from

0 mV to increasing absolute potential values to negative and positive direction at alternating signs (0 mV, -20 mV, +20 mV, -40 mV, +40 mV, etc.). The I-V relations determined in this way were only used for further analysis, if (i) the steady-state current before and after a step protocol was identical, and (ii) there was evidence for the contribution of single-unit currents to the steady-state current (such as transitions before or after the step protocols). In most cases, only outward currents at positive holding potentials allowed to discern single-channel openings for the calculation of I-V curves. Thus, single-channel conductances were usually calculated at positive command potentials. Generalized linear model analysis with binomial error distribution was used for statistical analysis to estimate channel activity in response to high intracellular Ca^{2+}, the PKC-activator PMA and/or 8bcGMP (Crawley 2002).

Results

To identify second messenger-dependent ion channels involved in sensitivity adjustment to odor concentration and duration, single-channel patch-clamp recordings were performed on primary cell

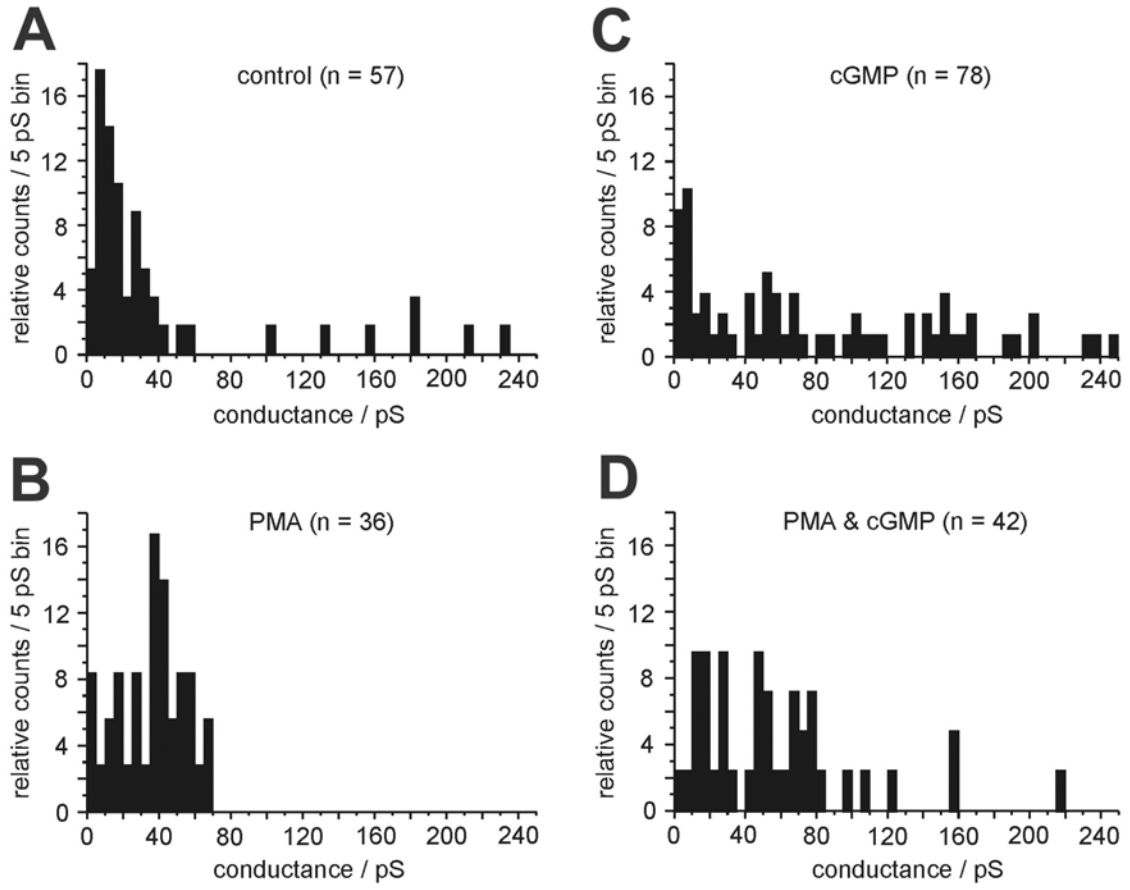

Figure 1 Frequency distribution histograms of single-channel conductances recorded with or without application of phorbol ester (PMA) and/or 8-bromo cGMP (8bcGMP) at 40 to 60 mV holding potential. **A.** In the absence of 8bcGMP and PMA, most recorded single-channels had a conductance below 60 pS. Single-channel conductances >100 pS were recorded occasionally. **B.** After application of PMA, single-channels with 10 and >100 pS were less frequently recorded. Instead, single-channels with a conductance of about 40, 60, and 70 pS were recorded. **C.** After application of 8bcGMP there was a tendency to large single-unit conductances. Single-channel conductances of about 10, 55, 70, and >100 pS were recorded. The 40 pS conductances were absent. **D.** After 8bcGMP and PMA application fewer 10 pS small-conductance channels were distinguishable among the currents that developed. The 40 pS conductances were absent. For statistical analysis see text.

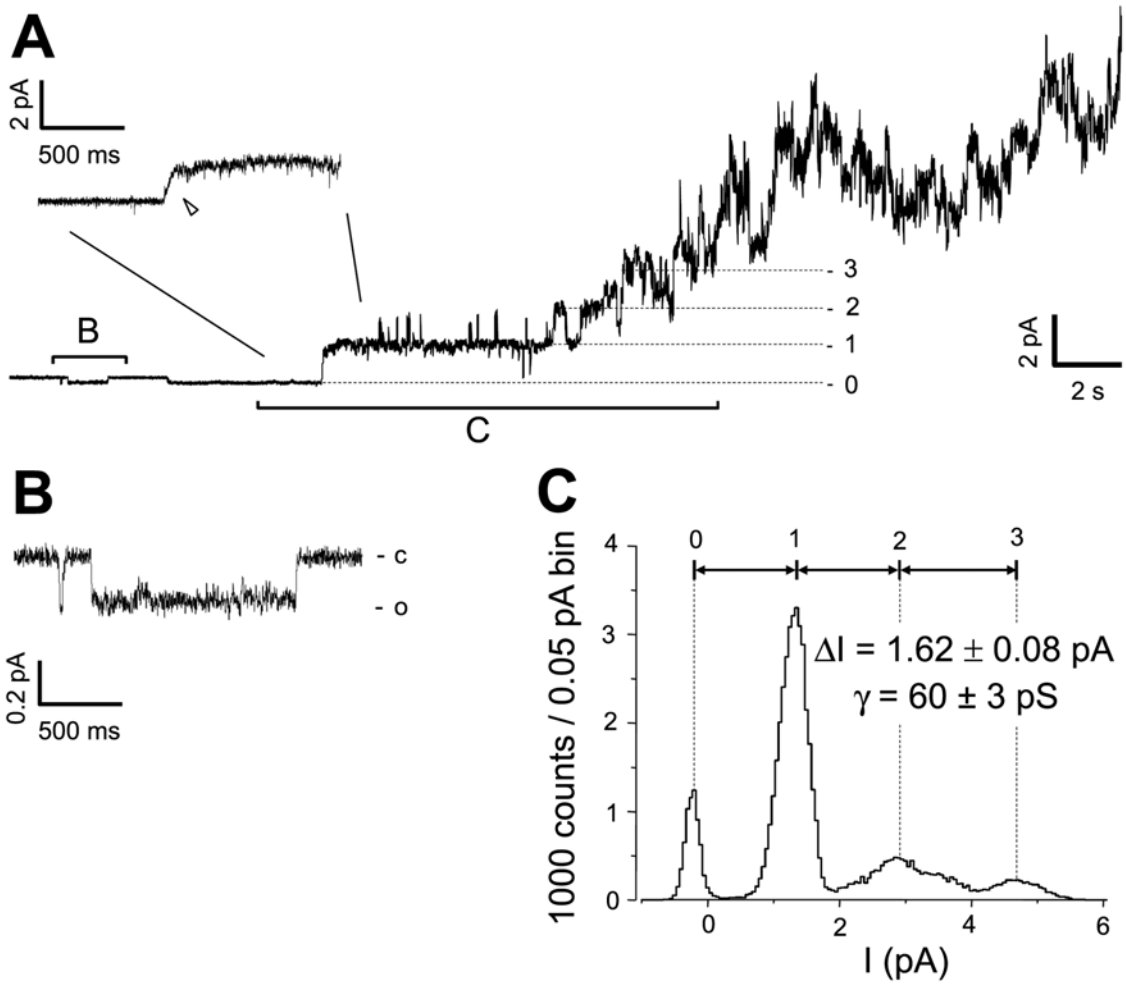

Figure 2 Small- and medium-conductance channels in cultured moth ORNs. **A.** A 60 pS channel was observed after previous PMA-application in an inside-out recording at +27 mV membrane potential. PMA was present in the dish before patch excision. The enlarged insert shows slow channel opening due to non-resolved substates (arrowhead). **B.** Before the activation of the medium-conductance channels a small-conductance channel with very long dwell times was active. This channel conducted inward currents at the positive membrane potential. **C.** Amplitude histogram of the section indicated in **A**. The numbers above the peaks correspond to the current levels indicated in **A**. The differences in the current levels (ΔI) were 1.62 ± 0.08 pA, corresponding to a single-unit conductance (γ) of 60 ± 3 pS (mean ± SD). After the activation of the third channel copy, distinct current levels could not be discerned anymore. Downward deflections from the closed state indicate inward current of positive ions, from the patch-electrode through the patch into the bath.

cultures of antennal ORNs of *M. sexta.* Ion channels were studied in response to high intracellular Ca^{2+}, the PKC-activator PMA and/or 8bcGMP. In inside-out patch-clamp recordings in high Ca^{2+} bath solution different ion channels were distinguished according to conductance, reversal potential, I-V relation and pharmacology. We focused on the effects of PKC and 8bcGMP on non-selective cation channels of medium-sized conductance and characterized Ca^{2+}-dependent channels that are closed by PKC and PKC-dependent ion channels that are closed by cGMP.

Ion channel classes observed after excision into high Ca^{2+}, in the presence or absence of PMA and/or 8bcGMP

Because pheromone stimulation causes rises in intracellular Ca^{2+} and activates a sequence of Ca^{2+}-dependent cation channels (Stengl 1993,

1994; Stengl et al. 1999) we, therefore, excised inside-out patches into solutions with high Ca^{2+}. In a total of 116 patch-clamp experiments, three classes of ion channels, small (≤ 20 pS), medium (between 20 and 100 pS), and large (>100 pS) were regularly recorded in high Ca^{2+} bath solution (Figs. 1, 2, 8). As judged from the reversal potential, from ion exchange-, and from blocking experiments, at least some of the small-conductance channels appeared to be Ca^{2+} channels (Figs. 1, 2; see below). These channels were not further analyzed, to focus on non-specific cation channels. The medium-conductance channels were mostly non-selective cation channels, because they reversed around 0 mV membrane potential under all ionic conditions and expressed considerable inward currents. Fewer K^+ channels with small outward currents at positive membrane potentials and without inward currents were also among the medium-conductance channels. The large-conductance channel-like events were apparently caused by Ca^{2+}-dependent, synchronized openings of chloride channels and non-selective cation channels as judged from the ion exchange and blocking experiments.

In the following, observations on patch excision-activated, PKC- and cGMP-dependent ion channels are summarized, normalized, quantified, and statistically analyzed (n = 213 experiments in 116 different recordings; Fig. 1). Then, the most prominent types of non-selective cation channels, namely about 30/35 pS, 40 pS, 55 pS, 60 pS, and 70 pS channels are further characterized. Recordings expressing very large currents without recognizable single-channel transitions were not included in the quantitative analysis.

Under control conditions (n = 57; Fig. 1A), without application of 8bcGMP and in the absence of PMA, mostly small-conductance channels (10-20 pS) and some medium- (about 30 pS), and large-conductance (>100 pS) channels opened. Pre-exposure to PMA (n = 36; Fig. 1B, 2) decreased the probability to detect 10 pS small- and >100 pS large-conductance channels. Instead, predominantly 40 and 60 pS medium-conductance channels opened, and few 70 pS medium-conductance channels were detected. Statistical analysis revealed a significant difference in the distribution of medium-conductance channels between control and the presence of PMA (Fig. 1A, B; $p < 0.05$), with significantly more openings of 40 pS medium-conductance channels in the presence of PMA ($p < 0.05$).

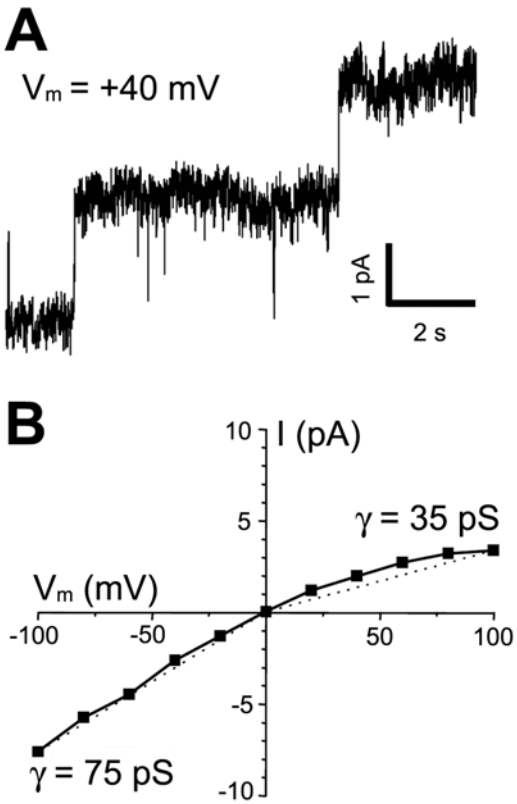

Figure 3 Patch excision-activated a medium-conductance channel of about 35 pS at positive holding potentials. **A.** A medium-conductance channel with dwell times of many seconds was active after patch-excision. **B.** A single-channel I-V relation showed that the medium-conductance channel is an inward rectifier with conductances (γ) of about 35 pS at positive potentials and 75 pS at negative potentials.

In the presence of 8bcGMP (n = 78; Fig. 1C, 6, 7), 10 pS small-, 55 and 70 pS medium-, and >100 pS large-conductance channels were observed. The 30 pS medium-conductance channels were less frequently detected as compared to recordings in the absence of 8bcGMP (Figs. 1A, B). Statistical analysis revealed a significant difference in the distribution of medium-conductance channels between the presence of PMA and the presence of 8bcGMP (Fig. 1B, C; $p < 0.01$), with significantly more openings of 40 pS channels in the presence of PMA ($p < 0.01$). For the large-conductance channels, significant differences between control and the presence of 8bcGMP (Fig. 1A, C; $p < 0.05$), as well as between the presence of PMA and the presence of 8bcGMP (Fig. 1B, C; $p < 0.05$) were observed.

After 8bcGMP application and additional pre-exposure to PMA (n = 42, Fig. 1D) small-conductance channels, and about 30 and 50 pS medium-conductance channels opened frequently. The 10 pS small- and 40 pS medium-conductance channels were less frequently recorded. Statistical analysis revealed a significant difference in the distribution of medium-conductance channels between the presence of 8bcGMP alone and the presence of 8bcGMP and PMA (Fig. 1C, D; $p < 0.01$). The open probability of 10 pS small-conductance channels was significantly reduced in the

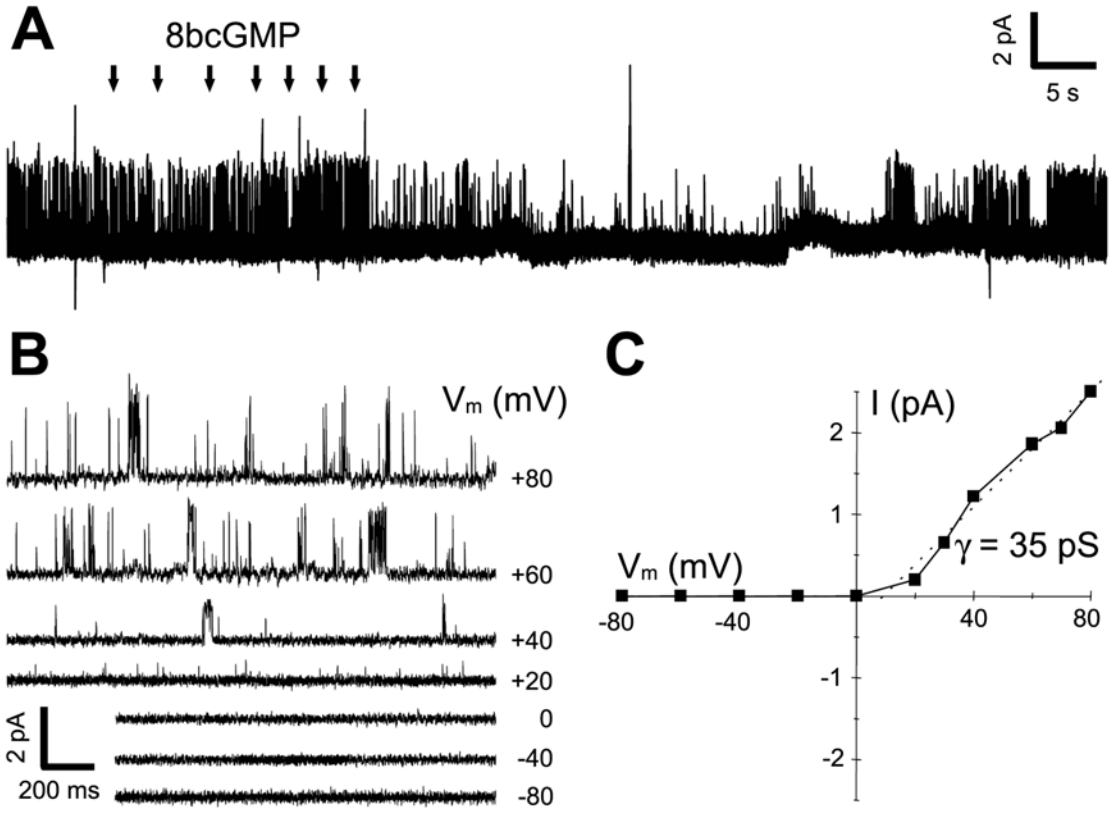

Figure 4 An outwardly rectifying medium-conductance channel of about 35 pS was transiently blocked by 8bcGMP. **A.** The application of several pulses of 8bcGMP (10 mM stock solution, several nl applied into 1 ml solution, arrows) to an inside-out patch at a membrane potential of +80 mV inhibited a single copy of an active channel. After about 40 s of wash the channel gradually regained its original activity. **B, C.** I-V relation of the same channel type obtained in a different inside-out recording. **B.** The patch was kept at different potentials for several seconds, and the single-unit conductance was determined by amplitude histograms (not shown). **C.** While the channel conducted no Cs^+ inward currents, the slope conductance (γ) of the outward currents was about 35 pS.

presence of 8bcGMP and PMA as compared to the control (Fig. 1A, D; $p < 0.05$).

In general, following application of PMA, the medium-conductance channels were observed more often, and the detection of single-channel currents became very difficult. In most recordings, large currents (up to several tens of nS in aggregate conductance) developed some time after patch-excision into high Ca^{2+} (58%), after PMA- (31%), and also after 8bcGMP-application (31%). Thus, no single-channel activity was distinguished. Only the fact that these large currents typically developed in the course of several 100 ms and occasionally inactivated later distinguished them from a broken seal. After patch-excision into high Ca^{2+} and after PMA- and/or 8bcGMP-application, different ion channels activated together, before large currents developed. Therefore, it was not possible to completely characterize the different ion channels involved. In the following, ion channels recorded at least once in isolation are distinguished according to conductance, reversal potential, I-V relation and pharmacology, and are grouped into three classes, small-, medium-,and large-conductance ion channels.

Small-conductance (2-20 pS) ion channels

Small-conductance channels of 2 to 20 pS single-unit conductance were detected in some of the recordings (n = 17 out of 116). When the absence of other active channels allowed the analysis of their kinetics (n = 3), the small-conductance channels displayed dwell times of many seconds (Fig. 2B). The fact that these channels were not recorded in the presence of Ca^{2+} channel blockers like 6 mM Ni^{2+}, suggests that at least some of them are Ca^{2+} channels.

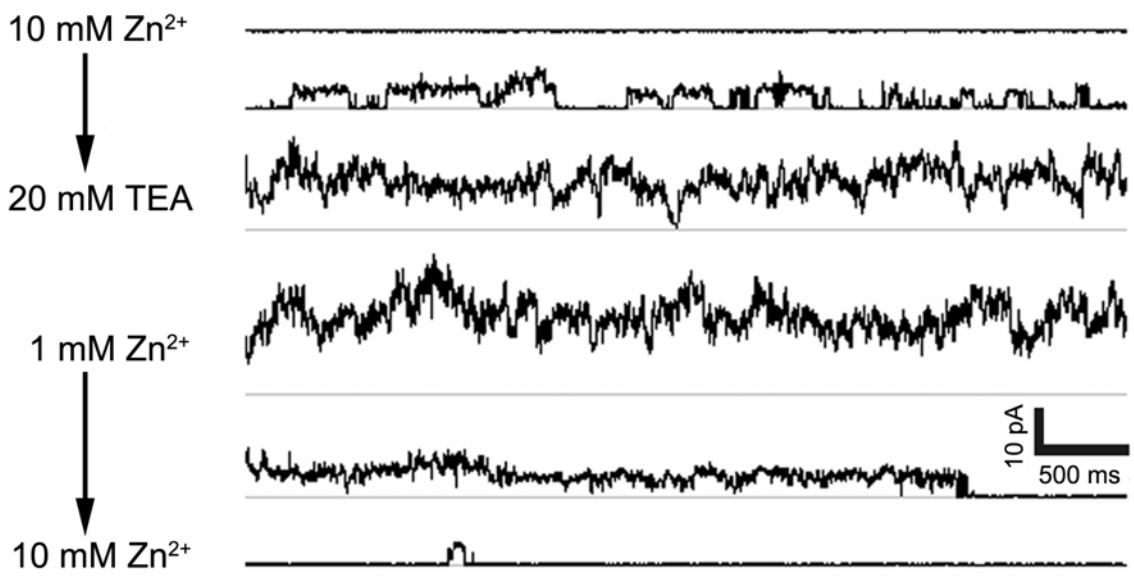

Figure 5 A medium-conductance channel of 40 pS was sensitive to 10 mM Zn^{2+}, but was not blocked in the presence of 20 mM TEA. About 25 s after an inside-out patch held at V_m = +80 mV was exposed to 10 mM Zn^{2+} bath solution; all previously active channels were closed (upper trace). When zinc was washed out with 20 mM TEA channel activity reappeared (second trace), until a large current developed without recognizable single channel events (third trace). In a bath solution containing 1 mM Zn^{2+} (fourth trace), channel activity was not notably affected. Switching back to 10 mM Zn^{2+} blocked the channel activity again (bottom two traces). Note, that distinct current levels were only determined during the wash out and wash in of 10 mM Zn^{2+} bath solution, as indicated by the arrows on the left. The amplitude histograms of traces 2 and 5 suggested a single-unit conductance of about 40 pS, with the presence of many substates (not shown). The grey lines indicate the zero-current levels. Traces were separated by about 1 min each, except for the last two traces, which are consecutive.

Since they were obscured by larger channels in most recordings, a more detailed analysis was not possible.

Medium-conductance (20-100 pS) ion channels

Most ion channels with conductances between 20 and 100 pS were non-selective cation channels with a reversal potential around 0 mV and linear or rectified I-V relations. K^+-selective channels could be distinguished from non-selective cation channels by their small outward currents, and the absence of inward currents. Without 20 mM TEA in the bath solution, non-selective cation channels were recorded in almost all experiments. Different subtypes of the medium-conductance channels were distinguished according to conductance, different I-V relations, pharmacology, and kinetics. The open times ranged from rapid flickering to dwell times of many seconds (Figs. 3-7).

Under control conditions, the most frequently recorded subtype of medium-conductance channels had about 75 pS at negative potentials and about 35 pS at positive potentials and activated spontaneously after patch-excision into bath solutions with high Ca^{2+} and Cs^+ pipette solution (Fig. 3). In the presence of 20 mM TEA, these medium-conductance channels were blocked (n = 3). Once activated, these channels did not inactivate after switching to bath solution with reduced Ca^{2+} concentration (10^{-7} M; n = 11). This channel type belongs to the cation channels of about 30 pS in Fig. 1.

Another type of medium-conductance channel of about 35 pS (Fig. 4) was blocked by application of 8bcGMP. The inactivation of this channel was observed in isolation only once. In most experiments, this channel was obscured by opening of other medium-conductance non-selective cation channels. Because this channel conducted no inward currents with Cs^+ in the patch pipette it appears to be a potassium channel.

Application of PMA revealed medium-conductance channels of about 60 pS with reversal potentials around 0 mV and a linear conductance. Usually, this channel was recorded in $\geq$ 3 copies per patch (Figs. 2A, C). Individual transitions between open and closed states took up to 100 ms, while sharp transitions occurred immediately before or after these slow transitions (n = 6 openings and 3 closings in different recordings). The individual transitions appeared to consist of several subconductance levels, which were too small to resolve. Spontaneous activation of the 60 pS channel always involved multiple copies in rapid succession, which suggests coupling among adjacent channels of the same type (Fig. 2). The 60 pS channel was recorded more frequently after application of PMA (Fig. 1), and was not detected in the presence of 20 mM TEA.

A subpopulation of medium-conductance channels activated spontaneously with a conductance of 40 pS at positive holding potentials. This channel was blocked by 10 mM, but not by 1 mM Zn^{2+} in the bath solution (n = 2 out of 7 observations), and was not affected by 20 mM TEA (Fig. 5). The 40 pS channel was more frequently observed in the presence of PMA (Fig. 1). Activation of medium-conductance channels was also recorded with 10 mM Zn^{2+} in the pipette solution (n = 25 out of 31), indicating that only a subpopulation of medium-conductance channels is zinc-sensitive.

After application of 8bcGMP, a 55 pS channel activated at +40 mV holding potential (Fig. 6). This cGMP-dependent ion channel showed a reversal potential around 0 mV and reduced inward current in the presence of 10 mM Zn^{2+} in the pipette solution (Fig. 7). The 55 pS channel was rarely seen during control conditions (Fig. 1A), but was recorded more frequently after 8bcGMP application (Figs. 1C, D; 6, 7). It is a

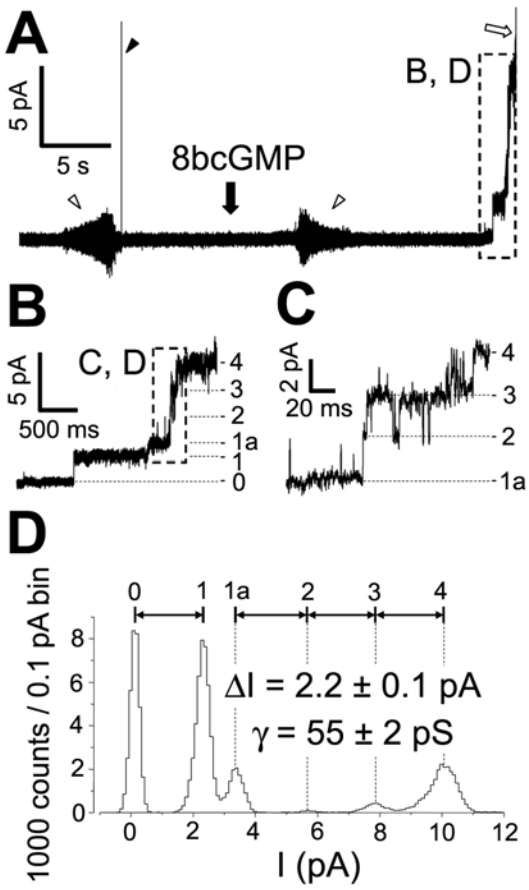

Figure 6 A 55 pS channel opened after application of 8bcGMP. **A.** At least 4 copies of a medium-conductance channel activated in an inside-out patch after puff application of 8bcGMP (10 mM stock solution) at +40 mV holding potential. The high-frequency artifacts (open arrowheads) indicate when the application pipette was moved into and out of the bath. The large capacitive transient (filled arrowhead) occurred when the application pipette first touched the surface of the bath. About 20 s after drug application to the vicinity of the cell several copies of a channel activated in rapid succession (indicated section shown at an enlarged time scale in **B**). About 2 s after the first observed channel activity, a current of >100 pA developed (open arrow; truncated), in which no single-channel currents were resolved. **C.** Enlarged view of the section indicated in **B** shows single-channel events. **D.** Amplitude histogram of the section shown in **B**. The differences in the current levels (ΔI) were 2.2 ± 0.1 pA, corresponding to a single-unit conductance ( ) of 55 ± 2 pS (mean ± SD). Another channel type with a smaller conductance caused the transition from current level 1 to 1a. Current levels in **B**-**D** correspond to each other.

non-selective cation channel which appears to be blocked by divalent cations (Fig. 7).

A 70 pS channel was blocked by application of 20 mM TEA (data not shown). This medium-conductance channel was only observed in the presence of 8bcGMP with or without PMA (Fig. 1). It activated and inactivated slowly at -40 mV holding potential, and expressed larger outward and reduced inward currents with Cs^+ in the pipette solution. Thus, the 70 pS channel appears to be a potassium channel.

Large-conductance ion channels (>100 pS)

In addition to the small- and the medium-conductance channels, large-conductance channels of >100 pS single-unit conductance were recorded. Like most of the medium-conductance channels, they typically activated after patch-excision without drug application or other obvious changes in the conditions. Frequently, the activation was correlated with the activation of medium-conductance channels, which suggests an unknown coupling mechanism. Apparent single-unit conductances of up to 550 pS were detected (Figs. 1, 8); in one recording even 1.7 nS. The transitions between the conductance states suggested the presence of multiple substates, or of multiple coupled ion channels. In most observations, the apparent single-unit conductance was below 250 pS (Fig. 8). Once activated, the large-conductance channels were affected only partly by replacing all cations in the bath solution with NMDG (n = 5 out of 7), a very large cation impermeant to most cation channels. The tested agents known as chloride channel blockers (6 mM Ni^{2+}, 10 mM Zn^{2+}, 1 mM SITS, 1 mM DIDS, 1 mM niflumic acid, 500 µM 9-AC, 100 µM PTX) did not influence the medium-conductance channels, and only partly affected the large-conductance channels (n > 10). Thus, the large-conductance channels were apparently conducted by non-selective cation and chloride channels, directly or indirectly activated by Ca^{2+}.

Discussion

In primary cell cultures of ORNs of *M. sexta*, we analyzed ion channels modulated by PKC and cGMP with inside-out patch-clamp recordings. The large diversity of interdependently activated ion channels allowed no detailed analysis but only a very general characterization of individual channels and their pharmacology in single-channel recordings. Nevertheless, new PKC- and cGMP-dependent ion channels were identified and interactions between the second messenger systems were detected, hinting at novel mechanisms of sensitivity modulation in the insect olfactory system.

Second messenger-mediated ion channels

Since ORNs can be clearly distinguished from other cell types in primary cell cultures (Stengl and Hildebrand 1990) the recorded ion channels probably belong to the olfactory signal transduction cascades. It is not possible, however, to distinguish between pheromone- and general odor-responsive ORNs from morphological markers only. Furthermore, it is not possible to determine whether different ORN classes exist, which express different sets of ion channels. The fact that in previous studies Ca^{2+}-dependent and PKC-dependent currents were expressed in almost all recordings, suggests that the respective ion channels are common to most ORNs and are shared between pheromone- and general odor-transduction cascades (Stengl et al. 1992; Stengl 1993, 1994). Whether all ORNs or only subgroups also possess cGMP-dependent ion channels remains to be examined.

At least some of the small-conductance channels recorded after patch-excision into high Ca^{2+} are likely to be voltage-dependent Ca^{2+} channels, since they were never observed in the presence of Ca^{2+} blockers (Stengl 1994; Lucas et al. 2002). Future whole-cell studies will examine Ca^{2+} channels in ORNs of *M. sexta* in more detail, since a thorough single-channel analysis was not possible.

The 30-35 pS inwardly rectified cation channel (Figs. 1A, 3) resembles the pheromone-activated cation channel, which was reported by Stengl et al (1992) with a conductance of 20 pS at +25 mV and 50 pS at -100 mV holding potential. Different patch-clamp configurations and ionic solutions may account for the differences in the conductance of this channel. In addition, this channel appears to be identical to the 37 pS (at +30 mV) cation channel which activated spontaneously after excision into the outside-out

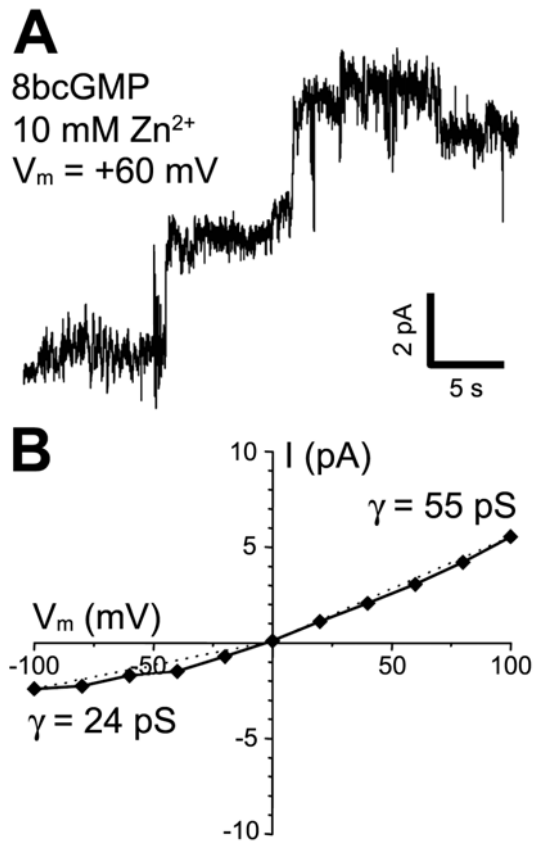

Figure 7 Patch excision-activated a medium-conductance channel of about 55 pS at positive holding potentials. **A.** Two copies of a 55 pS medium-conductance channel activated after 8bcGMP-application. **B.** A single-channel I-V relation obtained with voltage step protocols suggested a linear, zero-crossing current of 55 pS conductance (γ) at positive potentials. The inward currents were probably reduced by 10 mM Zn^{2+} included in the pipette solution.

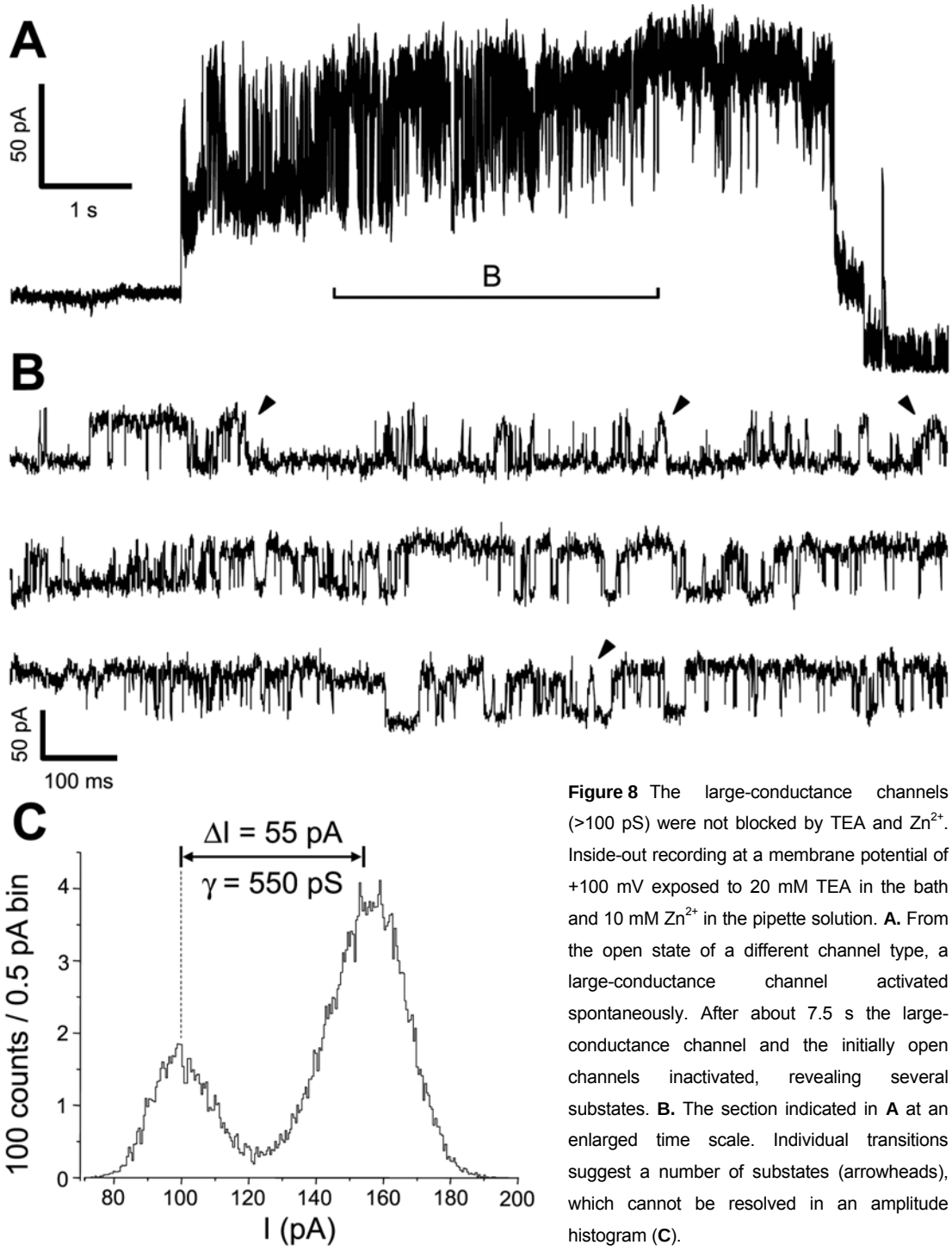

Figure 8 The large-conductance channels (>100 pS) were not blocked by TEA and Zn^{2+}. Inside-out recording at a membrane potential of +100 mV exposed to 20 mM TEA in the bath and 10 mM Zn^{2+} in the pipette solution. **A.** From the open state of a different channel type, a large-conductance channel activated spontaneously. After about 7.5 s the large-conductance channel and the initially open channels inactivated, revealing several substates. **B.** The section indicated in **A** at an enlarged time scale. Individual transitions suggest a number of substates (arrowheads), which cannot be resolved in an amplitude histogram (**C**).

mode (Stengl et al. 1992; Stengl 1993). The 30-35 pS channel is a Ca^{2+}-dependent cation channel and apparently underlies the second pheromone-dependent inward current component. It opened in Ca^{2+} concentrations higher than 10^{-6} M and was blocked by a Ca^{2+}-dependent negative feedback. The fact that the 30-35 pS channel opened readily over the course of minutes in excised patches, suggests that the high Ca^{2+} concentrations could not exert any negative feedback, since cytosolic factors, such as calmodulin, were missing. The channel was not affected by PKC activation, but was less often observed in the presence of cGMP. In ORNs of the silkmoth *Antheraea polyphemus*, a Ca^{2+}-activated cation channel of about 48 pS

conductance was blocked by cGMP (Zufall and Keil 1991). Since statistical analysis of this channel type was not possible, it could not be conclusively shown that this cation channel type in *M. sexta* is also blocked by cGMP.

The other type of 35 pS channel, which was blocked by cGMP, is most likely the previously described 30 pS delayed rectifier potassium channel, which was also blocked by cGMP, as well as cAMP and ATP (Zufall et al. 1991). This rapidly activating channel opens immediately after pheromone application, even before the cell depolarized (Stengl et al. 1992). If this channel type is present in the axons of ORNs, it contributes to the repolarization after the Na^+ channel opening and, thus, determines the duration of interspike intervals (Dolzer et al. 2001). It will be interesting to determine, whether the 35 pS channel belongs to the KCNQ ion channel family, underlying the M current in other species (reviewed by Hille 2001).

Among the PKC-dependent activated channels, only the 40 pS channel was significantly more often observed in the presence of PMA. Because the 40 pS channel was not affected by TEA, it can only partly underlie the previously described PKC-dependent non-Ca^{2+}-permeable, mostly TEA-blockable cation current which occurred after long pheromone stimulation (Stengl 1993; 1994). So far, the 60 pS PKC-dependent cation channel is the best candidate for the TEA-blockable, pheromone-dependent inward current component and further experiments need to test this hypothesis. The 40 pS cation channel which was not affected by TEA, has not been described before. Also, the 70 pS channel which was only observed in the presence of 8bcGMP and PMA awaits a further characterization. Since it was blocked by TEA and showed small, slowly activating outward and no inward currents, it seems to be a delayed rectifier potassium channel with slow kinetics. Whether this channel is encoded by the ether a-go-go (eag) potassium channel gene cloned from *M. sexta* (Keyser et al. 2003), remains to be examined.

The 55 pS cGMP-dependent activated cation channel shared properties with other CNG channels described from vertebrates (Kaupp and Seifert 2002; Craven and Zagotta 2006; Pifferi et al. 2006). It appeared to be a non-selective cation channel, which was blocked via Zn^{2+} in the recording electrode. However, in contrast to vertebrate CNG channels, it was not affected by the high intracellular Ca^{2+} concentration. It remains to be tested, whether addition of calmodulin together with high Ca^{2+} would block the 55 pS channel. Cloning and expression of CNG channels from *M. sexta* will facilitate the characterization of this cation channel in the future. Surprisingly, no dose-dependency was detected with the different cGMP concentrations tested. Apparently, all cGMP-dependent channels opened in concerted action. Whether this was due to a Ca^{2+}-dependent coupling mechanism remains to be examined.

The >100 pS large-conductance channels expressed very large currents which appeared to conduct non-selectively cations and anions, and apparently synchronized their channel openings via Ca^{2+}-dependent mechanisms. Since no reliable blockers of chloride channels in *M. sexta* are available, the further characterization of these channels is difficult and requires cloning and expression studies.

A hypothesis of sensitivity modulation in ORNs

In moth ORNs, pheromone stimuli open a characteristic sequence of three Ca^{2+}-dependent inward currents. The first two channels are down-regulated by Ca^{2+}-dependent negative feedback, while the third, a PKC-dependent inward current, is stable in the presence of second-long

pheromone stimulation (Stengl et al. 1992; Stengl 1993, 1994). Furthermore, minute-long pheromone stimulation elevates cGMP levels in ORNs of *M. sexta* (Stengl et al. 2001). Thus, cGMP elevations in ORNs correlate with the time course of long-term adaptation, while the PKC-dependent currents rather correlate with the time course of short-term adaptation, and Ca^{2+}/calmodulin-dependent negative feedback with mechanisms of desensitization. We, therefore, suggest that different sets of de- and hyperpolarizing ion channels, controlled by intracellular Ca^{2+}, Ca^{2+}-dependent kinase activity, and cyclic nucleotide concentrations, are responsible for the sliding modulation of pheromone-sensitivity during short- and long-term adaptation. Our findings are consistant with this hypothesis, since different sets of ion channels were observed in the presence or absence of high intracellular Ca^{2+}, 8bcGMP, or PKC activators. Further whole-cell and perforated patch-clamp recordings will investigate whether the ORNs of *M. sexta* express ion channels that are activated differentially by Ca^{2+}, 8bcGMP, or PKC activators. Finally, cloning and expression of the different second messenger-mediated ion channels together with RNA_i will further test our hypothesis.

Acknowledgements

The authors would like to thank Thomas Hörbrand, Karin Fischer, Holger Schmidt, Markus Hammer, Marion Zobel, Patrick Winterhagen, and Klaus Isselbächer for insect rearing, Ingrid Jakob and Philippe Lucas for valuable discussions and Günther Stöckl for technical help. This manuscript was significantly improved with the help of Uwe Homberg and unknown referees. This work was supported by DFG grants STE 531/5-1, 10-1, 10-2, 10-3 to Monika Stengl.

References

Boekhoff I, Strotmann J, Raming K, Tareilus E, Breer H. 1990. Odorant-sensitive phospholipase C in insect antennae. Cell Signal 2: 49-56.

Boekhoff I, Seifert E, Göggerle S, Lindemann M, Krüger BW, Breer H. 1993. Pheromone-induced second-messenger signaling in insect antennae. Insect Biochem Mol Biol 23(7): 757-762.

Craven KB, Zagotta WN. 2006. CNG and HCN channels: two peas, one pod. Annu Rev Physiol 68: 375-401.

Crawley MJ. 2002. Statistical Computing: An Introduction to Data Analysis using S-Plus. John Wiley & Sons, New York.

Dolzer J, Krannich S, Fischer K, Stengl M. 2001. Oscillations of the transepithelial potential of moth olfactory sensilla are influenced by octopamine and serotonin. J Exp Biol 204: 2781-2794.

Dolzer J, Fischer K, Stengl M. 2003. Adaptation in pheromone-sensitive trichoid sensilla of the hawkmoth *Manduca sexta*. J Exp Biol 206: 1575-1588.

Flecke C, Dolzer J, Krannich S, Stengl M. 2006. Perfusion with cGMP analogue adapts the action potential response of pheromone-sensitive sensilla trichoidea of the hawkmoth *Manduca sexta* in a daytime-dependent manner. J Exp Biol 209: 3898-3912.

Hamill OP, Marty A, Neher E, Sakmann B, Sigworth FJ. 1981. Improved patch-clamp techniques for high-resolution current recording from cells and cell-free membrane patches. Pflügers Arch 391: 85-100.

Hille B. 2001. Ion Channels of Exitable Membranes, Third Edition. Sunderland, Massachusetts: Sinauer Associates.

Jindra M, Huang JY, Malone F, Asahina M, Riddiford LM. 1997. Identification and mRNA developmental profiles of two ultraspiracle isoforms in the epidermis and wings of *Manduca sexta*. Insect Mol Biol 6: 41-43.

Kaissling K.-E, Zack-Strausfeld C, and Rumbo ER. 1986. Adaptation processes in insect olfactory receptors: their relation to transduction and orientation. Chem Senses 11: 574-577.

Kaupp UB, Seifert R. 2002. Cyclic nucleotide-gated ion channels. Physiol Rev 82: 769-824.

Keyser MR, Anson BD, Titus SA, Ganetzky B, Witten JL. 2003. Molecular characterization, functional expression, and developmental profile of an ether a-go-go K^+ channel in the tobacco hornworm *Manduca sexta*. J Neurobiol 55: 73-85.

Lucas P, Shimahara T. 2002. Voltage- and calcium-activated currents in cultured olfactory receptor neurons of male *Mamestra brassicae* (Lepidoptera). Chem Senses 27: 599-610.

Marion-Poll F, Tobin TR. 1992. Temporal coding of pheromone pulses and trains in *Manduca sexta*. J Comp Physiol A 171: 505-512.

Matthews HR, Reisert J. 2003. Calcium, the two-faced messenger of olfactory transduction and adaptation. Curr Opinion Neurobiol 13:469-475.

Pifferi S, Boccaccio A, Menini A. 2006. Cyclic nucleotide-gated ion channels in sensory transduction. FEBS Lett 580:2853-2859.

Redkozubov A. 2000. Guanosine 3',5'-cyclic monophosphate reduces the response of the Moth's olfactory receptor neuron to pheromone. Chem Sens 25: 381-385.

Stengl M. 1993. Intracellular-messenger-mediated cation channels in cultured olfactory receptor neurons. J Exp Biol 178: 125-147.

Stengl M. 1994. Inositol-trisphosphate-dependent calcium currents precede cation currents in insect olfactory receptor neurons *in vitro*. J Comp Physiol [A] 174: 187-194.

Stengl M, Hildebrand JG. 1990. Insect olfactory neurons *in vitro*: morphological and immunocytochemical characterization of male-specific antennal receptor cells from developing antennae of male *Manduca sexta*. J Neurosci 10(3): 837-847.

Stengl M, Zintl R. 1996. NADPH diaphorase activity in the antenna of the hawkmoth *Manduca sexta*. J Exp Biol 199(5): 1063-1072.

Stengl M, Zufall F, Hatt H, Hildebrand JG. 1992. Olfactory receptor neurons from antennae of developing male *Manduca sexta* respond to components of the species-specific sex pheromone in vitro. J Neurosci 12: 2523-2531.

Stengl M, Ziegelberger G, Boekhoff I, Krieger J. 1999. Perireceptor events and transduction mechanisms in insect olfaction. In: Insect Olfaction (ed. Hansson BS). Springer, 49-66.

Stengl M, Zintl R, de Vente J, Nighorn A. 2001. Localization of cGMP immunoreactivity and of soluble guanylyl cyclase in antennal sensilla of the hawkmoth *Manduca sexta*. Cell Tissue Res 304: 409-421.

Wegener JW, Breer H, Hanke W. 1997. Second messenger-controlled membrane conductance in locust (*Locusta migratoria*) olfactory neurons. J Insect Physiol 43: 595-603.

Ziegelberger G, van den Berg MJ, Kaissling K-E, Klumpp S, Schultz JE. 1990. Cyclic GMP levels and guanylate cyclase activity in pheromone-sensitive antennae of the silkmoths *Antheraea polyphemus* and *Bombyx mori*. J Neurosci 10(4): 1217-1225.

Zack-Strausfeld C, Kaissling K-E. 1986. Localized adaptation processes in olfactory sensilla of Saturniid moths. Chem Senses 11:499-512.

Zufall F, Keil TA. 1991. A Calcium-activated nonspecific cation channel from olfactory receptor neurons of the silkmoth *Antheraea polyphemus*. J Exp Biol 161: 455-468.

Zufall F, Stengl M, Franke C, Hildebrand JG, Hatt H. 1991. Ionic currents of cultured olfactory receptor neurons from antennae of male *Manduca sexta*. J Neurosci 11(4): 956-965.

Zufall F, Leinders-Zufall T. 2000. The cellular and molecular basis of odor adaptation. Chem Senses 25:473-481.

IV. Cyclic nucleotide-activated currents in cultured olfactory receptor neurons of the hawkmoth *Manduca sexta*.

Krannich S, Stengl M.

J Neurophysiol, under review.

ABSTRACT	81
INTRODUCTION	81
MATERIALS AND METHODS	82
Insects	82
Primary cell cultures	83
Solutions and reagents	83
Patch-clamp technique and data analysis	84
RESULTS	84
Cyclic nucleotides activate currents in moth ORNs	84
Cyclic nucleotides activate non-specific cation currents	87
Cyclic nucleotide-activated cation currents depend on the extracellular Ca^{2+} concentration	87
Cyclic nucleotide-activated currents are modulated by Ca^{2+}/CaM	90
Ni^{2+} and Zn^{2+} inhibit cyclic nucleotide-activated currents	90
Cyclic nucleotide-activated currents are modulated by extracellular Cl^-	91
Cyclic nucleotides activate currents independently of protein kinases	91
DISCUSSION	92
Moth ORNs appear to possess CNG channels	92
Prospective *Ms*CNG channels differ in their Ca^{2+}-dependency	94
Prospective *Ms*CNG channels differ in their Ca^{2+}/CaM-dependent inhibition	94
Lanthanum and transition metals inhibit prospective *Ms*CNG channels	95
Prospective *Ms*CNG channel permeability depends on the extracellular Cl^- concentration	95
A cAMP-activated Ca^{2+} inward current depends on protein kinase activity	95
Conclusions	96
ACKNOWLEDGEMENTS	96
REFERENCES	96
Supplementary Table 1	99

Cyclic nucleotide-activated currents in cultured olfactory receptor neurons of the hawkmoth *Manduca sexta*

Steffi Krannich[1,2] and Monika Stengl[1,2]

[1]Biology, Animal Physiology, Philipps-University of Marburg, Karl-von-Frisch-Straße, Marburg D-35043, Germany

[2]Institute of Biology, Animal Physiology, University of Kassel, Heinrich-Plett-Straße 40, Kassel D-34132, Germany

Correspondence to be sent to: Monika Stengl, Biology, Animal Physiology, Philipps-University of Marburg, Karl-von-Frisch-Straße, Marburg D-35032, Germany, e-mail: stengl@staff.uni-marburg.de

Abstract

Moth pheromones cause rises in intracellular Ca^{2+} concentrations that activate Ca^{2+}-dependent cation channels in antennal olfactory receptor neurons. In addition, mechanisms of adaptation and sensitization depend on changes in cyclic nucleotide concentrations. Here, cyclic nucleotide-activated currents in cultured olfactory receptor neurons of the moth *Manduca sexta* are described, which share properties with currents through vertebrate cyclic nucleotide-gated channels. The cyclic nucleotide-activated currents of *M. sexta* carried Ca^{2+} and monovalent cations. They were directly activated by cAMP and cGMP, modulated by Ca^{2+}/calmodulin, and inhibited by Lanthanum. *M. sexta* cyclic nucleotide-activated currents developed in an all or none-manner, which suggests that the underlying channels are coupled and act coordinately. At least one cAMP- and two cGMP-activated non-selective cation currents could be distinguished. Compared to the cAMP-activated current, both cGMP-activated currents appeared to conduct more Ca^{2+} and showed a stronger down-regulation by Ca^{2+}/calmodulin-dependent negative feedback. Furthermore, both cGMP-activated currents differed in their Ca^{2+}-dependent inhibition. Thus, *M. sexta* olfactory receptor neurons, like vertebrate sensory neurons, appear to express non-selective cyclic nucleotide-activated cation channels with different subunit compositions. Besides the non-selective cyclic nucleotide-activated cation currents, olfactory receptor neurons express a cAMP-dependent current. This current resembled a protein kinase-modulated low voltage-activated Ca^{2+} current.

Keywords: *Manduca sexta,* insect olfactory transduction, CNG channels, patch-clamp.

Introduction

Odors play a central role for the intra- and interspecific recognition and communication of insects. Male moths can detect almost single molecules of female sex pheromones (Kaissling and Priesner 1970). Accordingly, pheromone detection in moths is one of the best-studied models of how olfactory systems transduce odor information (Hildebrand 1995; Hansson 2002; Kaissling 2004; Rospars et al. 2007). Previous biochemical (Breer et al. 1990; Boekhoff et al. 1990), electrophysiological (Zufall and Hatt 1991; Zufall et al. 1991; Stengl et al. 1992; Stengl 1993, 1994; Wegener et al. 1997), and molecular genetic studies (Riesgo-Escovar et al. 1995; Jacquin-Joly

et al. 2002) extensively characterized the initial steps of the insect olfactory transduction cascade. It is largely unknown, however, how pheromones induce adaptation or sensitization of the insect olfactory transduction cascade. Available data demonstrate that pheromone stimuli induce slow and delayed increases in the cyclic guanosine monophosphate (cGMP) concentration in the olfactory receptor neurons (ORNs) of different moth species (Ziegelberger et al. 1990; Boekhoff et al. 1993). Tip recordings from trichoid sensilla of moths showed that cGMP reduces the action potential frequency upon pheromone stimulation, and thus may trigger long-term adaptation (Redkozubov 2000; Flecke et al. 2006). The increase of cGMP after adapting pheromone stimuli appears to activate protein kinase G (Boekhoff et al. 1993). In single channel recordings of *M. sexta* ORNs, millimolar concentrations of cGMP as well as cyclic adenosine monophosphate (cAMP) inhibited a pheromone-activated delayed rectifier potassium channel (Zufall et al. 1991; Stengl et al. 1992). Taken together, these findings suggest that cyclic nucleotides modulate olfactory transduction in moths.

In vertebrates, cyclic nucleotide-gated (CNG) channels have been extensively studied (Kaupp and Seifert 2002; Hofmann et al. 2005; Pifferi et al. 2006). Vertebrate olfactory CNG channels form heterotetrameric complexes composed of two principal CNGA2 subunits, a modulatory CNGA4, and a modulatory CNGB1b subunit (Sautter et al. 1998; Shapiro and Zagotta 1998; Bonigk et al. 1999; Zheng and Zagotta 2004). The subunit composition of vertebrate olfactory CNG channels determines their functional features like ligand sensitivity, ion selectivity, and gating properties (Munger et al. 2001; Bradley et al. 2005). Both cAMP and cGMP directly activate vertebrate olfactory CNG channels, which non-selectively conduct Ca^{2+} and monovalent cations (Frings et al. 1992, 1995; Dzeja et al. 1999). Since vertebrate olfactory CNG channels are negatively regulated by Ca^{2+}/calmodulin (CaM), Ca^{2+} influx through CNG channels probably leads to adaptation (Chen and Yau 1994; Zufall and Leinders-Zufall 2000; Bradley et al. 2001; Munger et al. 2001).

In insects, CNG channels have been characterized in the olfactory system of *Drosophila melanogaster* (Baumann et al. 1994; Miyazu et al. 2000), *Apis mellifera* (Gisselmann et al. 2003), and *Heliothis virescens* (Krieger et al. 1999). Here, we describe cyclic nucleotide-activated currents in the ORNs of *Manduca sexta*, which are likely to play a role for olfactory adaptation and sensitization. In whole-cell patch-clamp recordings, we found that cAMP and cGMP directly activated currents. Pharmacological and ion exchange experiments demonstrated that at least one cAMP- and two cGMP-activated non-selective cation currents occured in the ORNs of *M. sexta*. The cGMP-activated currents carried more Ca^{2+} and were stronger influenced by Ca^{2+}/CaM-dependent negative feedback than the cAMP-activated current. Furthermore, the cGMP-activated currents differed in their Ca^{2+}-dependent inhibition. Unlike cGMP, cAMP activated a previously undescribed Ca^{2+} current that resembled a protein kinase-modulated low voltage-activated (LVA) Ca^{2+} current.

Materials and Methods

Cell culture media were obtained from Gibco (Karlsruhe, Germany) or PAA (PAA Laboratories GmbH, Cölbe, Germany), reagents were purchased from Sigma (Taufkirchen, Germany), and salts for electrophysiological solutions from Merck (Frankfurt/M, Germany).

Insects

M. sexta (Johannson; Lepidoptera: Sphingidae) larvae were reared on an artificial diet (modified

after Bell and Joachim 1976). Larvae were maintained under long-day photoperiod (L:D 17:7) at 24 - 27°C and 40 - 60 % relative humidity. Pupae were staged using external markers (Jindra et al. 1997) and anesthetized by cooling until antennal flagella were dissected.

Primary cell cultures

The cell culture protocol was modified after Stengl and Hildebrand (1990). Briefly, antennae of male *M. sexta* pupae were dissected in Hanks' Balanced Salt Solution containing penicillin and streptomycin (HBSS/PS). Antennae were incubated for 5 min at room temperature in HBSS/PS containing 1.3 mM EGTA, rinsed in HBSS/PS, and dissociated in two batches for 5 and 3 min at 37°C in HBSS/PS containing 24 mM papain. Dissociation was stopped with Leibovitz L-15 medium supplemented with 10 % fetal bovine serum. The cell suspension was centrifuged at 90 to 110 rcf for 5 min and pellets were resuspended in HBSS/PS. Dispersed cells were plated on glass-bottom culture dishes, which were coated with concanavalin A and poly-L-lysine, and allowed to settle for 30 min. Then, 1 ml of a 2:1 cell culture medium (two parts of Leibovitz L-15 medium supplemented with 10 % fetal bovine serum and one part of *Manduca* embryonic cell line conditioned medium MRLL-CH1 (Eide et al. 1975)) was added. The medium was completely replaced within 24 h after dispersion. Cell cultures were maintained at 20°C and used for electrophysiology from 10 up to 25 days (Stengl and Hildebrand 1990).

Solutions and reagents

Solutions contained reagents at doses commonly used for patch-clamp recordings (Zufall et al. 1991; Stengl 1993, 1994). All solutions were adjusted to pH 7.1-7.2 and 370-380 mOsm for extracellular solutions and 340 mOsm for pipette solution, respectively. During recordings, cells were kept in 2 ml extracellular solution. Standard extracellular solution contained in mM: NaCl 156; KCl 4; $CaCl_2$ 6; glucose 5 and HEPES 10. To inhibit voltage-dependent sodium currents all extracellular solutions included 10^{-8} M tetrodotoxin. To investigate whether currents depend on the extracellular Ca^{2+} concentration, $CaCl_2$ in the extracellular solution was either reduced to 10^{-5} or 10^{-7} M (buffered with EGTA) or substituted with 6 mM $BaCl_2$. For simplicity, standard extracellular solution is referred to as "6Ca", solutions with reduced calcium concentration as "low Ca" and barium solution as "6Ba". To identify voltage-gated channels, extracellular solutions contained 6 mM $NiCl_2$ (6Ni) or 1 mM $ZnCl_2$ (1Zn). The Cl^--reduced extracellular solution (16 mM; "low Cl") was obtained by replacing NaCl with the sodium acetate salt. A gravity feed perfusion system controlled the exchange of extracellular solutions at a low flow rate. The complete exchange of extracellular solution took less than a minute. The ionic composition of the patch pipette solution was identical in all experiments (in mM): CsCl 160; $CaCl_2$ 1; EGTA 11 and HEPES 10. Cesium was used to prevent potassium-dependent outward currents.

Reagents were pipetted directly into the extracellular solution. At the beginning of each experiment, extracellular solution was pipetted directly onto the cells as a control. After a delay of at least 2 min, cyclic nucleotides were applied. The membrane-permeant cAMP and cGMP analogues 8-bromo cAMP and 8-bromo cGMP were dissolved in extracellular solution and applied at final concentrations ranging from 5 nM to 50 µM (Supplementary Tab. 1). The calmodulin (CaM) antagonist N-(6-aminohexyl)-5-chloro-1-naphthalenesulfonamid (W-7) and the non-specific inhibitor of Ca^{2+}-permeable cation channels, lanthanum (La^{3+}), were dissolved in water and applied at final concentrations of 10 to

50 µM for W-7 (Seno et al. 2005) and 0.05 to 1.1 mM for La^{3+}. The protein kinase inhibitors staurosporine (dissolved in dimethyl sulfoxid) and H7 (dissolved in EtOH) were applied at concentrations of 1 µM for staurosporine and 10 µM for H7 (Stengl 1993). Cell cultures were incubated with the respective protein kinase inhibitor for 15 to 30 min before breaking into whole-cell configuration and application of cyclic nucleotides.

Patch-clamp technique and data analysis

Patch-clamp recordings were performed in whole-cell configuration at room temperature according to the conventional patch-clamp method (Hamill et al. 1981). Cell cultures were monitored at 600x on an inverted microscope (Axioscope 135; Zeiss, Göttingen, Germany) equipped with phase-contrast optics. ORNs were identified on the basis of their morphology (Stengl and Hildebrand 1990). Patch electrodes were pulled from thick borosilicate glass capillaries (GC150T-10; Clark Electromedical Instruments, Reading, UK) with a micropipette puller (Sutter P97; Sutter, Novato, CA, USA). Fire-polished patch pipettes with a tip resistance of 2 to 8 MΩ when filled with pipette solution were used to obtain seals of several GΩ on the cell membrane. Junction potential was nullified prior to seal formation, and capacitance and series resistance of the patch pipette were compensated. For whole-cell recordings, the membrane potential was clamped at -60 mV. After breaking into whole-cell configuration and a delay of at least 2 min for the stabilization of outward currents, the experiment was started. Three consecutive voltage ramp protocols from -100 mV to +100 mV, with 500 ms each, were applied to establish current-voltage (I-V) relations.

Data acquisition was carried out with an Axopatch 1D amplifier using a Digidata 1200B interface (Molecular Devices Corp., Union City, CA, USA). Data acquisition and analyses were performed with pClamp (version 9; Molecular Devices Corp.). Currents recorded during voltage protocols were sampled at 20 kHz and low-pass filtered at 2 kHz. A MiniDigi acquisition device (MiniDigi1A; Molecular Devices Corp.) was used to continuously sample currents at 1 kHz and to record the time of drug application on a second acquisition channel. The figures show representative traces corrected for leak currents. The mean current amplitudes were determined at -100 mV. All data were presented as mean ± SEM. Statistical significance (p-value of <0.05) was evaluated by means of the two-tailed Student's t-test. Increase of current amplitude was measured at ±100 mV and normalized to the maximum current amplitude obtained in control conditions. Inhibition of current amplitude was measured at ±100 mV and plotted as percentage of the maximum current amplitude obtained under control conditions.

Results

Cyclic nucleotides activate currents in moth ORNs

To characterize cyclic nucleotide-activated currents, we stimulated *M. sexta* ORNs (n = 188) in whole-cell patch-clamp recordings with the membrane-permeable cAMP and cGMP analogues 8-bromo cAMP and 8-bromo cGMP. Since a detailed analysis of all concentrations (5 nM to 50 µM) did not reveal statistically significant differences in the frequency of activation, current amplitude, reversal potential, and latency of activation over the total number of ORNs tested (Supplementary Tab. 1), we pooled the data.

Cyclic nucleotide application typically induced a step-wise increasing inward current with a delay of several seconds up to several minutes (cAMP 126 ± 9 s, n = 82 ORNs; cGMP 110 ± 10 s, n = 75 ORNs). The amplitude of the inward current typically reached a plateau and did not decline over the course of the recording (Fig. 1A, B). Both

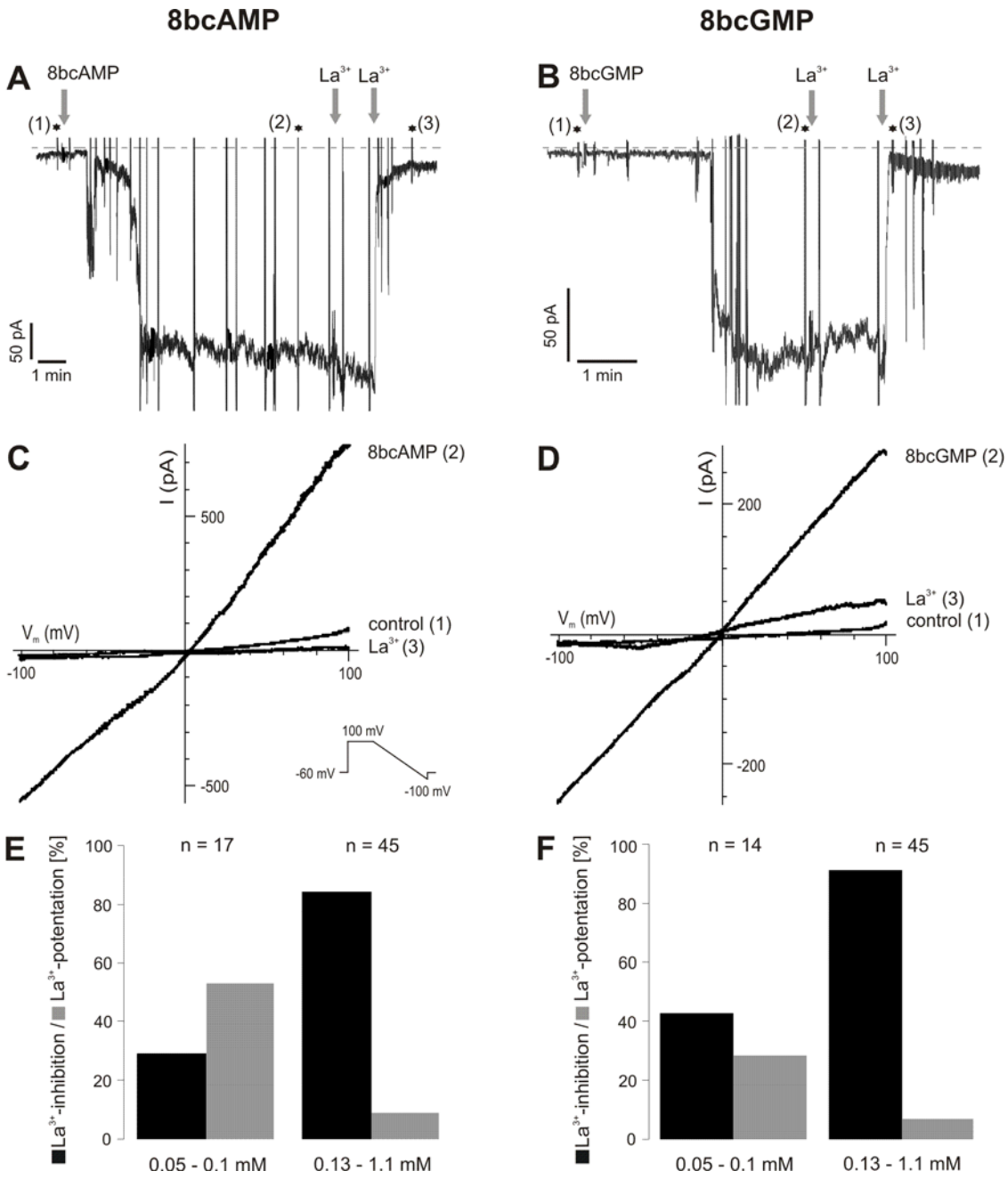

Figure 1 Whole-cell patch-clamp recordings of cultured *M. sexta* ORNs. Application of 0.5 µM 8bcAMP (**A**) or 0.5 µM 8bcGMP (**B**) activated La^{3+}-sensitive inward currents at -60 mV membrane potential in standard extracellular solution. While 50 µM La^{3+} did not influence the current (first application), 600 µM La^{3+} (second application) inhibited the inward current. The dashed line indicates 0 pA level. The large transient interruptions of the inward current are voltage ramp protocols. Asterisks indicate voltage ramp protocols used to establish I-V relations before (control; 1), after 8bcAMP- (**C**) or 8bcGMP- (**D**) application (2), and after La^{3+}-application (3). Both cyclic nucleotides activated La^{3+}- sensitive, non-selective cation currents with reversal potentials around 0 mV. **(E, F)** La^{3+} had a dose-dependent effect. Whereas low La^{3+} concentrations (50 to 100 µM; grey) sometimes potentiated cyclic nucleotide-activated currents, high La^{3+} concentrations (0.13 to 1.1 mM; black) usually inhibited cyclic nucleotide-activated currents. In some ORNs, La^{3+} had no effect.

cyclic nucleotides induced a current with a linear I-V relation in standard extracellular solution (6Ca; Tab. 1; Fig. 1C, D). The cAMP-activated current had a mean reversal potential of 0.2 ± 1.6 mV and a mean amplitude of 608 ± 114 pA (*n* = 49 of 56 ORNs; Fig. 1C). The cGMP-activated current did not significantly differ from the cAMP-activated current and had a mean reversal

Table 1 Cyclic nucleotide-activated currents in moth ORNs.

	n		activation (%)		rectification		reversal potential (mV)		mean amplitude (pA)	
	cAMP	*cGMP*	*cAMP*	*cGMP*	*cAMP*	*cGMP*	*cAMP*	*cGMP*	*cAMP*	*cGMP*
6Ca	56	52	88	83	linear	linear	0.2 ± 1.6	1.6 ± 1.2	608 ± 114	918 ± 208
+ staurosporine	8	9	88*	67	linear	linear	5.7 ± 2.3	8.0 ± 8.7	607 ± 343	738 ± 253
+ H7	9	7	67*	86	linear/ inward	inward	5.7 ± 3.6	5.3 ± 3.3	330 ± 243	142 ± 55
6Ba	6	8	100	88	linear	linear	-0.4 ± 1.6	-3.6 ± 3.1	749 ± 199	1054 ± 719
low Ca	17	16	77	81	linear/ inward	linear	-0.5 ± 4.3	6.8 ± 4.9	1001 ± 391	997 ± 280

n = number of ORNs recorded, + incubation with protein kinase inhibitor in 6Ca, *except activation of $I_{Ca(cAMP)}$. See Materials and Methods for solutions. Data represent mean ± SEM.

potential of 1.6 ± 1.2 mV, and a mean amplitude of 918 ± 208 pA (*n* = 43 of 52 ORNs; Fig. 1D). Application of La^{3+} (Tab. 2), a non-specific blocker of Ca^{2+}-permeable cation channels, significantly inhibited both cyclic nucleotide-activated currents ($p < 0.01$; Fig. 1), i.e. 71.6 ± 3.5 % of the cAMP-activated current (*n* = 41 of 49 ORNs), and 68.1 ± 2.6 % of the cGMP-activated current (*n* = 45 of 50 ORNs), respectively. The La^{3+}-induced current inhibition did not significantly differ between cAMP- and cGMP-activated currents. However, La^{3+} inhibited the inward current of both cyclic nucleotide-activated currents significantly stronger than the outward current ($p < 0.01$). The remaining La^{3+}-independent outwardly rectified current had a mean reversal potential of -5.4 ± 2 mV for cAMP- and -1.8 ± 1.5 mV for cGMP-activated currents.

Both cyclic nucleotide-activated currents showed a La^{3+} concentration dependency (Fig. 1A, B, E, F). Low La^{3+} concentrations (50 to 100 µM) inhibited cAMP-activated currents in ~29 % of ORNs, but potentiated them in ~53 % of ORNs (*n* = 17 applications). High La^{3+} concentrations (0.13 to 1.1 mM) inhibited cAMP-activated currents in ~84 % of ORNs, and potentiated them in only ~9 % of ORNs (*n* = 45 applications; Fig. 1E). Similarly, low La^{3+} concentrations inhibited cGMP-activated currents in ~43 % of ORNs, and potentiated them in ~29 % of ORNs (*n* = 14 applications). High La^{3+} concentrations inhibited the cGMP-activated current in ~91 % of ORNs, and potentiated them in only ~7 % of ORNs (*n* = 45 applications; Fig. 1F). In the remaining ORNs, La^{3+} had no effect.

Table 2 Pharmacological properties of cyclic nucleotide-activated currents.

	n		inhibition (%)		activation (%)		rectification		reversal potential	
	cAMP	*cGMP*	*cAMP*	*cGMP*	*cAMP*	*cGMP*	*cAMP*	*cGMP*	*cAMP*	*cGMP*
++ W-7	12	14	0	14	67	50	linear	linear	-0.5 ± 1.7 mV	1.2 ± 4.3 mV
++ La^{3+}	49	50	83	91	11	7	outward	outward	-5.4 ± 2.0 mV	-1.8 ± 1.5 mV
6Ca > low Ca	8	7	0	14	100	71	linear	linear	persisted	persisted
low Ca > 6Ca	7	9	71	33	14	66	linear/ outward	linear	persisted	persisted
> 6Ni	13	14	54	64	31	21	outward	outward	persisted	persisted
> 1Zn	7	6	71	100	14	0	outward	outward	persisted	persisted
> low Cl	9	7	11	14	56	71	outward	linear/ outward	negative	negative

n = number of ORNs recorded, ++ bath application, > perfusion. Remaining ORNs showed no effect. See Materials and Methods for solutions. Data represent mean ± SEM.

Cyclic nucleotides activate non-selective cation currents

To investigate whether cAMP- and cGMP-activated currents depend on the extracellular Ca^{2+} concentration, $CaCl_2$ was reduced in the extracellular solution to either 10^{-5} or 10^{-7} M (low Ca), or substituted with 6 mM $BaCl_2$ (6Ba; Tab. 1). Both cAMP and cGMP induced currents in low Ca and 6Ba solution. Subsequent La^{3+}-application inhibited these currents. In low Ca solution (see Fig. 4A-C, traces (1)), cAMP induced a linear or inwardly rectified current with a mean reversal potential of -0.5 ± 4.3 mV and a mean amplitude of 1001 ± 391 pA (*n* = 13 of 17 ORNs). Similarly, the cGMP-activated current showed a linear I-V relation, a mean reversal potential of 6.8 ± 4.9 mV, and a mean amplitude of 997 ± 280 pA (*n* = 13 of 16 ORNs). In 6Ba solution, both cyclic nucleotides induced currents with a linear I-V relation. The cAMP-activated current (Fig. 2A) had a mean reversal potential of -0.4 ± 1.6 mV and a mean amplitude of 749 ± 199 pA (*n* = 6 ORNs). The cGMP-activated current (Fig. 2B) had a mean reversal potential of -3.6 ± 3.1 mV and a mean amplitude of 1054 ± 719 pA (*n* = 7 of 8 ORNs). The mean amplitudes or reversal potentials of the cAMP- and cGMP-activated currents did not significantly differ in the different extracellular solutions. In some experiments (*n* = 8 of 14 ORNs), 6Ba solution induced a small inward current through Ca^{2+} channels (Fig. 2B).

To examine whether K^+ and Na^+ equally contribute to the cAMP- and cGMP-activated currents (cAMP *n* = 5 ORNs; cGMP *n* = 3 ORNs, data not shown), cyclic nucleotide-activated currents were recorded with standard Cs^+ pipette solution (160 mM), and successively exposed to extracellular solution containing 160 mM Cs^+, K^+, and Na^+, respectively. The conductance sequence for outward currents was measured relative to Cs^+ at +100 mV. The conductance sequence of the cAMP-activated current was: K^+ (1.3) : Na^+ (1.2) : Cs^+ (1), and that of the cGMP-activated current was: K^+ (1.2) : Na^+ (1) ~ Cs^+ (1).

Cyclic nucleotide-activated currents depend on the extracellular Ca^{2+} concentration

To investigate the Ca^{2+}-dependency of cyclic nucleotide-activated currents, ORNs were exposed to different extracellular Ca^{2+} concentrations. In a first set of experiments, ORNs were initially kept in 6Ca solution, stimulated with cyclic nucleotides,

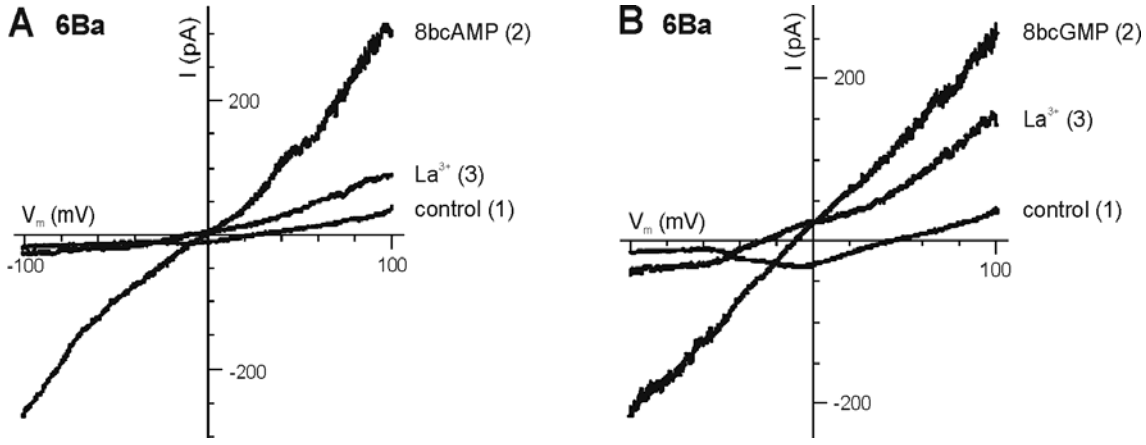

Figure 2 Cyclic nucleotides activated non-selective cation currents. I-V relations of currents activated after application of 1.5 µM 8bcAMP **(A**, 2**)** or 0.3 µM 8bcGMP **(B**, 2**)** in extracellular solution with 6 mM $BaCl_2$ (6Ba) substituted for $CaCl_2$. Subsequent La^{3+}-application (3) inhibited the cyclic nucleotide-activated currents. The 6Ba solution sometimes induced a small inward current (control; 1) through Ca^{2+} channels **(B)**.

and then perfused with low Ca solution (10^{-5} M; Tab. 2). Both the cAMP-activated (*n* = 8 ORNs; Fig. 3A) and the cGMP-activated (*n* = 5 of 7 ORNs; Fig. 3B) currents increased in low Ca solution significantly ($p < 0.01$; Fig. 3C). Subsequent La^{3+}-application inhibited the cyclic nucleotide-activated currents (Fig. 3). After perfusion with low Ca solution, both cyclic nucleotide-activated currents expressed a linear I-V relation with a constant mean reversal potential.

In a second set of experiments, ORNs were at first kept in low Ca solution, stimulated with cyclic nucleotides, and then perfused with 6Ca solution (Tab. 2). In 5 of 7 ORNs, perfusion with 6Ca solution significantly inhibited 35 ± 4 % of the cAMP-activated current ($p < 0.01$; Fig. 4A, D). The mean reversal potential of the linear or outwardly rectified cAMP-activated current remained unchanged. The cGMP-activated current showed a comparatively complex Ca^{2+}-dependency. In general, the cGMP-activated current significantly increased after perfusion with 6Ca solution ($p < 0.05$; *n* = 6 of 9 ORNs; Fig. 4C, E). However, in 3 of 9 ORNs, perfusion with 6Ca solution significantly inhibited 56.5 ± 7.9 % of the cGMP-activated current ($p < 0.01$; Fig. 4B, D). The cGMP-activated current showed a significantly stronger current inhibition in 6Ca solution than the cAMP-activated current ($p < 0.05$). The mean reversal potential of the linear cGMP-activated currents remained unchanged. Following perfusion with 6Ca solution, La^{3+}-application further inhibited 61 ± 11.7 % of the remaining cyclic nucleotide-activated currents (*n* = 3 ORNs, data not shown), but did not significantly change the mean reversal potential.

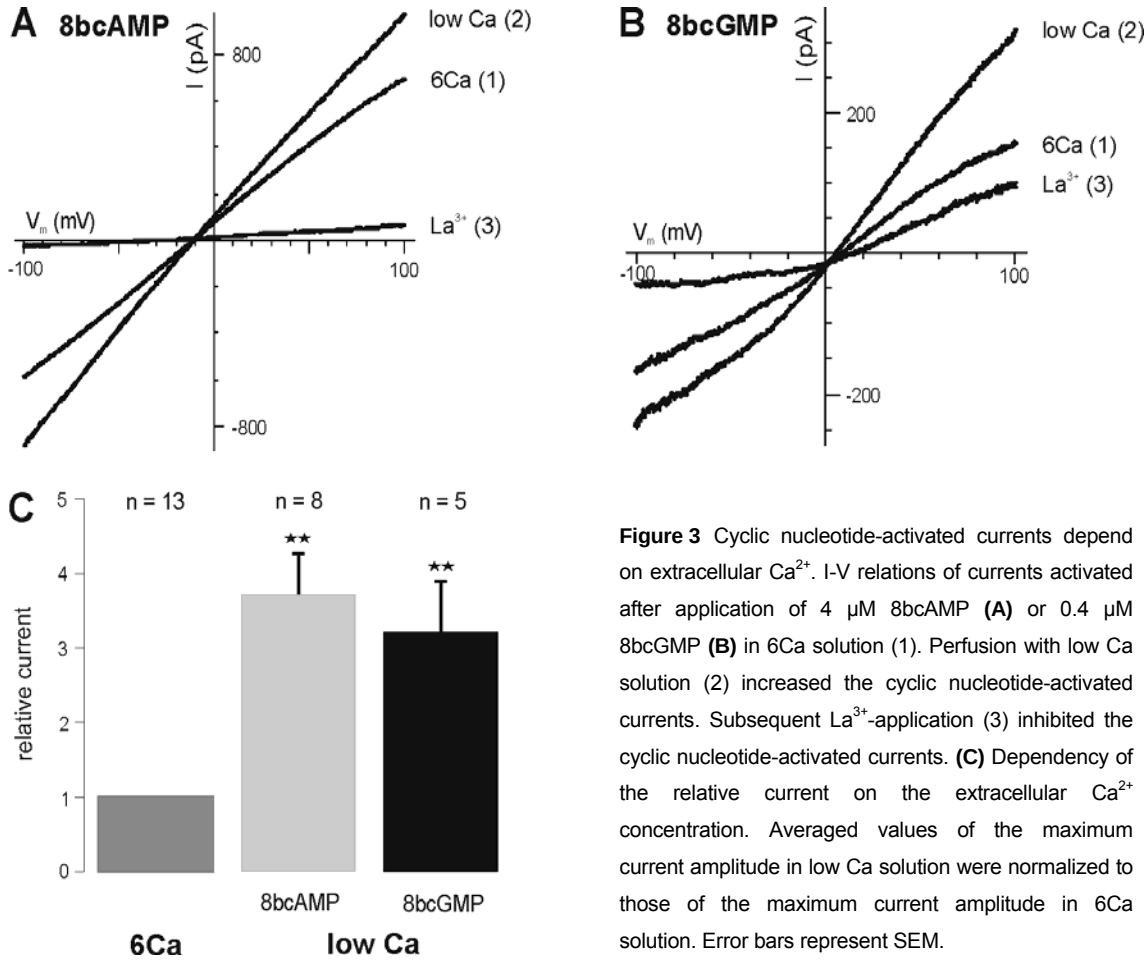

Figure 3 Cyclic nucleotide-activated currents depend on extracellular Ca^{2+}. I-V relations of currents activated after application of 4 µM 8bcAMP **(A)** or 0.4 µM 8bcGMP **(B)** in 6Ca solution (1). Perfusion with low Ca solution (2) increased the cyclic nucleotide-activated currents. Subsequent La^{3+}-application (3) inhibited the cyclic nucleotide-activated currents. **(C)** Dependency of the relative current on the extracellular Ca^{2+} concentration. Averaged values of the maximum current amplitude in low Ca solution were normalized to those of the maximum current amplitude in 6Ca solution. Error bars represent SEM.

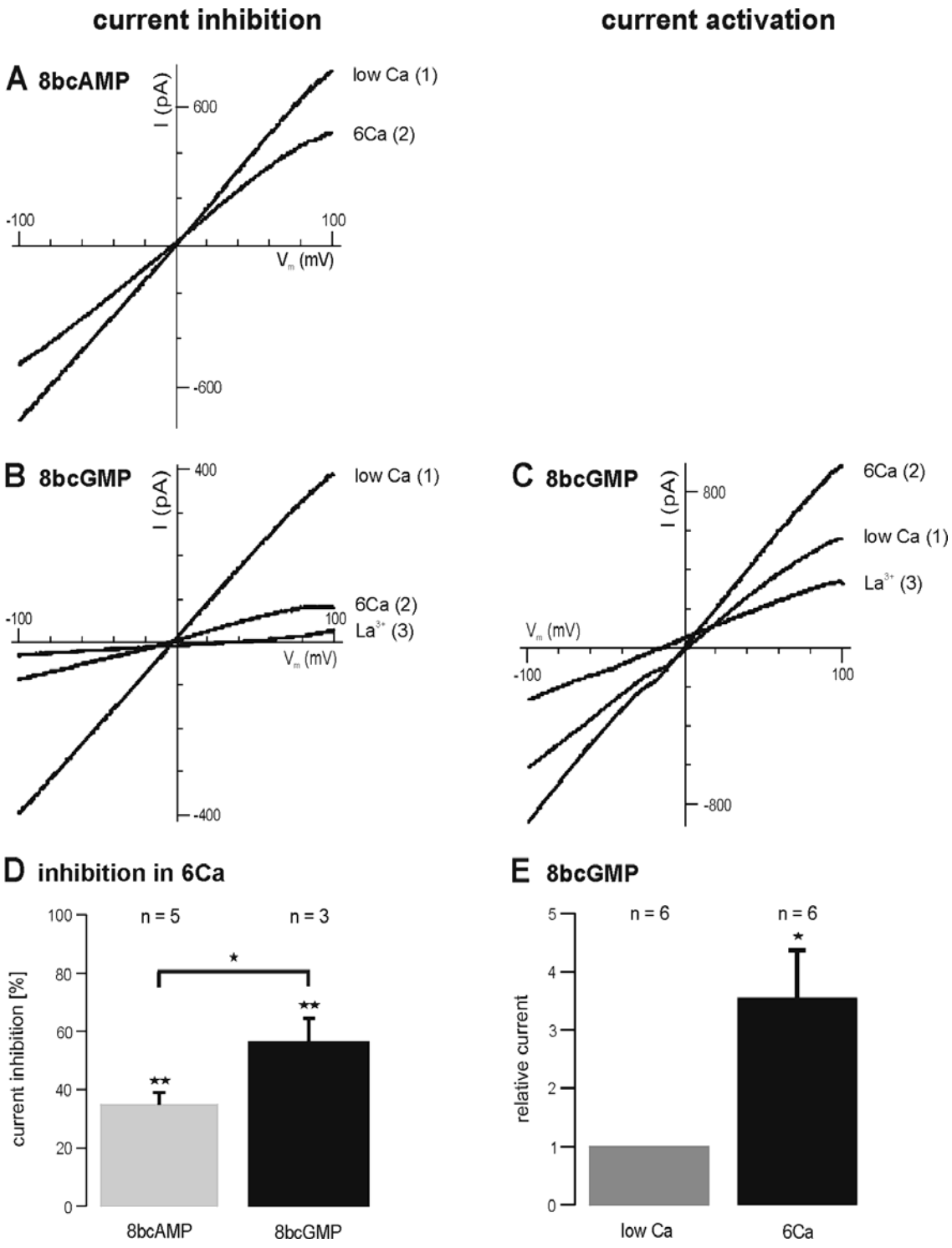

Figure 4 Cyclic nucleotide-activated currents differed in their Ca^{2+}-dependency. I-V relations of currents activated after application of 0.3 µM 8bcAMP **(A)**, 5 nM **(B)** or 0.3 µM 8bcGMP **(C)** in low Ca solution (1). Perfusion with 6Ca solution (2) decreased the cAMP-activated current (A). In contrast, 8bcGMP appeared to activate two different currents. Perfusion with 6Ca solution decreased the cGMP-activated current in 3 of 9 ORNs (B), but increased the cGMP-activated current in 6 of 9 ORNs (C). Subsequent La^{3+}-application (3) inhibited the cyclic nucleotide-activated currents. **(D)** Mean inhibition of cyclic nucleotide-activated currents in 6Ca solution as percentage of the maximum current amplitude in low Ca solution. 6Ca solution significantly stronger decreased the cGMP-activated current than the cAMP-activated current (*; $p < 0.05$). **(E)** Dependency of the relative cGMP-activated current on the extracellular Ca^{2+} concentration. Averaged values of maximum current amplitudes in 6Ca solution were normalized to those of the maximum current amplitudes in low Ca solution. Error bars represent SEM.

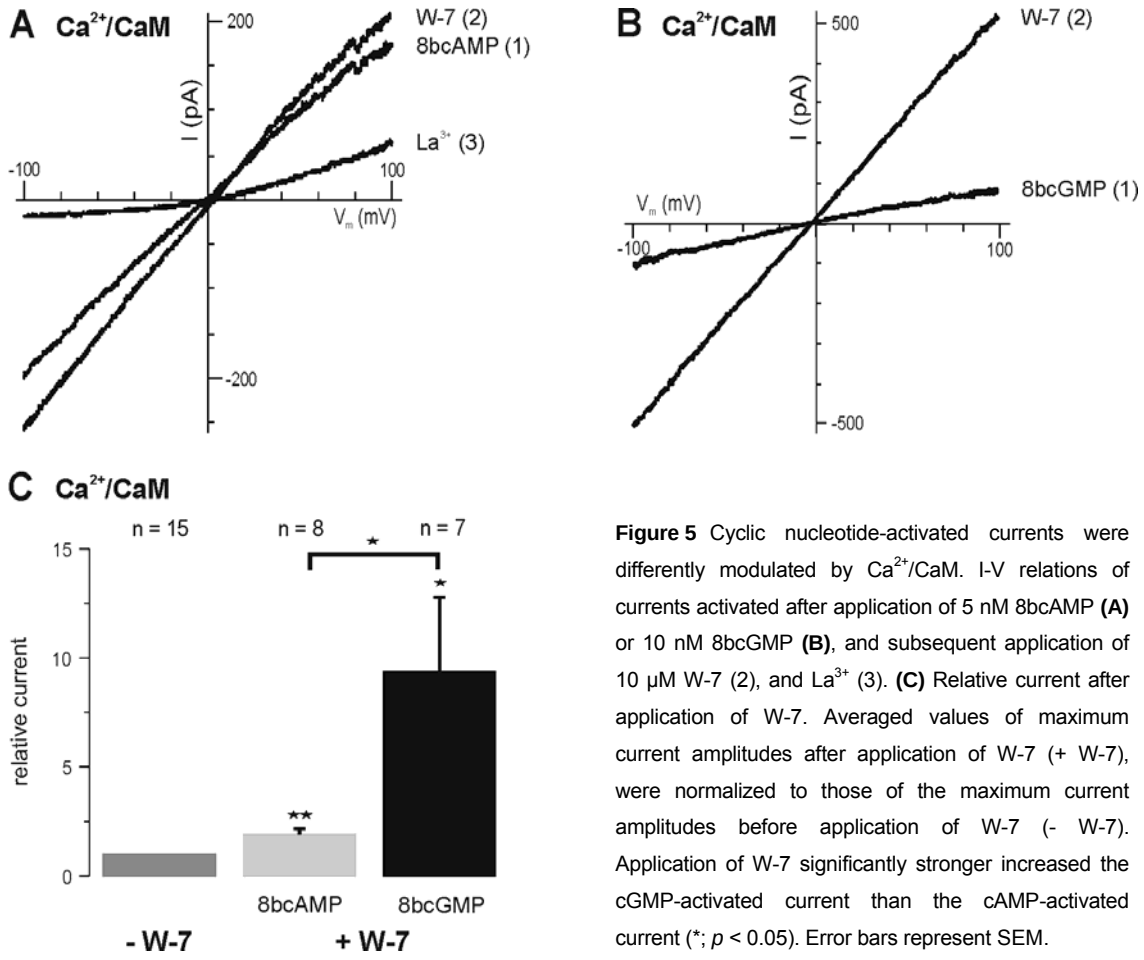

Figure 5 Cyclic nucleotide-activated currents were differently modulated by Ca^{2+}/CaM. I-V relations of currents activated after application of 5 nM 8bcAMP **(A)** or 10 nM 8bcGMP **(B)**, and subsequent application of 10 µM W-7 (2), and La^{3+} (3). **(C)** Relative current after application of W-7. Averaged values of maximum current amplitudes after application of W-7 (+ W-7), were normalized to those of the maximum current amplitudes before application of W-7 (- W-7). Application of W-7 significantly stronger increased the cGMP-activated current than the cAMP-activated current (*; $p < 0.05$). Error bars represent SEM.

Cyclic nucleotide-activated currents are modulated by Ca^{2+}/CaM

To test whether Ca^{2+}/CaM inhibits cyclic nucleotide-activated currents, the CaM antagonist W-7 was applied. Application of W-7 (10 to 50 µM) alone did not elicit a current response (n = 14 ORNs), but significantly increased the cyclic nucleotide-activated currents (Tab. 2). Application of W-7 induced a ~2-fold increase of the cAMP-activated current ($p < 0.01$; n = 8 of 12 ORNs; Fig. 5A, C), and a ~10-fold increase of the cGMP-activated current ($p < 0.05$; n = 7 of 14 ORNs; Fig. 5B, C). Thus, W-7 increased the cGMP-activated current significantly stronger than the cAMP-activated current ($p < 0.05$; Fig. 5C). Apart from the differing current amplitudes, the properties of the cyclic nucleotide-activated currents remained unchanged, i.e. the currents still showed a linear I-V relation, a mean reversal potential of -0.5 ± 1.7 mV for cAMP-, and 1.2 ± 4.3 mV for cGMP-activated currents, and inhibition by La^{3+}.

Ni^{2+} and Zn^{2+} inhibit cyclic nucleotide-activated currents

Transition metals like Ni^{2+} and Zn^{2+} inhibit Ca^{2+} permeable channels. Thus, to further characterize the Ca^{2+}-dependency of cyclic nucleotide-activated currents, ORNs were kept in 6Ca solution, stimulated with cyclic nucleotides, and then exposed to solutions containing 6 mM $NiCl_2$ (6Ni), or 1 mM $ZnCl_2$ (1Zn; Tab. 2). Both the 6Ni and 1Zn solution significantly reduced the cAMP- and the cGMP-activated currents ($p < 0.01$). Perfusion with 6Ni solution inhibited 56 ± 7.3 % of the cAMP-activated current (n = 7 of 13 ORNs, Fig. 6), while 1Zn solution inhibited 31.1 ± 5.4 % (n = 5 of 7 ORNs; Fig. 6). Thus, the 6Ni solution induced a significantly stronger current decline

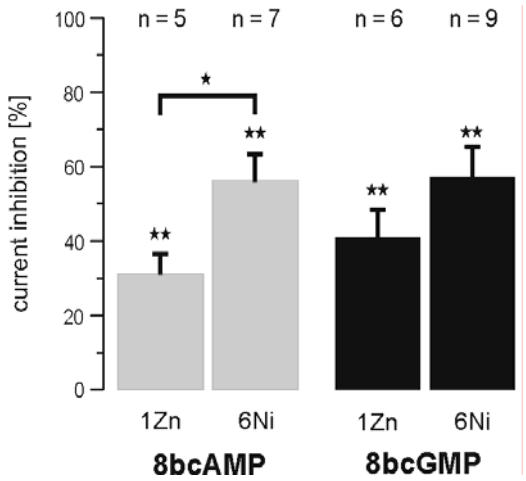

Figure 6 Ni^{2+} and Zn^{2+} inhibit cyclic nucleotide-activated currents. Mean inhibition of cyclic nucleotide-activated currents in 1Zn or 6Ni solution as percentage of the maximum current amplitude obtained before addition of transition metals. 6Ni significantly stronger inhibited the cAMP-activated current than 1Zn (*; $p < 0.05$). Error bars represent SEM.

than the 1Zn solution ($p < 0.05$). The mean reversal potential of the outwardly rectified currents remained unchanged in both solutions. Similarly, perfusion with 6Ni solution inhibited 57.3 ± 8 % of the cGMP-activated current (n = 9 of 14 ORNs, Fig. 6), and 1Zn solution inhibited 40.9 ± 7.6 % (n = 6 ORNs; Fig. 6). In contrast to the cAMP-activated current, the cGMP-activated current appeared to be equally inhibited by the 6Ni and 1Zn solution. The mean reversal potential of the outwardly rectified currents remained unchanged in both solutions. La^{3+} inhibited 61.5 ± 6.3 % of the remaining cyclic nucleotide-activated currents in 6Ni solution (n = 13 of 16 ORNs), and 72.3 ± 7.1 % in 1Zn solution (n = 5 of 6 ORNs; data not shown), but did not significantly change the mean reversal potential. In some experiments, however, perfusion with 6Ni solution increased cAMP- (n = 4 of 13 ORNs) or cGMP-activated currents (n = 3 of 14 ORNs; data not shown).

Cyclic-nucleotide-activated currents are modulated by extracellular Cl^-

To investigate whether Cl^- currents constitute a fraction of the cyclic nucleotide-activated currents, ORNs were kept in 6Ca solution, stimulated with cyclic nucleotides, and then exposed to an extracellular solution with a reduced Cl^--concentration (low Cl; Tab. 2). In 6Ca solution, cAMP-activated currents had a mean reversal potential of -0.2 ± 3 mV, which significantly shifted to -11.6 ± 4 mV in low Cl solution ($p < 0.05$; n = 9 ORNs). Similarly, the mean reversal potential of cGMP-activated currents significantly shifted from 7.1 ± 8 mV in 6Ca solution to -14.3 ± 3.9 mV in low Cl solution ($p < 0.05$; n = 7 ORNs). Perfusion with low Cl solution typically increased both the cAMP- (n = 5 of 9 ORNs; Fig 7A) and the cGMP-activated currents (n = 5 of 7 ORNs; Fig. 7B). Subsequent La^{3+}-application inhibited 82.9 ± 4 % of the cyclic nucleotide-activated currents in low Cl solution (n = 10 ORNs; Fig. 7), but did not significantly change the mean reversal potential.

Cyclic nucleotides activate currents independently of protein kinases

To investigate whether cAMP- and cGMP-activated currents depend on protein kinases, ORNs were pre-incubated with the protein kinase inhibitors staurosporine (1 µM) or H7 (10 µM) for at least 15 min, and then stimulated with cyclic nucleotides. Both protein kinase inhibitors did not prevent cAMP- and cGMP-activated non-selective cation currents (Tab. 1). In the presence of staurosporine, both cyclic nucleotide-activated currents showed a linear I-V relation (Fig. 8A, B). The cAMP-activated current had a mean reversal potential of 5.7 ± 2.3 mV and a mean amplitude of 607 ± 343 pA (n = 7 of 8 ORNs; Fig. 8A). Comparably, the cGMP-activated current had a mean reversal potential of 8 ± 8.7 mV and a mean amplitude of 738 ± 253 pA (n = 6 of 9 ORNs; Fig. 8B). In the presence of H7, both cyclic nucleotides predominantly activated an inwardly rectified current (Fig. 8C, D). The cAMP-activated current had a mean reversal potential of 5.7 ±

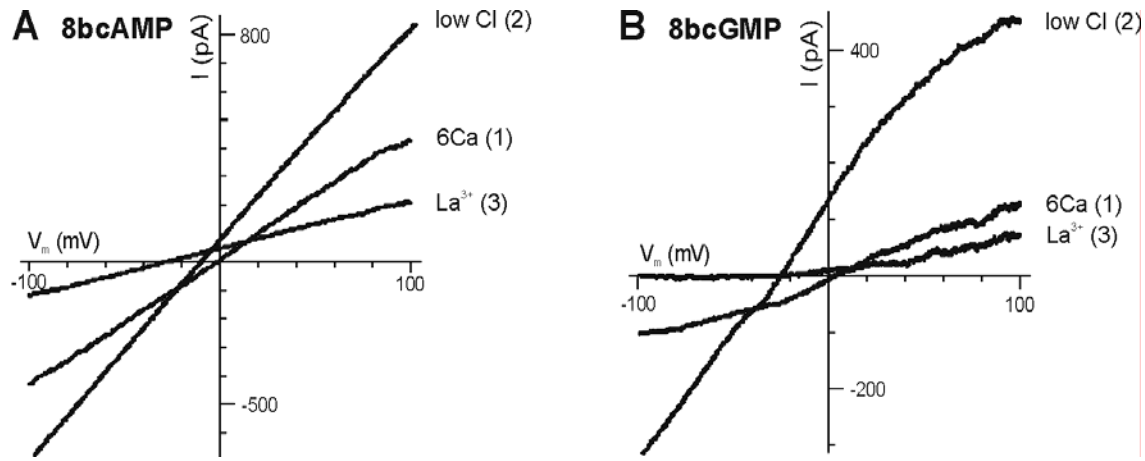

Figure 7 Cyclic nucleotide-activated currents depend on the extracellular Cl^- concentration. I-V relations of currents activated after application of 0.4 µM 8bcAMP **(A)** or 0.5 µM 8bcGMP **(B)** in 6Ca solution (1). Perfusion with low Cl solution (2) significantly shifted the reversal potential of both cyclic nucleotide-activated currents to more negative values. Subsequent La^{3+}-application (3) inhibited the cyclic nucleotide-activated currents, but did not significantly change the mean reversal potential.

3.6 mV, and a mean amplitude of 330 ± 243 pA (*n* = 6 of 9 ORNs; Fig. 8C). Similarly, the cGMP-activated current had a mean reversal potential of 5.3 ± 3.3 mV, and a mean amplitude of 142 ± 55 pA (*n* = 6 of 7 ORNs; Fig. 8D). Subsequent La^{3+}-application inhibited both cyclic nucleotide-activated currents.

Unlike cGMP, cAMP activated an additional inward current in the presence of H7 and staurosporine. This current immediately appeared after cAMP application and showed the typical I-V relation of a LVA Ca^{2+} current, activating at about -60 mV and a peak at about -20 mV (Fig. 8C). The cAMP-activated Ca^{2+} inward current ($I_{Ca(cAMP)}$) declined within seconds to minutes or was superimposed by the cAMP-activated non-selective cation current. In the presence of H7, the $I_{Ca(cAMP)}$ had a mean amplitude of -39.8 ± 9.1 pA and a mean reversal potential of 44.3 ± 8.3 mV (*n* = 8 of 9 ORNs). Three ORNs exclusively showed the $I_{Ca(cAMP)}$. In the presence of staurosporine, cAMP-application induced the $I_{Ca(cAMP)}$ in 4 of 7 ORNs (data not shown). In these ORNs, the $I_{Ca(cAMP)}$ had a mean amplitude of -11.3 ± 0.3 pA, and a mean reversal potential of 14.3 ± 8.8 mV. One ORN exclusively showed the $I_{Ca(cAMP)}$.

Discussion

Here, we used whole-cell patch-clamp recordings to characterize cyclic nucleotide-activated currents in cultured ORNs of *M. sexta* that are possibly involved in olfactory adaptation and sensitization. Pharmacological and ion exchange experiments distinguished at least one cAMP- and two cGMP-activated non-selective cation currents, which significantly differed in their Ca^{2+}-dependency and Ca^{2+}/CaM-dependent inhibition. Furthermore, a cAMP-dependent LVA Ca^{2+} current was described for the first time that was modulated by protein kinases.

Moth ORNs appear to possess CNG channels

In *M. sexta* ORNs, cyclic nucleotide-activated currents show similar properties as currents through vertebrate olfactory CNG channels. Since cGMP has been shown to activate a 55 pS non-selective cation channel in single channel recordings (Dolzer et al. 2008), our findings suggest that cyclic nucleotide-activated currents depend on prospective *M. sexta* cyclic nucleotide-gated (*Ms*CNG) channels. Like vertebrate olfactory CNG channels (Kaupp and Seifert 2002; Hofmann et al. 2005; Pifferi et al. 2006), the prospective

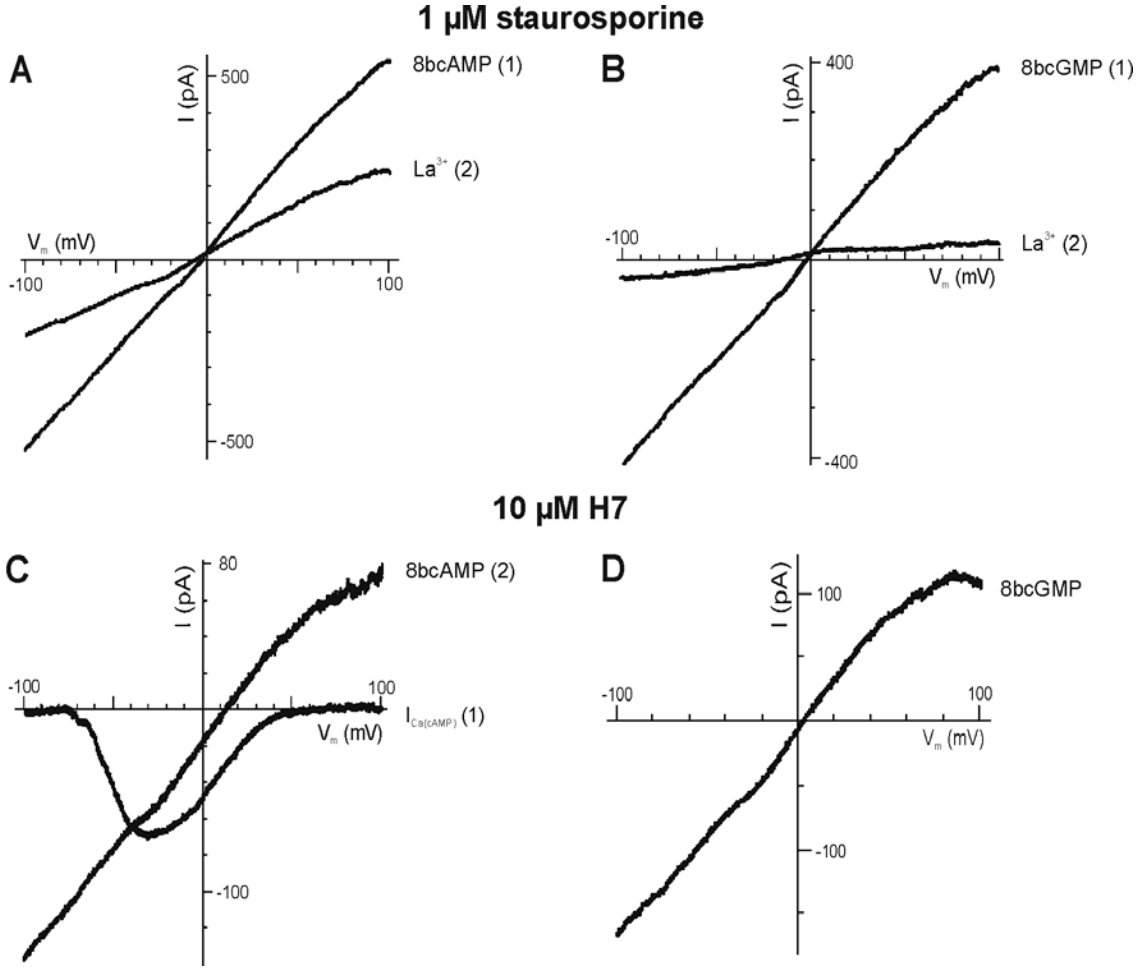

Figure 8 Cyclic nucleotides activated currents in the presence of protein kinase inhibitors. I-V relations of currents activated after application of 0.5 µM 8bcAMP **(A)** and 0.5 µM 8bcGMP **(B)** in the presence of 1 µM staurosporine, or 1.5 µM 8bcAMP **(C)** and 1.5 µM 8bcGMP **(D)** in the presence of 10 µM H7. Subsequent La^{3+}-application (2) inhibited the cyclic nucleotide-activated currents. **(C)** In the presence of 10 µM H7, an inward current ($I_{Ca(cAMP)}$) developed immediately after 8bcAMP-application. The $I_{Ca(cAMP)}$ showed the characteristics of a LVA Ca^{2+} current. While the $I_{Ca(cAMP)}$ (1) declined within seconds to minutes, the cAMP-activated non-selective cation current (2) developed.

*Ms*CNG channels are Ca^{2+} permeable non-selective cation channels that are directly activated by both cAMP and cGMP. Both prospective *Ms*CNG channels and vertebrate olfactory CNG channels show weak voltage-dependency and do not desensitize in the continuous presence of cyclic nucleotides. In addition, prospective *Ms*CNG channels and vertebrate olfactory CNG channels are modulated by Ca^{2+}/CaM. Like vertebrate olfactory CNG channels, the prospective *Ms*CNG channels differ in ligand sensitivity, ion selectivity, and gating properties.

Unlike vertebrate olfactory CNG channels, however, prospective *Ms*CNG channels did not change their response to varying concentrations of cAMP and cGMP. This lack of dose-dependency was also found for cGMP-activated channels in single channel recordings of *M. sexta* ORNs (Dolzer et al. 2008). Since both cAMP and cGMP typically induced a step-wise inward current, prospective *Ms*CNG channels are probably coupled and act coordinately. Accordingly, in single channel recordings of *M. sexta* ORNs, large conductance events consisted of several simultaneous subconductance events

in the open state (Dolzer et al. 2008). In the rat olfactory system, the principal CNG channel subunit CNGA2 localizes to lipid rafts (Brady et al. 2004) that facilitate the lateral assembly of signaling cascades (Simons and Toomre 2000), and hence likely coordinate gating. Compartmentalization of vertebrate olfactory CNG channels ensures rapid and efficient cyclic nucleotide signaling (Brady et al. 2004). Since prospective *Ms*CNG channels appear to open in a concerted manner, several lipid rafts possibly congregate prospective *Ms*CNG channels in the cell membrane of ORNs and act coordinately.

Prospective *Ms*CNG channels differ in their Ca^{2+}-dependency

Like homomeric olfactory CNG channels (Frings et al. 1995, Seifert et al. 1999), prospective *Ms*CNG channels differ in their sensitivity to extracellular Ca^{2+}. Increases of extracellular Ca^{2+} inhibited the cAMP-activated currents, and one type of the cGMP-activated currents. This fits with the finding that high extracellular Ca^{2+} concentrations generally inhibit monovalent cation currents and turn vertebrate olfactory CNG channels into "pure" Ca^{2+} channels (Frings et al. 1995; Dzeja et al. 1999). Noteworthy, Ca^{2+} significantly stronger inhibited cGMP-activated currents than cAMP-activated currents. Since the molecular structure of the channel pore determines the Ca^{2+}-permeability of vertebrate CNG channels (Root and MacKinnon 1993; Eismann et al. 1994; Sesti et al. 1995; Seifert et al. 1999), the prospective cAMP- and cGMP-dependent *Ms*CNG channels are likely to differ in their pore region. Besides the inhibitory effect of Ca^{2+} on cAMP- and cGMP-activated currents, Ca^{2+} also increased the current through at least one additional cGMP-dependent prospective *Ms*CNG channel. It is so far unknown, however, which ORNs express which specific prospective *Ms*CNG channel. Since ORNs did not differ in their morphology in primary cell culture (Stengl and Hildebrand 1990), we arranged ORNs into different subpopulations according to their electrophysiological properties. Because the increase of external Ca^{2+} induced opposite effects on cGMP-activated currents, at least two types of prospective cGMP-dependent *Ms*CNG channels appear to be expressed in moth ORNs.

Prospective *Ms*CNG channels differ in their Ca^{2+}/CaM-dependent inhibition

Cyclic nucleotides do not directly inactivate vertebrate olfactory CNG channels, but instead induce adaptation of the respective channels via Ca^{2+}/CaM-dependent negative feedback (Chen and Yau 1994; Trudeau and Zagotta 2003; Bradley et al. 2005). In *M. sexta* ORNs, the CaM antagonist W-7 increased the amplitude of cyclic nucleotide-activated currents. Thus, Ca^{2+}/CaM obviously provide negative feedback on these currents in the continuous presence of cyclic nucleotides. In the vertebrate olfactory system, native CNG channels are composed of two CNGA2, a CNGA4, and a CNGB1b subunit (Sautter et al. 1998; Shapiro and Zagotta 1998; Bonigk et al. 1999; Zheng and Zagotta 2004). The CNGA2 subunit contains a CaM binding site and controls gating (Liu et al. 1994), while the modulatory subunits CNGA4 and CNGB1b contain IQ-motifs that regulate the kinetic of Ca^{2+}/CaM-mediated inhibition. Native CNG channels are rapidly inhibited by Ca^{2+}/CaM. However, vertebrate olfactory CNG channels which consist of only CNGA2 subunits or two differing subunits (CNGA2+CNGA4/B1b) show a distinctively reduced current decline due to a reduced rate of Ca^{2+}/CaM binding to the CNGA2 subunit (Bradley et al. 2001, 2004; Munger et al. 2001). Since W-7 induced a stronger activation of the cGMP- than the cAMP-activated currents in

M. sexta ORNs, the corresponding prospective *Ms*CNG channels may differ in their subunit composition.

Lanthanum and transition metals inhibit prospective *Ms*CNG channels

Several studies used La^{3+} to inhibit Ca^{2+}-permeable cation channels such as TRP-channels (Clapham et al. 2005), Ca^{2+}-activated chloride channels (Tokimasa and North 1996), or store-operated Ca^{2+} channels (I_{CRAC}; Hoth and Penner 1993). In *M. sexta* ORNs, La^{3+} inhibited at least 83 % of cyclic nucleotide-activated currents. Low La^{3+} concentrations, however, also potentiated cyclic nucleotide-activated currents through prospective *Ms*CNG channels. Because the structure of prospective *Ms*CNG channels is unknown, and La^{3+} has not been used as an antagonist on CNG channels before, the dose-dependent effects of La^{3+} on prospective *Ms*CNG channels remain unclear. Nevertheless, a comparable dose-dependency of La^{3+} has been described for mouse TRPC5 channels. At the extracellular mouth of the TRPC5 channel pore, lanthanides bind to specific glutamate residues, which likely act as "gatekeepers" controlling cation entry (Jung et al. 2003). Remarkably, in *M. sexta* ORNs, low La^{3+} concentrations appear to potentiate more cAMP- than cGMP-activated currents. Thus, cAMP- and cGMP-dependent prospective *Ms*CNG channels may differ in their channel pore composition.

Like La^{3+}, transition metals as Ni^{2+} and Zn^{2+} also alter the sensitivity of CNG channels (Ildefonse et al. 1992, Karpen et al. 1993; Gordon and Zagotta 1995a, b). Ni^{2+}, for instance, inhibits the CNGA2 channel in the vertebrate olfactory system (Gordon and Zagotta 1995a). In *M. sexta* ORNs, both Ni^{2+} and Zn^{2+} inhibited cyclic nucleotide-activated currents. This corresponds to the finding that Zn^{2+} inhibited a cGMP-activated non-selective cation channel of *M. sexta* ORNs in single channel recordings (Dolzer et al. 2008). Remarkably, La^{3+} inhibited the remaining part of the cyclic nucleotide-activated currents. This suggests that transition metals and La^{3+} bind to different sites of prospective *Ms*CNG channels. However, La^{3+} typically did not completely inhibit cyclic nucleotide-activated currents. Since the reversal potentials of the cyclic nucleotide-activated currents did not significantly change upon La^{3+} application, the remaining La^{3+}-insensitive current was not characterized.

Prospective *Ms*CNG channel permeability depends on the extracellular Cl^- concentration

Cyclic nucleotides induce an intracellular Ca^{2+}-increase in vertebrate ORNs that subsequently leads to the activation of Ca^{2+}-activated Cl^- channels (Frings et al. 2000). The secondary Cl^- efflux forms a large fraction of the current through vertebrate olfactory CNG channels. When Cl^- is replaced with larger anions, the corresponding current is eliminated (Kleene 1993). In *M. sexta* ORNs, however, the replacement of Cl^- with acetate typically increased both cAMP- and cGMP-activated currents. Thus, Cl^- seems to inhibit monovalent cation flux through prospective *Ms*CNG channels. Since the replacement of Cl^- with acetate also significantly shifted the reversal potentials of the cyclic nucleotide-activated currents to more negative values, Cl^- carries a fraction of the respective currents.

A cAMP-activated Ca^{2+} inward current depends on protein kinase activity

In the presence of protein kinase inhibitors, an additional cAMP-dependent Ca^{2+} inward current ($I_{Ca(cAMP)}$) often preceded the cAMP-activated non-selective cation current. In a few recordings, the $I_{Ca(cAMP)}$ was not followed by cAMP-activated non-selective cation currents. In other recordings, the $I_{Ca(cAMP)}$ was missing and cAMP only activated non-selective cation currents. Thus, the $I_{Ca(cAMP)}$

does not induce non-selective cation currents through prospective *Ms*CNG channels. The $I_{Ca(cAMP)}$ instead shows the typical characteristics of a LVA Ca^{2+} current (Nilius et al. 2006) with an activation threshold at -60 mV, and a peak current at -20 mV. The $I_{Ca(cAMP)}$ only occurred in the presence of protein kinase inhibitors upon cAMP-, but not cGMP-application. Thus, the $I_{Ca(cAMP)}$ likely depends on cAMP and protein kinase-mediated phosphorylation.

Conclusions

To our knowledge, there are only few reports on CNG channels in moths. In *Heliothis virescens*, a cAMP- and hyperpolarization-activated CNG channel localized to antennal cells (Krieger et al. 1999). A clone from a cDNA library of *Spodoptera littoralis* (P. Lucas and E. Jaquin-Joly, personal communication) showed high sequence similarity to invertebrate hyperpolarization-activated CNG channels (Krieger et al. 1999, Gisselmann et al. 2003, Quesneville et al. 2005). In addition, preliminary PCR studies suggested at least two CNG channel types in *M. sexta*, among them one with sequence similarity to a subunit of the heterotetrameric CNG channels and another one with sequence similarity to hyperpolarization-activated CNG channels (M. Stengl and A. Nighorn, unpublished).

Our patch-clamp results suggest that *M. sexta* ORNs express at least one cAMP- and two cGMP-dependent prospective *Ms*CNG channels. These prospective *Ms*CNG channels differ in their Ca^{2+}-dependency and Ca^{2+}/CaM-dependent inhibition. Therefore, like vertebrate olfactory CNG channels, prospective *Ms*CNG channels are probably composed of principal and modulatory subunits, and differ in their subunit composition. Besides the prospective *Ms*CNG channels, *M. sexta* ORNs express at least one cAMP-activated, protein kinase-dependent LVA Ca^{2+} current. Furthermore, *M. sexta* ORNs express a delayed rectifier potassium channel of unknown molecular identity, which is inhibited by cyclic nucleotides (Zufall et al. 1991; Stengl et al. 1992). Thus, a multitude of cyclic nucleotide-activated channels - non-selective cation, potassium and calcium channels - are present in ORNs. Since both cAMP and cGMP activated at least 81% of ORNs, most ORNs appear to co-express cAMP- and cGMP-dependent prospective *Ms*CNG channels. The prospective *Ms*CNG channels, therefore, are likely to play a prominent role for the modulation of the olfactory transduction cascade. Current molecular cloning studies aim to identify the *Ms*CNG channels that are involved in olfactory transduction.

Acknowledgments

The authors would like to thank Jonas Benzler, Cornelia Ellendt, Sandy Fastner, and Martina Kern for insect rearing; Philippe Lucas for valuable discussions; Christian Wegener and Matthias Vömel for help with the manuscript. This work was supported by the DFG grant STE 531/13-1,2 to Monika Stengl.

References

Baumann A, Frings S, Godde M, Seifert R, Kaupp UB. Primary structure and functional expression of a *Drosophila* cyclic nucleotide-gated channel present in eyes and antennae. *EMBO J* 13: 5040-5050, 1994.

Bell RA, Joachim FA. Techniques for rearing laboratory colonies of the tobacco hornworm, *Manduca sexta* and pink ballworms. *Ann Entomol Soc Am* 69: 365-373, 1976.

Boekhoff I, Strotmann J, Raming K, Tareilus E, Breer H. Odorant-sensitive phospholipase C in insect antennae. *Cell Signal* 2: 49-56, 1990.

Boekhoff I, Seifert E, Goggerle S, Lindemann M, Kruger BW, Breer H. Pheromone-induced second-messenger signaling in insect antennae. *Insect Biochem Mol Biol* 23: 757-762, 1993.

Bonigk W, Bradley J, Muller F, Sesti F, Boekhoff I, Ronnett GV, Kaupp UB, Frings S. The native rat olfactory cyclic nucleotide-gated channel is composed of three distinct subunits. *J Neurosci* 19: 5332-5347, 1999.

Bradley J, Reuter D, Frings S. Facilitation of calmodulin-mediated odor adaptation by cAMP-gated channel subunits. *Science*

*2*94: 2176-2178, 2001.

Bradley J, Bonigk W, Yau KW, Kaupp UB. Calmodulin permanently associates with rat olfactory CNG channels under native conditions. *Nat Neurosci* 7: 705-710, 2004.

Bradley J, Reisert J, Frings S. Regulation of cyclic nucleotide-gated channels. *Curr Opin Neurobiol* 15: 343-349, 2005.

Brady JD, Rich TC, Le X, Stafford K, Fowler CJ, Lynch L, Karpen JW, Brown RL, Martens JR. Functional role of lipid raft microdomains in cyclic nucleotide-gated channel activation. *Mol Pharmacol* 65: 503-511, 2004.

Breer H, Boekhoff I, Tareilus E. Rapid kinetics of second messenger formation in olfactory transduction. *Nature* 345: 65-68, 1990.

Chen TY, Yau KW. Direct modulation by Ca^{2+}-calmodulin of cyclic nucleotide-activated channel of rat olfactory receptor neurons. *Nature* 368: 545-548, 1994.

Clapham DE, Julius D, Montell C, Schultz G. International Union of Pharmacology. XLIX. Nomenclature and structure-function relationships of transient receptor potential channels. *Pharmacol Rev* 57: 427-450, 2005.

Dolzer J, Krannich S, Stengl M. Pharmacological investigation of protein kinase C- and cGMP-dependent ion channels in cultured olfactory receptor neurons of the hawkmoth *Manduca sexta*. *Chem Sens*: in press.

Dzeja C, Hagen V, Kaupp UB, Frings S. Ca^{2+} permeation in cyclic nucleotide-gated channels. *EMBO J* 18: 131-144, 1999.

Eide PE, Caldwell JM, Marks EP. Establishment of two cell lines from embryonic tissue of the tobacco hornworm, *Manduca sexta* (L). *In Vitro* 11: 395-399, 1975.

Eismann E, Muller F, Heinemann SH, Kaupp UB. A single negative charge within the pore region of a cGMP-gated channel controls rectification, Ca^{2+} blockage, and ionic selectivity. *Proc Natl Acad Sci USA* 91: 1109-1113, 1994.

Flecke C, Dolzer J, Krannich S, Stengl M. Perfusion with cGMP analogue adapts the action potential response of pheromone-sensitive sensilla trichoidea of the hawkmoth *Manduca sexta* in a daytime-dependent manner. *J Exp Biol* 209: 3898-3912, 2006.

Frings S, Lynch JW, Lindemann B. Properties of cyclic nucleotide-gated channels mediating olfactory transduction. Activation, selectivity, and blockage. *J Gen Physiol* 100: 45-67, 1992.

Frings S, Seifert R, Godde M, Kaupp UB. Profoundly different calcium permeation and blockage determine the specific function of distinct cyclic nucleotide-gated channels. *Neuron* 15: 169-179, 1995.

Frings S, Reuter D, Kleene SJ. Neuronal Ca^{2+}-activated Cl^- channels - homing in on an elusive channel species. *Prog Neurobiol* 60: 247-289, 2000.

Gisselmann G, Warnstedt M, Gamerschlag B, Bormann A, Marx T, Neuhaus EM, Stoertkuhl K, Wetzel CH, Hatt H. Characterization of recombinant and native Ih-channels from *Apis mellifera*. *Insect Biochem Mol Biol* 33: 1123-1134, 2003.

Gordon SE, Zagotta WN. Localization of regions affecting an allosteric transition in cyclic nucleotide-activated channels. *Neuron* 14: 857-864, 1995a.

Gordon SE, Zagotta WN. Subunit interactions in coordination of Ni^{2+} in cyclic nucleotide-gated channels. *Proc Natl Acad Sci USA* 92: 10222-10226, 1995b.

Hamill OP, Marty A, Neher E, Sakmann B, Sigworth FJ. Improved patch-clamp techniques for high-resolution current recording from cells and cell-free membrane patches. *Pflugers Arch* 391: 85-100, 1981.

Hansson BS. A bug's smell--research into insect olfaction. *Trends Neurosci* 25: 270-274, 2002.

Hildebrand JG. Analysis of chemical signals by nervous systems. *Proc Natl Acad Sci USA* 92: 67-74, 1995.

Hofmann F, Biel M, Kaupp UB. International Union of Pharmacology. LI. Nomenclature and structure-function relationships of cyclic nucleotide-regulated channels. *Pharmacol Rev* 57: 455-462, 2005.

Hoth M, Penner R. Calcium release-activated calcium current in rat mast cells. *J Physiol* 465: 359-386, 1993.

Ildefonse M, Crouzy S, Bennett N. Gating of retinal rod cation channel by different nucleotides: Comparative study of unitary currents. *J Membr Biol* 130: 91-104, 1992.

Jacquin-Joly E, Francois MC, Burnet M, Lucas P, Bourrat F, Maida R. Expression pattern in the antennae of a newly isolated lepidopteran Gq protein alpha subunit cDNA. *Eur J Biochem* 269, 2133-2142, 2002.

Jindra M, Huang JY, Malone F, Asahina M, Riddiford LM. Identification and mRNA developmental profiles of two ultraspiracle isoforms in the epidermis and wings of *Manduca sexta*. *Insect Mol Biol* 6: 41-43, 1997.

Jung S, Muhle A, Schaefer M, Strotmann R, Schultz G, Plant TD. Lanthanides potentiate TRPC5 currents by an action at extracellular sites close to the pore mouth. *J Biol Chem* 278: 3562-3571, 2003.

Kaissling KE. Physiology of pheromone reception in insects (an example of moths). *ANIR* 6: 73-91, 2004.

Kaissling KE, Priesner E. Smell threshold of the silkworm. *Naturwissenschaften* 57: 23-28, 1970.

Karpen JW, Brown RL, Stryer L, Baylor DA. Interactions between divalent cations and the gating machinery of cyclic GMP-activated channels in salamander retinal rods. *J Gen Physiol* 101: 1-25, 1993.

Kaupp UB, Seifert R. Cyclic nucleotide-gated ion channels. *Physiol Rev* 82: 769-824, 2002.

Kleene SJ. Origin of the chloride current in olfactory transduction. *Neuron* 11: 123-132, 1993.

Krieger J, Strobel J, Vogl A, Hanke W, Breer H. Identification of a cyclic nucleotide- and voltage-activated ion channel from insect antennae. *Insect Biochem Mol Biol* 29: 255-267, 1999.

Liu M, Chen TY, Ahamed B, Li J, Yau KW. Calcium-calmodulin modulation of the olfactory cyclic nucleotide-gated cation channel. *Science* 266: 1348-1354, 1994.

Miyazu M, Tanimura T, Sokabe M. Molecular cloning and

characterization of a putative cyclic nucleotide-gated channel from *Drosophila melanogaster*. *Insect Mol Biol* 9: 283-292, 2000.

Munger SD, Lane AP, Zhong H, Leinders-Zufall T, Yau KW, Zufall F, Reed RR. Central role of the CNGA4 channel subunit in Ca^{2+}-calmodulin-dependent odor adaptation. *Science* 294: 2172-2175, 2001.

Nilius B, Talavera K, Verkhratsky A. T-type calcium channels: The never ending story. *Cell Calcium* 40: 81-88, 2006.

Quesneville H, Bergman CM, Andrieu O, Autard D, Nouaud D, Ashburner M, Anxolabehere D. Combined evidence annotation of transposable elements in genome sequences. *PLoS Comput Biol* 1: 166-175, 2005.

Pifferi S, Boccaccio A, Menini A. Cyclic nucleotide-gated ion channels in sensory transduction. *FEBS Lett* 580: 2853-2859, 2006.

Redkozubov A. Guanosine 3',5'-cyclic monophosphate reduces the response of the Moth's olfactory receptor neuron to pheromone. *Chem Senses* 25: 381-385, 2000.

Riesgo-Escovar J, Raha D, Carlson JR. Requirement for a phospholipase C in odor response: overlap between olfaction and vision in *Drosophila*. *Proc Natl Acad Sci USA* 92: 2864-2868, 1995.

Root MJ, MacKinnon R. Identification of an external divalent cation-binding site in the pore of a cGMP-activated channel. *Neuron* 11: 459-466, 1993.

Rospars JP, Lucas P, Coppey M. Modelling the early steps of transduction in insect olfactory receptor neurons. *Biosystems* 89: 101-109, 2007.

Sautter A, Zong X, Hofmann F, Biel M. An isoform of the rod photoreceptor cyclic nucleotide-gated channel beta subunit expressed in olfactory neurons. *Proc Natl Acad Sci USA* 95: 4696-4701, 1998.

Seifert R, Eismann E, Ludwig J, Baumann A, Kaupp UB. Molecular determinants of a Ca^{2+}-binding site in the pore of cyclic nucleotide-gated channels: S5/S6 segments control affinity of intrapore glutamates. *EMBO J* 18: 119-130, 1999.

Seno K, Nakamura T, Ozaki M. Biochemical and physiological evidence that calmodulin is involved in the taste response of the sugar receptor cells of the blowfly, *Phormia regina*. *Chem Senses* 30: 497-504, 2005.

Sesti F, Eismann E, Kaupp UB, Nizzari M, Torre V. The multi-ion nature of the cGMP-gated channel from vertebrate rods. *J Physiol* 487: 17-36, 1995.

Shapiro MS, Zagotta WN. Stoichiometry and arrangement of heteromeric olfactory cyclic nucleotide-gated ion channels. *Proc Natl Acad Sci USA* 95: 14546-14551, 1998.

Simons K, Toomre D. Lipid rafts and signal transduction. *Nat Rev Mol Cell Biol* 1: 31-39, 2000.

Stengl M. Intracellular-messenger-mediated cation channels in cultured olfactory receptor neurons. *J Exp Biol* 178: 125-147, 1993.

Stengl M. Inositol-trisphosphate-dependent calcium currents precede cation currents in insect olfactory receptor neurons in vitro. *J Comp Physiol [A]* 174: 187-194, 1994.

Stengl M, Hildebrand JG. Insect olfactory neurons in vitro: morphological and immunocytochemical characterization of male-specific antennal receptor cells from developing antennae of male *Manduca sexta*. *J Neurosci* 10: 837-847, 1990.

Stengl M, Zufall F, Hatt H, Hildebrand JG. Olfactory receptor neurons from antennae of developing male *Manduca sexta* respond to components of the species-specific sex pheromone in vitro. *J Neurosci* 12: 2523-2531, 1992.

Tokimasa T, North RA. Effects of barium, lanthanum and gadolinium on endogenous chloride and potassium currents in *Xenopus* oocytes. *J Physiol* 496: 677-686, 1996.

Trudeau MC, Zagotta WN. Calcium/calmodulin modulation of olfactory and rod cyclic nucleotide-gated ion channels. *J Biol Chem* 278: 18705-18708, 2003.

Wegener JW, Breer H, Hanke W. Second messenger-controlled membrane conductance in locust (*Locusta migratoria*) olfactory neurons. *J Insect Physiol* 43: 595-603, 1997.

Zheng J, Zagotta WN. Stoichiometry and assembly of olfactory cyclic nucleotide-gated channels. *Neuron* 42: 411-421, 2004.

Ziegelberger G, van den Berg MJ, Kaissling KE, Klumpp S, Schultz JE. Cyclic GMP levels and guanylate cyclase activity in pheromone-sensitive antennae of the silkmoths *Antheraea polyphemus* and *Bombyx mori*. *J Neurosci* 10: 1217-1225, 1990.

Zufall F, Hatt H. Dual activation of a sex pheromone-dependent ion channel from insect olfactory dendrites by protein kinase C activators and cyclic GMP. *Proc Natl Acad Sci USA* 88: 8520-8524, 1991.

Zufall F, Leinders-Zufall T. The cellular and molecular basis of odor adaptation. *Chem Senses* 25: 473-481, 2000.

Zufall F, Stengl M, Franke C, Hildebrand JG, Hatt H. Ionic currents of cultured olfactory receptor neurons from antennae of male *Manduca sexta*. *J Neurosci* 11: 956-965, 1991.

Supplementary Table 1 Cyclic nucleotide-activated currents in moth ORNs seem to lack dose-dependency.

	n		**n activation**		**mean amplitude (pA)**		**reversal potential (mV)**		**latency (s)**	
	cAMP	*cGMP*	*cAMP*	*cGMP*	*cAMP*	*cGMP*	*cAMP*	*cGMP*	*cAMP*	*cGMP*
10^{-9} M	22	19	21	18	646 ± 220	1158 ± 387	0.2 ± 1.4	0.9 ± 0.9	139 ± 15	83 ± 14
10^{-7} M	23	26	18	21	594 ± 120	767 ± 267	2.9 ± 2.2	2.1 ± 3.2	116 ± 19	93 ± 17
10^{-6} M	47	34	40	27	695 ± 159	793 ± 227	0.7 ± 2.1	4.4 ± 2.3	121 ± 13	126 ± 17
10^{-5} M	4	13	3	9	750 ± 366	733 ± 216	-1.2 ± 2.6	3.6 ± 4.2	167 ± 78	153 ± 45

n = number of ORNs recorded, n activation = number of ORNs that activated a current at the corresponding concentration of cyclic nucleotides. The listed parameters did not significantly differ. The table indicates that also within the same concentration of cyclic nucleotides a great variability in the examined parameters exists. Data represent mean ± SEM.

Appendix A

Hyperpolarization-activated cyclic nucleotide-modulated currents in cultured olfactory receptor neurons of *Manduca sexta*.

Properties of HCN channels

Cyclic nucleotide-dependent channels belong to two families: cyclic nucleotide-gated (CNG) channels and hyperpolarization-activated cyclic nucleotide-modulated (HCN) channels (Hofmann et al. 2005). Both CNG and HCN channels are part of the superfamily of voltage-gated K^+-channels. Yet, CNG channels are less voltage-dependent than HCN channels. In contrast to most voltage-gated channels, HCN channels open at hyperpolarizing and close at depolarizing potentials. The cyclic nucleotides adenosine monophosphate (cAMP) and guanosine mono-phosphate (cGMP) modulate the permeability of HCN channels (Robinson and Siegelbaum 2003, Craven and Zagotta 2006). Typically, HCN channels conduct a mixed current of monovalent cations, but prefer K^+ over Na^+. Divalent cations like Ca^{2+} or Mg^{2+} slightly permeate, but do not block HCN channels (Dzeja et al. 1999; Yu et al. 2004). The current generated by HCN channels is usually termed hyperpolarization-activated current (I_h current; Yanagihara and Irisawa 1980). In neurons, I_h currents contribute to the resting potential and also play a role for the generation of pacemaker potentials (Pape 1996, Robinson and Siegelbaum 2003).

I_h currents in moth ORNs

In whole-cell patch-clamp recordings on cultured *Manduca sexta* olfactory receptor neurons (ORNs), the membrane-permeable cAMP and cGMP analogues 8bcAMP and 8bcGMP activated an inward current at hyperpolarizing potentials. The current characteristics resembled those of I_h currents with activation at about -110 mV, a reversal potential of about -50 mV, and a peak current at -80 mV. Both cAMP and cGMP directly

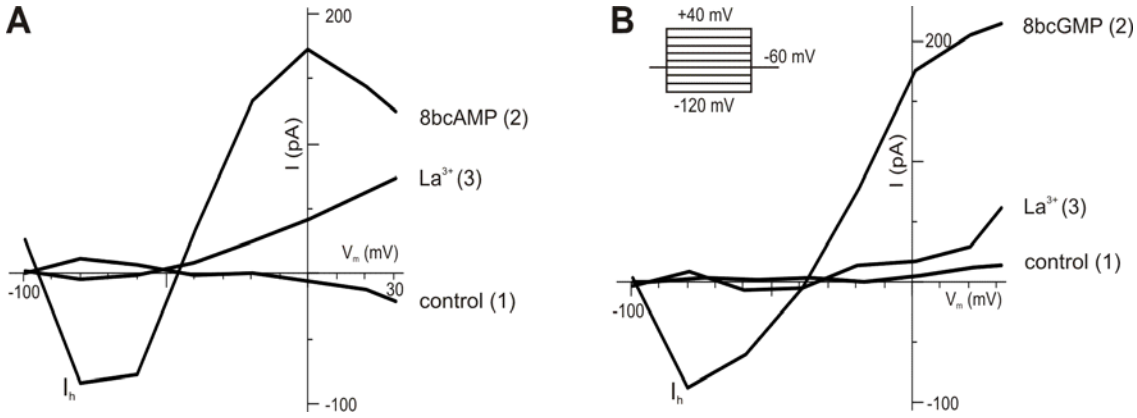

Figure A1 I_h current in moth ORNs. Voltage step protocols were used to establish I-V relations before (control, 1), after cyclic nucleotide-application (2), and after La^{3+}-application (3). Stimulation with 0.5 µM 8bcAMP (**A**) or 1.5 µM 8bcGMP (**B**) induced a hyperpolarization-activated current (I_h) with a peak at -80 mV. Subsequent La^{3+}-application inhibited the I_h current.

activated I_h currents, and the activation did not depend on the extracellular Ca^{2+} concentration (10^{-5} M Ca^{2+}; *n* = 13 ORNs). The cAMP-activated I_h current had a mean amplitude of -86 ± 20 pA (*n* = 29 of 96 ORNs; Fig. A1A) while the cGMP-activated I_h current had a mean amplitude of -70 ± 11 pA (*n* = 21 of 93 ORNs; Fig. A1B). Application of lanthanum (La^{3+}), a non-specific blocker of Ca^{2+}-permeable cation channels, completely inhibited the I_h currents (*n* = 32 of 34 ORNs; Fig. A1).

Possible role of the I_h currents in moth ORNs

We here characterized hyperpolarization-activated cyclic nucleotide-modulated currents in about 23 % of cultured ORNs of the moth *M. sexta*. In the moth *Heliothis virescens*, a cAMP-activated HCN channel, which localized to the antennal cells, was described (Krieger et al. 1999). The antennae and the CNS of *M. sexta* also appear to express ion channels with sequence similarity to HCN channels (M. Stengl, personal communication). However, nothing is known about the spatial distribution of HCN channels in insect ORNs. The moth HCN channels might play a similar role as vertebrate HCN channels, which control pacemaker activity. Like vertebrate heart cells, ORNs from insect antennae show spontaneous activity (Kaissling 1986, Dolzer et al. 2001) and an increased action potential frequency upon odorant stimulation (Dubin and Harris 1997) while the decrease in action potential frequency seems at least partly mediated by cGMP-dependent ion channels (Flecke et al. 2006). Thus, HCN channels might be necessary to distinguish olfactory input with high resolution in time.

References

Craven KB, Zagotta WN (2006). CNG and HCN channels: two peas, one pod. *Annu Rev Physiol* 68: 375-401.

Dolzer J, Krannich S, Fischer K, Stengl M (2001). Oscillations of the transepithelial potential of moth olfactory sensilla are influenced by octopamine and serotonin. *J Exp Biol* 204: 2781-2794.

Dubin AE, Harris GL (1997). Voltage-activated and odor-modulated conductances in olfactory receptor neurons of *Drosophila melanogaster*. *J Neurobiol* 32: 123-137.

Dzeja C, Hagen V, Kaupp UB, Frings S (1999). Ca^{2+} permeation in cyclic nucleotide-gated channels. *EMBO J* 18: 131-144.

Flecke C, Dolzer J, Krannich S, Stengl M (2006). Perfusion with cGMP analogue adapts the action potential response of pheromone-sensitive sensilla trichoidea of the hawkmoth *Manduca sexta* in a daytime-dependent manner. *J Exp Biol* 209: 3898-3912.

Hofmann F, Biel M, Kaupp UB (2005). International Union of Pharmacology. LI. Nomenclature and structure-function relationships of cyclic nucleotide-regulated channels. *Pharmacol Rev* 57: 455-462.

Kaissling KE (1986). Chemo-electrical transduction in insect olfactory receptor neurons. *Ann Rev Neurosci* 9: 121-145.

Krieger J, Strobel J, Vogl A, Breer H (1999). Identification of a cyclic nucleotide- and voltage-activated ion channel from insect antennae. *Insect Biochem Mol Biol* 29: 255-267.

Pape HC (1996). Queer current and pacemaker: the hyperpolarization-activated cation current in neurons. *Annu Rev Physiol* 58: 299-327.

Robinson RB, Siegelbaum SA (2003). Hyperpolarization-activated cation currents: From molecules to physiological function. *Annu Rev Physiol* 65: 453-480.

Yanagihara K, Irisawa H (1980). Inward current activated during hyperpolarization in the rabbit sinoatrial node cell. *Pflügers Arch* 358: 11-19.

Yu X, Duan KL, Shang CF, Yu HG, Zhou Z (2004). Calcium influx through hyperpolarization-activated cation channels (I(h) channels) contributes to activity-evoked neuronal secretion. *Proc Natl Acad Sci USA* 101: 1051-1056.

Appendix B

Protein kinase C-dependent currents in cultured olfactory receptor neurons of *Manduca sexta*.

Two models of PKC activation

Odorants bind to G-protein-coupled receptors (GPCRs) that interact with phospholipase C (PLC). The PLC then cleaves phosphatidylinositol 4,5-bisphosphate to generate the second messengers inositol 1,4,5-triphosphate (IP_3) and 1,2-diacylglycerol (DAG; Bruch 1996). IP_3 activates Ca^{2+}-dependent channels, and hence causes depolarization (Stengl 1994). The intracellular Ca^{2+} increase leads to the recruitment of cytosolic protein kinase C (PKC) to the plasma membrane. There, PKC is activated by membrane-bound DAG. The activated PKC and other GPCR kinases phosphorylate the GPCRs and thereby terminate signal transduction (Boekhoff and Breer 1992; Bruch 1996; Becker and Hannun 2005). Within seconds, the PKC is returned to the cytosol and DAG is metabolized (Oancea and Meyer 1998). Apart from the activation of PLC, GPCRs can interact with phospholipase D that cleaves phosphatidylcholine into phosphatidic acid (PA) and choline. A phosphohydrolase may then convert PA into DAG (Becker and Hannun 2005). DAG from this source is sustained in the membrane and induces prolonged PKC translocation (Ha and Exton 1993). Phorbol esters activate PKC and, therefore, can be used to mimic transient and sustained DAG signals.

PKC-dependent currents in moth ORNs

In cultured *Manduca sexta* olfactory receptor neurons (ORNs), application of 10 nM of the phorbol ester phorbol 12-myristate-13-acetate (PMA) activated a Ca^{2+}-independent non-specific cation current in whole-cell patch-clamp recordings (Stengl 1993), as well as 40 and 60 pS non-specific cation channels in single channel patch-clamp recordings (see Chapter 3). In extracellular solution containing 6 mM Ca^{2+}, the PKC-

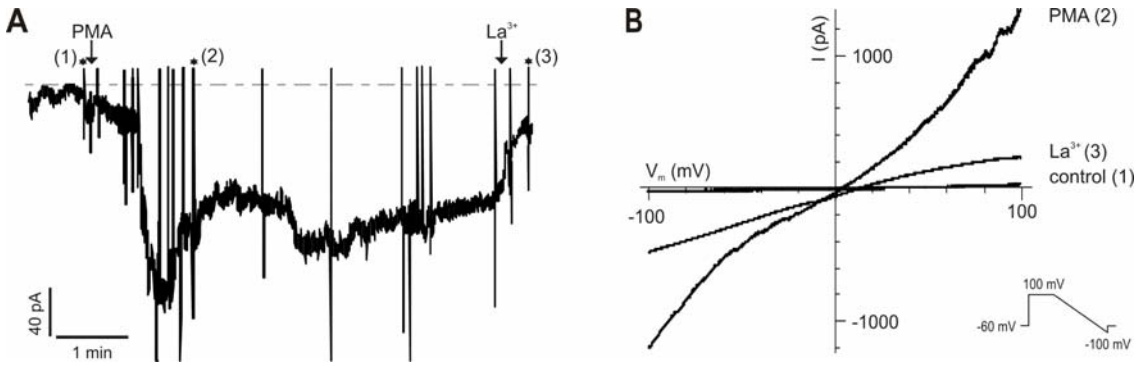

Figure B1 A PKC-dependent current in moth ORNs. (**A**) Stimulation with 250 nM PMA activates a La^{3+}-sensitive inward current at -60 mV membrane potential in extracellular solution containing 6 mM Ca^{2+}. Dashed line indicates 0 pA level. The large transient interruptions are voltage-ramp protocols. Asterisks indicate protocols used to establish I-V relations before (control; 1) and after PMA-application (2), and after La^{3+}-application (3; **B**).

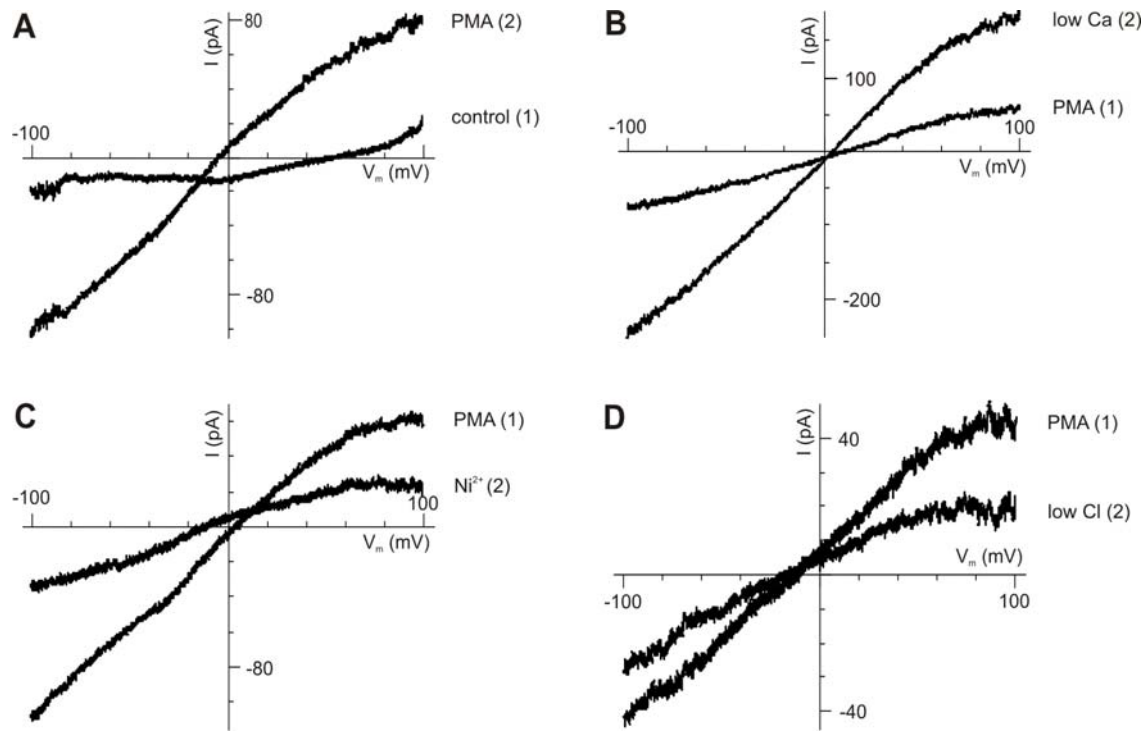

Figure B2 Properties of the PKC-dependent current. (**A**) Stimulation with 250 nM PMA activates a non-specific cation current (2) in extracellular solution containing 6 mM Ba^{2+} substituted for Ca^{2+}. (**B**) The PKC-dependent current (1) increased following perfusion with reduced extracellular Ca^{2+} solution (low Ca, 2). The PKC-dependent current (1) inhibited following perfusion with 6 mM extracellular Ni^{2+} solution (**C**, 2) or reduced extracellular Cl^- solution (low Cl; **D**, 2).

dependent current (Stengl 1993) showed a linear I-V relation, a reversal potential around 0 mV, and a mean amplitude of -45 ± 16 pA at -110 mV. In extracellular solution with reduced Ca^{2+} concentration (10^{-7} M) the mean amplitude was -64 ± 34 pA. Application of extracellular solution containing 20 mM of the cation channel blocker tetraethylammonium chloride inhibited the PKC-dependent current (Stengl 1993) and the 60 pS cation channel, but did not affect the 40 pS cation channel (see Chapter 3).

Here, whole-cell patch-clamp recordings of *M. sexta* ORNs revealed a second type of PKC-dependent non-specific cation current. In extracellular solution containing 6 mM Ca^{2+}, application of 250 nM PMA activated a current with a linear I-V relation, a reversal potential of -0.5 ± 2.2 mV, and a mean amplitude of -598 ± 122 pA at -100 mV (*n* = 41 of 55 ORNs; Fig. B1). Application of PMA in extracellular solution with reduced Ca^{2+} concentration (10^{-5} or 10^{-7} M) activated the PKC-dependent current. This PKC-dependent current also showed a linear I-V relation, a reversal potential of -8.5 ± 4.2 mV, and a mean amplitude of -439 ± 246 pA at -100 mV (*n* = 9 of 11 ORNs; Fig. B2A). Application of PMA in extracellular solution containing 6 mM Ca^{2+} and subsequent perfusion with extracellular solution with reduced Ca^{2+} concentration (10^{-5} M; Fig. B2B) increased the PKC-dependent current amplitude without changing the reversal potential (*n* = 6 of 7 ORNs). Subsequent application of lanthanum (La^{3+}), a non-specific blocker of Ca^{2+}-permeable cation channels, significantly inhibited 80.4 ± 3 % of the PKC-dependent current (*n* = 20 of 25 ORNs; $p < 0.01$; Fig. B1). Perfusion with extracellular solution containing 6 mM of the calcium channel blocker Ni^{2+} also significantly inhibited 78.8 ± 6.9 % of the PKC-dependent current (*n* = 9 of 11 ORNs; $p < 0.01$; Fig. B2C) without changing the reversal

potential. Thus, as opposed to the previously described PKC-dependent current (Stengl 1993), the PKC-dependent current observed here carried both Ca^{2+} and monovalent cations. Furthermore, this PKC-dependent current at least partly carried Cl^-, because perfusion with extracellular solution with reduced Cl^- concentration significantly inhibited 27.7 ± 6 % of the PKC-dependent current (n = 4 of 7 ORNs; $p < 0.01$; Fig. B2D) without changing the reversal potential.

Differential PKC stimulation

A transient odorant-induced increase in IP_3 is assumed to promote a transient elevation of DAG and activation of PKC. This transient PKC activation terminates the IP_3-mediated odorant response (Boekhoff and Breer 1992). Stengl (1993) showed that short-term application of PMA induced a non-specific cation current. The PKC-dependent current did not depend on Ca^2. Because this current was blocked TEA-dependently, it might correspond to the 60 pS PKC-dependent channel found in single channel patch-clamp recordings (see Chapter 3). In the moth *Antherea polyphemus*, short-term application of DAG and phorbol ester activated a 56 pS odorant-dependent channel in the dendritic membrane of ORNs. These results indicated that PKC-mediated channel phosphorylation is involved for transducing odorant information (Zufall and Hatt 1991; Maida et al. 2000). Here, PMA was permanently applied with the extracellular solution and induced a second type of PKC-dependent non-specific cation currents in about 75 % of cultured ORNs. This PKC-dependent current carried Ca^{2+}, monovalent cations, and Cl^-. Since the current properties differed from the PKC-dependent current described before (Stengl 1993), this PKC-dependent current might correspond to the 40 pS PKC-dependent channel described in single channel recordings or to the large-conductance Cl^- channels that were not further characterized (see Chapter 3). Since long-lasting Ca^{2+} changes were known to influence gene expression, the second type of PKC-dependent current may play a role for long-term cellular processes such as adaptation (Nishizuka 1995; Becker and Hannun 2003).

References

Becker KP, Hannun YA (2003). cPKC-dependent sequestration of membrane-recycling components in a subset of recycling endosomes. *J Biol Chem* 278: 52747-52754.

Becker KP, Hannun YA (2005). Protein kinase C and phospholipase D: intimate interactions in intracellular signalling. *CMLS* 62: 1448-1461.

Boekhoff I, Breer H (1992). Termination of second messenger signaling in olfaction. *Proc Natl Acad Sci USA* 89: 471-474.

Bruch RC (1996). Phosphoinositide second messengers in olfaction. *Comp Biochem Physiol* 113B: 451-459.

Ha KS, Exton JH (1993). Differential translocation of protein kinase C isozymes by thrombin and platelet-derived growth factor. A possibly function for phosphatidylcholine-derived diacylglycerol. *J Biol Chem* 268: 10534-10539.

Maida R, Redkozubov A, Ziegelberger G (2000). Identification of PLCβ and PKC in pheromone receptor neurons of *Antheraea polyphemus*. *Neuroreport* 11: 1773-1776.

Nishizuka Y (1995). Protein kinase C and lipid signaling for sustained cellular responses. *FASEB J* 9: 484-496.

Oancea E, Meyer T (1998). Protein kinase C as a molecular machine for decoding calcium and diacylglycerol signals. *Cell* 95: 307-318.

Stengl M (1993). Intracellular-messenger-mediated cation channels in cultured olfactory receptor neurons. *J Exp Biol* 178: 125-147.

Stengl M (1994). Inositol-trisphosphate-dependent calcium currents precede cation currents in insect olfactory receptor neurons in vitro. *J Comp Physiol A* 174: 187-194.

Zufall F, Hatt H (1991). Dual activation of a sex pheromone-dependent ion channel from insect olfactory dendrites by protein kinase C activators and cyclic GMP. *Proc Natl Acd Sci USA* 88: 8520-8524.

Appendix C

Cross-talk of second messenger pathways in cultured olfactory receptor neurons of *Manduca sexta*.

ORNs harbor different second messenger pathways

Depending on stimulus length and strength, odorants activate different second messenger pathways in insect olfactory receptor neurons (ORNs). Short-term pheromone stimulation activates phospholipase C (PLC), which converts phosphatidylinositol 4,5-bisphosphate into inositol 1,4,5-triphosphate (IP_3) and 1,2-diacylglycerol (DAG). IP_3 and DAG in turn activate cation channels involved in insect pheromone transduction (Zufall and Hatt 1991; Stengl 1994; Pophof and Van der Goes van Naters 2002; see Chapter 1, 2). In contrast, minute-long pheromone stimulation increases the cyclic guanosine monophosphate (cGMP) concentration in the ORNs (Ziegelberger et al. 1990; Boekhoff et al. 1993). Cyclic nucleotides directly activate cyclic nucleotide-gated (CNG) cation channels that probably mediate sensitization and adaptation of the olfactory response (Baumann et al. 1994; Krieger et al. 1999; Gisselmann et al. 2003; see Chapter 3, 4).

Since IP_3-dependent currents occurred in about 90 % (Stengl 1994), DAG-dependent currents in about 65 % (see Chapter 2), and cyclic nucleotide-dependent currents in about 81 % of cultured *M. sexta* ORNs (see Chapter 4), it is likely that IP_3/DAG- and cyclic nucleotide-dependent pathways coexist within the same ORN. Previous studies on invertebrate and vertebrate ORNs suggested that at least IP_3 and cAMP interact during olfactory transduction (Ache and Zhainazarov 1995). Inhibition of the IP_3-dependent protein kinase C (PKC) resulted in a potentiation of the cAMP-mediated olfactory response. *Vice versa*, inhibition of the cAMP-dependent protein kinase A increased the IP_3-mediated olfactory response (Frings 1993; Gomez et al. 2000). In the vertebrate visual system, DAG analogues inhibited cGMP-activated currents through CNG channels suggesting that DAG and cGMP may also interact (Gordon et al. 1995; Crary et al. 2000). In vertebrate ORNs, however, PKC, and not DAG, inhibited cGMP-activated currents through CNG channels suggesting that PKC and cGMP interact as well (Muller et al. 1998, 2001).

Interactions of second messengers

We showed in whole-cell patch-clamp recordings that application of the cAMP analogue 8bcAMP, the cGMP analogue 8bcGMP, the DAG analogue 1,2-dioctanoyl-*sn*-glycerol (DOG), or the PKC activator phorbol 12-myristate-13-acetate (PMA) induced different non-specific cation currents in cultured *Manduca sexta* ORNs (see Chapter 1-4, Appendix A, B).

Here, we investigated in a first set of experiments whether application of DOG or PMA alters cyclic nucleotide-activated currents (Fig. C1). Application of 500 nM DOG induced a ~2-fold increase of the cGMP-activated current in 5 of 9 ORNs ($p < 0.01$; Fig. C1A). The remaining four ORNs did not respond to DOG. Application of 250 nM PMA increased the cGMP-activated

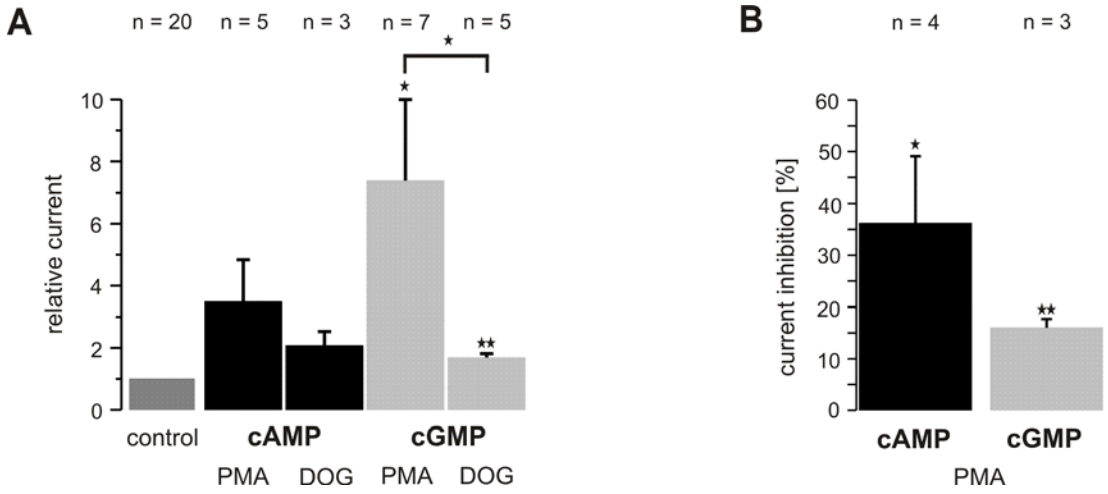

Figure C1 Interaction of the cyclic nucleotide signaling pathways with DAG/PKC. (**A**) In most ORNs, application of 250 nM PMA or 500 nM DOG did not significantly change the cAMP-activated current, but significantly increased the cGMP-activated current. (**B**) In few ORNs, PMA significantly inhibited the cyclic nucleotide-activated currents. Error bars represent SEM.

current ~7-fold in 7 of 10 ORNs ($p < 0.05$). Thus, PMA caused a significantly stronger increase than DOG ($p < 0.05$; Fig. C1A). In the remaining three ORNs, PMA significantly inhibited 16 ± 1.7 % of the cGMP-activated current ($p < 0.01$; Fig. C1B). The cAMP-activated current did not significantly increase upon application of DOG in 3 of 7 ORNs (Fig. C1A), and was unaffected in the remaining four ORNs. Similarly, PMA did not significantly increase the cAMP-activated current in 5 of 10 ORNs (Fig. C1A). In 4 of 10 ORNs, however, PMA significantly inhibited 36.2 ± 12.9 % of the cAMP-activated current ($p < 0.05$; Fig. C1B).

In a second set of experiments, we analyzed whether application of cyclic nucleotides alters PMA- or DOG-activated currents (Fig. C2). Application of cAMP induced a ~2-fold increase of the PMA-activated current in 3 of 7 ORNs ($p < 0.05$; Fig. C2A). In 4 of 7 ORNs, however, cAMP-

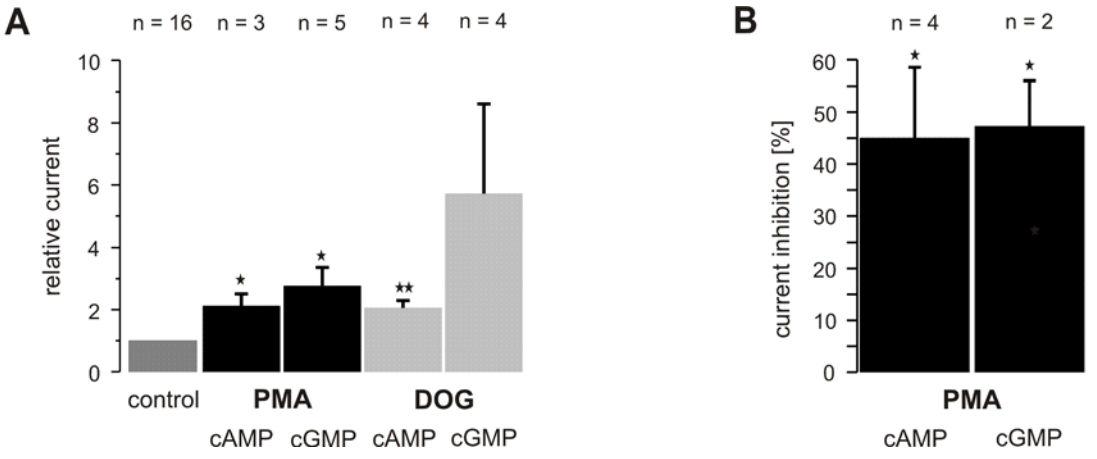

Figure C2 Interaction of the DAG/PKC signaling pathways with cyclic nucleotides. (**A**) In most ORNs, application of 500 nM 8bcAMP or 8bcGMP significantly increased the PMA-activated current. The DOG-activated current significantly increased after 8bcAMP-application, whereas 8bcGMP did not significantly change the DOG-activated current. (**B**) In few ORNs, cyclic nucleotides significantly inhibited the PMA-activated currents. Error bars represent SEM.

application significantly inhibited 45 ± 13.5 % of the PMA-activated current ($p < 0.05$; Fig. C2B). Application of cGMP increased the PMA-activated current ~3-fold in 5 of 11 ORNs ($p < 0.05$; Fig. C2A). In 2 of 11 ORNs, cGMP significantly inhibited 47.3 ± 8.7 % of the PMA-activated current ($p < 0.05$; Fig. C2B). In the remaining four ORNs, cGMP did not affect the PMA-activated current. Application of cAMP induced a ~2-fold increase of the DOG-activated current in 4 of 6 ORNs ($p < 0.01$; Fig. C2A), and had no effect in the remaining two ORNs. The DOG-activated current did not significantly increase upon application of cGMP in 4 of 9 ORNs (Fig. C2A), and was unaffected in the remaining five ORNs.

Cross-talk in moth ORNs

Several second messenger pathways mediate olfactory transduction in ORNs. In case multiple pathways are present in the same ORN, these pathways can directly or indirectly alter the activity of each other in a process termed cross-talk. In lobster ORNs (Boekhoff et al. 1994; Hatt and Ache 1994), olfactory transduction results in the synthesis of both IP_3 and cAMP. While IP_3 evokes excitation, cAMP inhibits the ORN. In vertebrate ORNs, IP_3 and cAMP also activate opposing conductances. Which of the respective pathways is excitatory or inhibitory depends on the species (Ache and Zhainazarov 1995). The antagonistic properties of the cAMP and IP_3 signaling pathways allow the fine-tuning of the olfactory response. In some ORNs, e.g. in those of the catfish, both cAMP and IP_3 are excitatory and induce an increase of the intracellular Ca^{2+} concentration. The Ca^{2+} increase then inhibits the olfactory transduction cascade (Miyamoto et al. 1992). In the ORNs of *M. sexta*, the second messengers cAMP and cGMP, DAG/PKC, and IP_3 also induced an increase in the intracellular Ca^{2+} concentration and, therefore, likely mediate excitation (Stengl 1994; see Chapter 1-4, Appendix A, B). It is still unclear, however, if different second messenger pathways localize to the same ORN and affect each other.

As opposed to rod CNG channels (Gordon et al. 1995; Crary et al. 2000), we here found that the DAG analogue DOG did not inhibit cyclic nucleotide-activated currents in moth ORNs. Instead, DOG often increased the amplitude of cyclic nucleotide-activated currents. *Vice versa*, cyclic nucleotides often increased the amplitude of DOG-activated currents. These results suggest that at least some moth ORNs co-express DAG-gated channels and CNG channels.

Similarly to vertebrate olfactory CNG channels (Muller et al. 1998, 2001), we here found that the PKC activator PMA inhibited cyclic nucleotide-activated currents in a subset of moth ORNs. Concomitantly, cyclic nucleotides inhibited the amplitude of the PMA-activated currents in some ORNs. In most ORNs, however, PMA increased the amplitude of cyclic nucleotide-activated currents. *Vice versa*, cyclic nucleotides often increased the amplitude of PMA-activated currents. These results suggest that at least in some moth ORNs cyclic nucleotides and PKC may affect each other.

References

Ache BW, Zhainazarov A (1995). Dual second-messenger pathways in olfactory transduction. *Curr Opin Neurobiol* 5: 461-466.

Baumann A, Frings S, Godde M, Seifert R, Kaupp UB (1994). Primary structure and functional expression of a *Drosophila* cyclic nucleotide-gated channel present in eyes and antennae. *EMBO J* 13: 5040-5050.

Boekhoff I, Seifert E, Goggerle S, Lindemann M, Kruger BW, Breer H (1993). Pheromone-induced second-messenger signaling in insect antennae. *Insect Biochem Mol Biol* 23: 757-762.

Boekhoff I, Michel WC, Breer H, Ache BW (1994). Single odors differentially stimulate dual second messenger pathways in lobster olfactory receptor cells. *J Neurosci* 14: 3304-3309.

Crary JI, Dean DM, Nguitragool W, Kurshan PT, Zimmerman AL

(2000). Mechanism of inhibition of cyclic nucleotide-gated ion channels by diacylglycerol. *J Gen Physiol* 116: 755-768.

Frings S (1993). Protein kinase C sensitizes olfactory adenylate cyclase. *J Gen Physiol* 101: 183-205.

Gisselmann G, Warnstedt M, Gamerschlag B, Bormann A, Marx T, Neuhaus EM, Stoertkuhl K, Wetzel CH, Hatt H (2003). Characterization of recombinant and native Ih-channels from *Apis mellifera*. *Insect Biochem Mol Biol* 33: 1123-1134.

Gomez G, Rawson NE, Cowart B, Lowry LD, Pribitkin EA, Restrepo D (2000). Modulation of odor-induced increases in $[Ca^{2+}]_i$ by inhibitors of protein kinases A and C in rat and human olfactory receptor neurons. *Neurosci* 98: 181-189.

Gordon SE, Downing-Park J, Tam B, Zimmermann AL (1995). Diacylglycerol analogs inhibit the rod cGMP-gated channel by a phosphorylation-independent mechanism. *Biophys J* 69: 409-417.

Hatt H, Ache BW (1994). Cyclic nucleotide- and inositol phosphate-gated ion channels in lobster olfactory receptor neurons. *Proc Natl Acad Sci USA* 91:6264-6268.

Krieger J, Strobel J, Vogl A, Hanke W, Breer H (1999). Identification of a cyclic nucleotide- and voltage-activated ion channel from insect antennae. *Insect Biochem Mol Biol* 29: 255-267.

Miyamoto T, Restrepo D, Cragoe EJ, Teeter EH (1992). IP_3- and cAMP-induced responses in isolated olfactory receptor neurons from the channel catfish. *J Membr Biol* 127: 173-183

Muller F, Bonigk W, Sesti F, Frings S (1998). Phosphorylation of mammalian olfactory cyclic nucleotide-gated channels increases ligand sensitivity. *J Neurosci* 18: 164-173.

Muller F, Vantler M, Weitz D, Eismann E, Zoche M, Koch KW, Kaupp UB (2001). Ligand sensitivity of the α2 subunit from the bovine cone cGMP-gated channel is modulated by protein kinase C but not by calmodulin. *J Physiol Lond* 532: 399-409.

Pophof B, Van der Goes van Naters W (2002). Activation and inhibition of the transduction process in silkmoth olfactory receptor neurons. *Chem. Senses* 27, 435-443.

Stengl M (1994). Inositol-trisphosphate-dependent calcium currents precede cation currents in insect olfactory receptor neurons *in vitro*. *J Comp Physiol A* 174: 187-194.

Ziegelberger G, van den Berg MJ, Kaissling KE, Klumpp S, Schultz JE (1990). Cyclic GMP levels and guanylate cyclase activity in pheromone-sensitive antennae of the silkmoths *Antheraea polyphemus* and *Bombyx mori*. *J Neurosci* 10: 1217-1225.

Zufall F, Hatt H (1991). Dual activation of a sex pheromone-dependent ion channel from insect olfactory dendrites by protein kinase C activators and cyclic GMP. *Proc Natl Acad Sci USA* 88: 8520-8524.

Conclusions

In the insect olfactory system, pheromone perception involves the generation of the second messengers inositol 1,4,5-triphosphate (IP_3) and 1,2-diacylglycerol (DAG). While several studies analyzed the function of IP_3, the specific role of DAG remained largely unexplored. Thus, in the first part of my PhD thesis (Chapter 1, 2), whole-cell and inside-out patch-clamp recordings were used to characterize the effects of DAG on moth olfactory receptor neurons (ORNs). Previous findings suggested that pheromone transduction also depends on the intracellular concentration of cyclic nucleotides. Thus, in the second part of my PhD thesis, single channel (Chapter 3) and whole-cell (Chapter 4) patch-clamp recordings were used to investigate whether cyclic nucleotides activate ion channels in moth ORNs.

The DAG pathway

In the invertebrate visual system, DAG has been shown to directly modulate the activity of several ion channels of the transient receptor potential (TRP) channel family. Recent studies on the vertebrate olfactory system suggested that DAG directly activates ion channels of the classical TRP subfamily (TRPC). Here, we describe for the first time DAG-dependent non-specific cation currents in the ORNs of

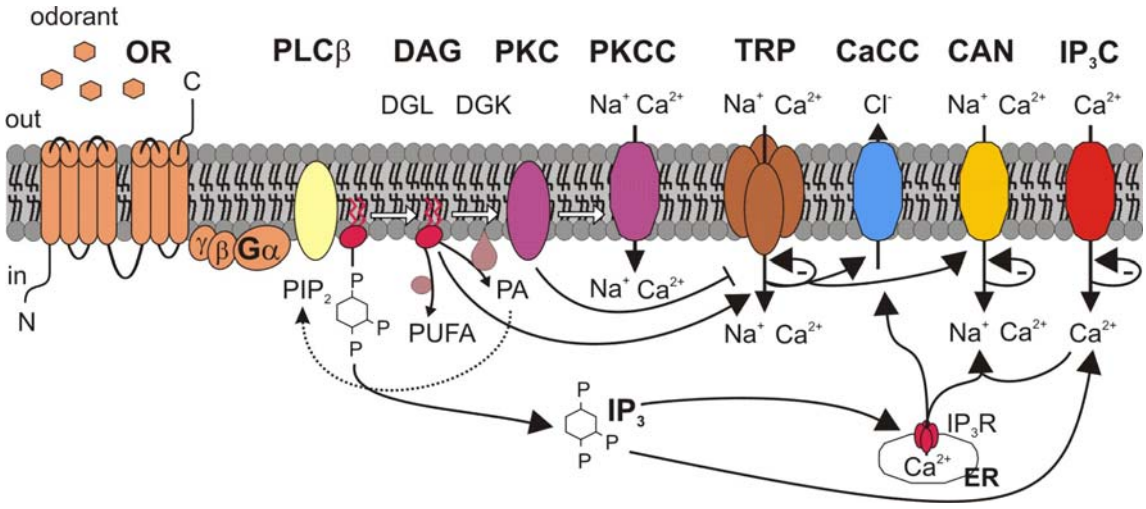

Figure 7 The IP_3 and DAG signaling pathway in moth ORNs. Odorants bind to G-protein-coupled odorant receptors (OR) that interact with phospholipase Cβ (PLCβ). PLCβ hydrolyzes phosphatidylinositol 4,5-bisphosphate (PIP_2) into inositol 1,4,5-triphosphate (IP_3) and diacylglycerol (DAG). IP_3 leads to an influx of Ca^{2+} through IP_3-dependent channels (IP_3C) in the cell membrane. In addition, IP_3 releases Ca^{2+} from the endoplasmic reticulum (ER) through IP_3 receptors (IP_3R). DAG activates protein kinase C (PKC), which in turn activates PKC-dependent cation channels (PKCC). In addition, DAG activates ion channels that show similar electrophysiological properties as those of the transient receptor potential (TRP) channel family. These putative moth DAG-gated TRP-like channels are inhibited by PKC. The intracellular increase of Ca^{2+} following IP_3- or DAG-gated channel activation further leads to the activation of Ca^{2+}/CaM-dependent cation channels (CAN) and Ca^{2+}-activated Cl^- channels (CaCC). DAG is metabolized by either DAG lipase (DGL) that hydrolyzes DAG to produce poly-unsaturated fatty acids (PUFA), or by DAG kinase (DGK) that phosphorylates DAG to produce phosphatidic acid (PA). PA represents the first step in PIP_2 recycling. Most likely, both pathways are present in the same moth ORN.

two moth species, *Spodoptera littoralis* (Chapter 1) and *Manduca sexta* (Chapter 2). In whole-cell and inside-out patch-clamp recordings, DAG activated currents in a protein kinase C- (PKC) independent way. Ca^{2+}/calmodulin (CaM) modulated the DAG-dependent currents. Inhibition of DAG kinase, the DAG-degrading enzyme, resulted in the activation of DAG-dependent currents. Lanthanum, a non-specific blocker of Ca^{2+}-permeable cation channels, and PKC inhibited the DAG-dependent currents (Fig. 7). Thus, the electrophysiological properties of the moth DAG-dependent currents resembled those of currents through transient receptor potential (TRP) channels. Since RT-PCR experiments showed that two RNA transcripts with high sequence similarity to the *Drosophila melanogaster* TRPL channel are present in the *M. sexta* brain and antennae, the putative moth DAG-gated channels likely represent TRP-like channels. Accordingly, DAG or one of its metabolites is involved in the moth olfactory transduction cascade and probably plays a decisive role in the transduction of olfactory information.

Summary and perspectives

- In the olfactory system of *M. sexta*, DAG-dependent currents occurred in about 65 % of cultured ORNs (Chapter 2), whereas IP_3-dependent currents were found in about 90 % of cultured ORNs (Stengl 1994). Thus, in most ORNs, DAG and IP_3 are likely to interact during olfactory transduction. At least some ORNs probably express only DAG- or IP_3-dependent currents. The question arises if the different current types play specific roles for signal transmission.
- Since about 65 % of the cultured ORNs of *M. sexta* show DAG-dependent currents and about 38 % of the cultured ORNs were activated pheromone-dependently (Stengl et al. 1992), it is likely that DAG is involved in the perception of general odorants. In future experiments, it will be investigated if pheromone-sensitive ORNs express DAG-dependent currents.
- TRP-like ion channels are probably expressed in moths (Chapter 2). It will be investigated in future experiments if TRP-like channels localize to ORNs and are DAG-sensitive.

The cyclic nucleotide pathway

In vertebrate ORNs, the cyclic nucleotides adenosine monophosphate (cAMP) and guanosine monophosphate (cGMP) directly activate cyclic nucleotide-gated (CNG) channels in a Ca^{2+}/CaM-dependent manner and, therefore, probably play key roles in olfactory adaptation and sensitization. Only few studies described CNG channels in insect ORNs. The identified insect CNG channels belong to the subfamily of hyperpolarization-activated cyclic nucleotide-modulated (HCN) channels. Here, we described in single channel (Chapter 3) and whole-cell patch-clamp recordings (Chapter 4) cyclic nucleotide-dependent non-specific cation channels in the ORNs of *M. sexta* that have similar properties as vertebrate CNG channels, and are likely to be involved in adaptation and sensitization of moth ORNs. In whole-cell patch-clamp recordings, both cAMP and cGMP activated these putative *Ms*CNG channels in a protein kinase-independent way. Lanthanum and the transition metals Ni^{2+} and Zn^{2+} inhibited the putative *Ms*CNG channels (Fig. 8). Since the putative *Ms*CNG channels differed in their Ca^{2+}/CaM-dependency, they appear to be composed of different subunits. At least one cAMP- and two cGMP-dependent putative *Ms*CNG channels could be distinguished in *M. sexta* ORNs. Apart from the putative *Ms*CNG channels, ORNs of *M. sexta* appear to possess putative HCN channels (Appendix B). Finally, a previously unknown

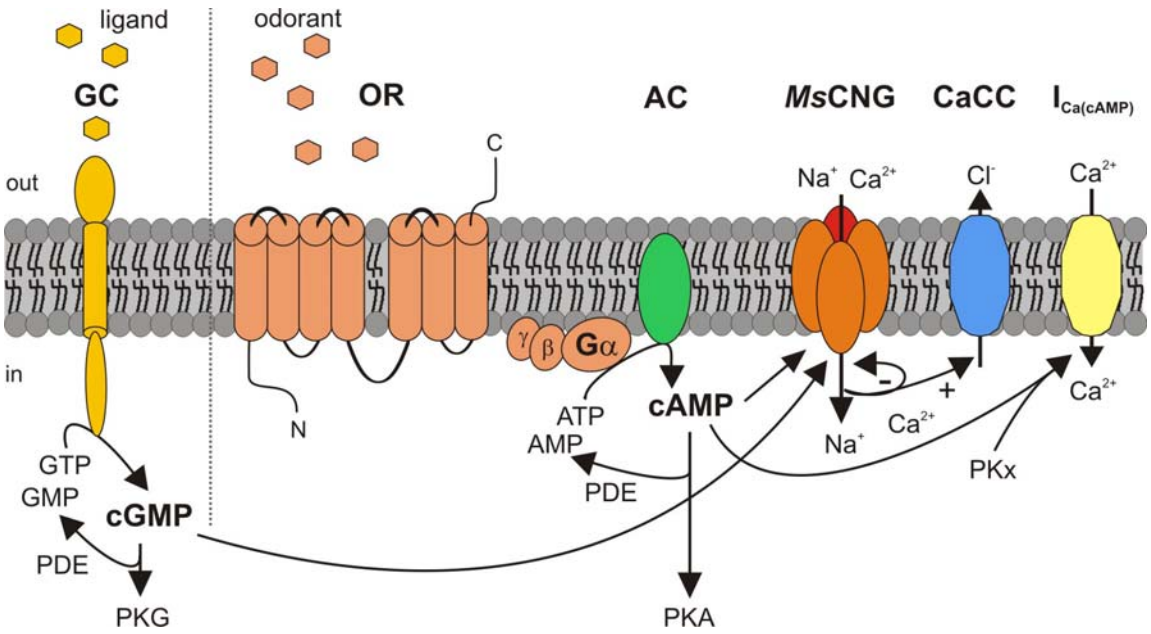

Figure 8 The cAMP and cGMP signaling pathway in moth ORNs. Odorants bind to G-protein-coupled odorant receptors (OR) that interact with an adenylyl cyclase (AC). The activation of AC leads to an increase of the cyclic adenosine monophosphate (cAMP) concentration. The ligand-mediated activation of a receptor guanylyl cyclase (GC) increases the cyclic guanosine monophosphate (cGMP) concentration. Both cAMP and cGMP in turn directly activate putative cyclic nucleotide-activated channels (*Ms*CNG) in the ORNs of *M. sexta* as well as the respective protein kinase (PKA, PKG). The activation of putative *Ms*CNG channels increases the intracellular Ca^{2+} concentration that leads to the subsequent activation of Ca^{2+}-activated Cl^- channels (CaCC). The Ca^{2+} increase stimulates the hydrolyzation of cAMP and cGMP through phosphodieasterases (PDE). In addition, in ORNs of *M. sexta* occurred a novel cAMP- and protein kinase-dependent low voltage-activated Ca^{2+} current ($I_{Ca(cAMP)}$). Most likely, both pathways are present in the same moth ORN.

low voltage-activated (LVA) Ca^{2+} current, which activated cAMP- and protein kinase-dependently, was found in the ORNs of *M. sexta* (Fig. 8). Thus, there are multiple cyclic nucleotide-dependent channels in moth ORNs. Since cyclic nucleotides and PKC differentially activated specific ion channels, and cGMP is involved in long-term adaptation while PKC mediates short-term adaptation, the corresponding ion channels might allow fine-tuning of the olfactory response.

Summary and perspectives

- Patch-clamp recordings suggested that moth ORNs express ion channels that are similar to vertebrate CNG channels. Preliminary RT-PCR experiments suggested that CNG-like channels were expressed in the moth antennae. In future experiments, it will be analyzed whether these channels localize to ORNs and respond to cyclic nucleotides.
- In the olfactory system of *M. sexta*, about 81 % of cultured ORNs expressed cyclic-nucleotide-activated currents (Chapter 4) and about 23 % of cultured ORNs expressed hyperpolarization-activated cyclic nucleotide-modulated currents (Appendix A). The functional role of the putative moth cyclic nucleotide-gated channels (*Ms*CNG and HCN) in the olfactory transduction cascade will be investigated in future experiments.

References

Stengl M (1994). Inositol-trisphosphate-dependent calcium currents precede cation currents in insect olfactory receptor neurons *in vitro*. *J Comp Physiol [A]* 174: 187-194.

Stengl M, Zufall F, Hatt H, Hildebrand JG (1992). Olfactory receptor neurons from antennae of developing male *Manduca sexta* respond to components of the species-specific sex pheromone *in vitro*. *J Neurosci* 12: 2523-2531.

Acknowledgements

I'm very grateful to Prof. Dr. Monika Stengl for supervising my PhD thesis. At all times, she provided means and support for the careful realization of my experiments. She always encouraged me to follow my own ideas and enabled me to work independently.
I also thank Prof. Dr. Uwe Homberg for surveying my PhD thesis, and Prof. Dr. Monika Hassel, and Prof. Dr. Roland Brandl for their contribution in the examination commission.

Special thanks to Dr. Philippe Lucas. He excellently supervised me during my one-year stay at INRA Versailles. Together we enjoyed a lot of fruitful discussions, and I thank him for countless practical hints. My stay at INRA Versailles was supported by the Marie Curie Fellowship Association.

I'm also very grateful to Dr. Jan Dolzer. He was my first scientific teacher and trained me in electrophysiology. Hopefully, one day I will be as good as he at always giving helpful advice.

The list of students and colleagues that were involved in insect rearing is long. Thanks to each one.

Last but not least, I want to thank everybody, former or present member, of the Neurobiology group in Marburg for good atmosphere and company.

Finally, special thanks to Matze, my family and friends for their encouragement and all-time assistance.

Ich versichere, dass ich meine Dissertation

Electrophysiological and pharmacological characterization of ion channels involved in moth olfactory transduction cascades

(Elektrophysiologische und pharmakologische Charakterisierung von Ionenkanälen in den olfaktorischen Transduktionskaskaden von Nachtschmetterlingen)

selbständig, ohne unerlaubte Hilfe angefertigt und mich dabei keiner anderen als der von mir ausdrücklich bezeichneten Quellen und Hilfen bedient habe.

Die Dissertation wurde in der jetzigen oder einer ähnlichen Form noch bei keiner anderen Hochschule eingereicht und hat noch keinen sonstigen Prüfungszwecken gedient.

Marburg 2008

(Steffi Krannich)

Curriculum vitae
STEFFI KRANNICH

Current address
FB Biology, Animal Physiology
Karl-von-Frisch Straße
35032 Marburg/Germany
phone: +49 6421 28 23416
email: Krannics@students.uni-marburg.de

Personal

Date and place of birth	:	21.05.1978 in Zwickau (Germany)
Marital status	:	Single

Education

2003 - present	Doctoral thesis, Philipps-University Marburg, Germany
2002.10.	Diploma, Philipps-University Marburg, Germany; Title of diploma thesis: Immunocytochemical characterization of luminal cells of the antennal system of the hawkmoth *Manduca sexta*.
1999 - 2002	Undergraduate, Philipps-University Marburg, Germany
1996 - 1999	Undergraduate, University of Bremen, Germany
1984 - 1996	High School, Georgengymnasium Zwickau, Germany

Academic appointment

2007 - 2008	Research assistant, University of Kassel, Germany
2004 - 2007	Research assistant, Philipps-University Marburg, Germany
2003 - 2004	Research assistant, INRA Versailles, France

Fellowship

2003.02. - 2004.01.	One-year stage trainee, INRA Versailles, France. This work was supported by the Marie Curie Fellowship Association.

Teaching

Tutor in undergraduate courses:

- Animal physiology (muscle physiology, sensory transduction)
- Zoology (morphology of vertebrates and invertebrates)
- Biology for medical students (chronobiology, sensory transduction)

Publication list

Reviewed articles:

- Dolzer J, Krannich S, Stengl M (2008). Pharmacological investigations of protein kinase C- and cGMP-dependent ion channels in cultured olfactory receptor neurons of the hawkmoth *Manduca sexta*. *Chem Senses*: in press.
- Flecke C, Dolzer J, Krannich S, Stengl M (2006). Perfusion with cGMP analogue adapts the action potential response of pheromone-sensitive sensilla trichoidea of the hawkmoth *Manduca sexta* in a daytime-dependent manner. *J Exp Biol* 209: 3898 - 3912.
- Dolzer J, Krannich S, Fischer K, Stengl M (2001). Oscillations of the transepithelial potential of moth olfactory sensilla are influenced by octopamine and serotonin. *J Exp Biol* 204: 2781 - 2794.

Submitted:

- Krannich S, Stengl M. Cyclic nucleotide-activated currents in cultured olfactory receptor neurons of the hawkmoth *Manduca sexta*. *J Neurophysiol*
- Pézier A, Papaefthimiou C, Krannich S, Acquistapace A, Stengl M, Lucas P. Diacylglycerol activates cation channels in moth olfactory receptor neurons. *J Neurophysiol*

Abstracts:

- Stengl M, Flecke C, Krannich S, Dolzer J, Riedinger K (2008). Modulation of pheromone transduction in olfactory sensilla of the hawkmoth *Manduca sexta*. Signalling in Sensory Systems, 28th Blankenese Conference, p29.
- Krannich S, Ackermann F, Lucas P, Stengl M (2005). Does diacylglycerol gate a conductance via TRP-like ion channels in the moth *Manduca sexta*. Signalling in Sensory Systems, 25th Blankenese Conference, p62.
- Pézier A, Papaefthymiou C, Krannich S, Stengl M, Lucas P (2005). Involvement of Diacylglycerol in insect olfactory transduction. An electrophysiological study in the moth *Spodoptera littoralis*. Signalling in Sensory Systems, 25th Blankenese Conference, p73.
- Seidel K, Krannich S, Schuckel J, Stengl M (2005). Luminal cells in the antenna of the hawkmoth *Manduca sexta* stained with antibodies against HRP, cGMP, fascicline, and the circadian clock protein PERIOD. Signalling in Sensory Systems, 25th Blankenese Conference, p74.
- Krannich S, Lucas P, Stengl M (2005). Diacylglycerol in moth olfactory transduction. NWG Göttingen, Proc 6th German Neurosci Soc Conf, Thieme, Stuttgart, 131B: p534.
- Krannich S, Papaefthymiou C, Stengl M, Lucas P (2004). Diacylglycerol is involved in moth olfactory transduction. 7th International Congress of Neuroethology, Nyborg/Denmark, P114: p109.
- Flecke C, Dolzer J, Krannich S, Stengl M (2002). Effects of cyclic nucleotides on olfactory sensilla and olfactory receptor neurons of the hawkmoth *Manduca sexta*. 15th Meeting of the European Chemoreception Research Organization. Chem Senses 28:E1-E69.
- Dolzer J, Flecke C, Krannich S, Stengl M (2002). Effects of cyclic nucleotides in tip-recordings of olfactory sensilla and patch clamp recordings of cultured olfactory receptor neurons of the hawkmoth *Manduca sexta*. 95. DZG meeting Halle, Zoology 105, Suppl. V: p40.

- Krannich S, Stengl M (2002). Luminal cells in the adult antenna of the hawkmoth *Manduca sexta*. 95. DZG meeting Halle, Zoology 105, Suppl. V, p43.
- Dolzer J, Krannich S, Flecke C, Stengl M (2001). Effects of biogenic amines and cyclic nucleotides on unstimulated olfactory sensilla of the hawkmoth *Manduca sexta*. NWG Göttingen Proc 4th German Neurosci Soc Conf, Vol. 1, Thieme, Stuttgart, 190.
- Dolzer J, Krannich S, Fischer K, Stengl M (2000). Tip recordings from unstimulated trichoid sensilla of the hawkmoth *Manduca sexta*: action potential bursts, oscillating transepithelial potential, and pharmacology. 22th AChemsS meeting Erlangen, AChemS 22: p33.

Marburg 2008

Steffi Krannich